Reconstitution of Biosynthetic Gene Clusters for Bioactive Fungal Metabolites

Ying Ye

Dissertation

Hokkaido University

2017

Contents

Chapter 1. Introduction

1-1. Fungal secondary metabolites

Fungi grown in different environments produce various secondary metabolites (SM) during their life time. Most of these fungal SMs exhibit bioactivities. The most well-known example is penicillin isolated from *Penicillium* species as the antibiotic[1]. Besides penicillin, there are many other important compounds isolated from fungi with beneficial bioactivities toward humans (Figure 1-1). Lovastatin isolated from *Aspergillus terreus* was used as inhibitor of cholesterol biosynthesis[2]. Aphidicolin was isolated from the fungus *Cephalosporum aphidicola* as a tetracyclic diterpene antibiotic, it is a specific inhibitor of nuclear DNA replication in eukaryotes[3]. Pleuromutilin, also a diterpenoid antibiotics, was isolated from *Pleurotus mutilus.* It interacted with the ribosomal peptidyl transferase center to inhibit protein synthesis in bacteria[4].

On the other hand, some fungal metabolites can also be detrimental to human life. Mycotoxins are defined as secondary metabolites produced by fungi that are capable of causing disease and death in humans and other animals[5]. A famous example is aflatoxins, which is produced in several fungal strains such as *Aspergillus flavus* and *Aspergillus parasiticus.* It was implicated in the death of more than 100 thousand turkeys that was fed on fungus contaminated foodstuffs[6].

Studies on biosynthesis of these fungal secondary metabolites may not only help to produce the useful compounds but also to have a deeper knowledge of harmful toxics to avoid their adverse effects.

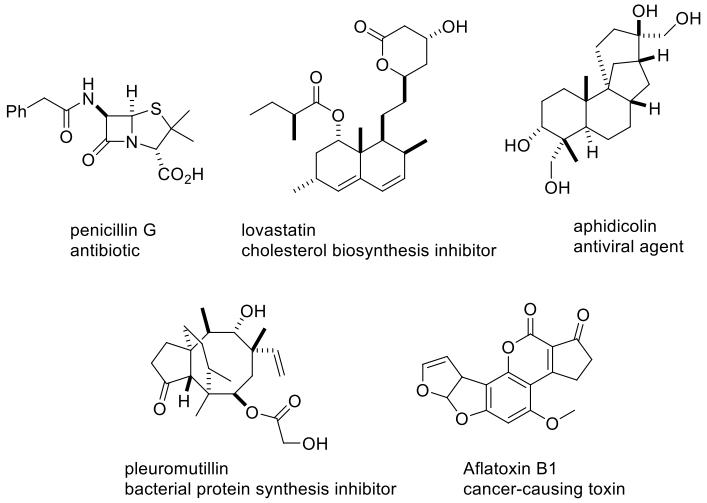

Figure 1-1 Fungal secondary metabolites

1-2. Gene cluster for fungal secondary metabolites.

Although natural products have great structure variety, they actually are biosynthesized in a few general pathways. The key enzymes in each common pathway for skeleton construction include non-ribosomal peptide synthetases (NRPS), polyketide synthase (PKS), terpene synthases (TS) and so on. To further modify the core structure and regulate the production, there are also tailoring enzymes in the later stage of biosynthetic pathway, such as oxidases, prenyltransferases, transcription regulators and transporters. A biosynthetic gene cluster (BGC) can be defined as a physically clustered group of two or more genes in a particular genome that together encode a biosynthetic pathway for the production of a specialized metabolite (including its chemical variants)[7]. Many gene clusters have been characterized such as the case of fumigaclavines in *Aspergillus fumigatus*[8] (Figure 1-2). On the other hand, large numbers of isolated natural compounds have no information of their BGCs, and many functionally unknown BGCs speculated by bioinformatics are waiting to be characterized[9,10].

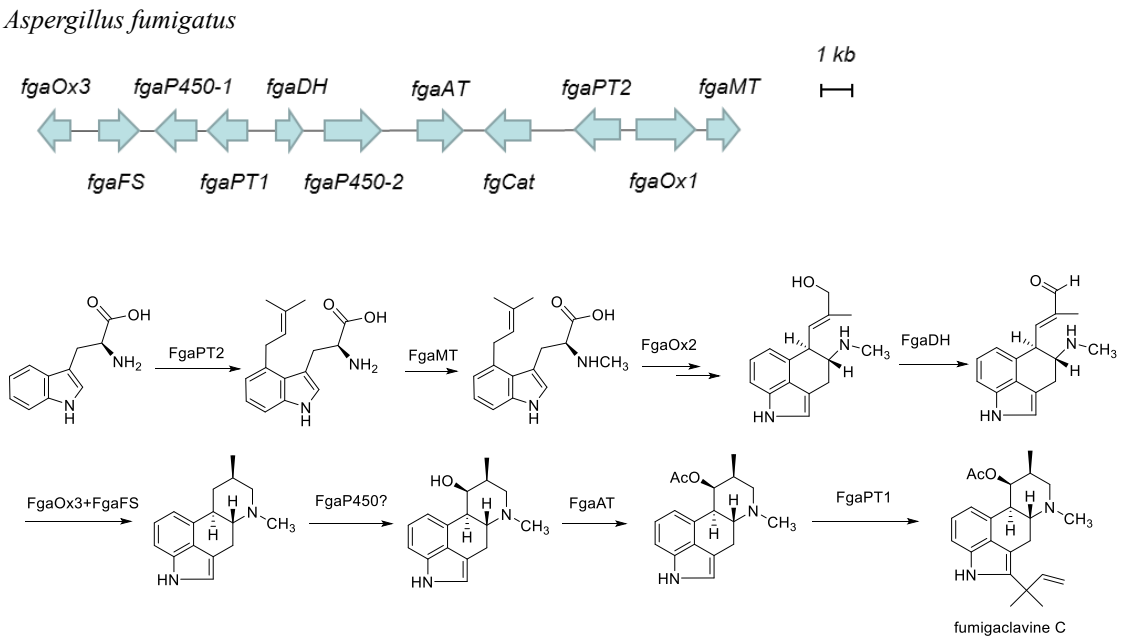

Figure 1-2. Example of biosynthetic gene cluster of fumigaclavines in *Aspergillus fumigatus*

Traditionally, the biosynthetic gene clusters were identified through sequencing of cosmid plasmids. After elucidating the location of the core enzymes such as NRPS and PKS. The problem was that it was difficult to sequence and find the complete composition of a BGC longer than 20 Kbps. With

the development of whole genome sequencing technology, over 800 fungal genome sequences are publicly available[11]. It becomes easy to access genomic data and get the full pictures of BGCs. Furthermore, using BLAST (Basic Local Alignment Search Tool) to search the homologues of studied enzymes, researchers may find many more unknown enzymes possibly catalyzing novel reactions. Together with other programs such as pfam[12], 2ndFind[13], antiSMASH[14], the process of enzyme motif analysis, functional prediction and BCG identification from the huge body of genome sequence information has been greatly facilitated.

1-3. Approaches to characterize the functions of the biosynthetic enzymes.

There are several approaches to characterize the functions of biosynthetic enzymes[15, 16], three examples are listed here: 1) gene disruption. 2) manipulating pathway-specific transcription factors 3) heterologous expression. Specifically:

(1) Gene disruption is one of the common way to investigate the function of gene(s) of interests. The traditional method is through homologous recombination, in which more than 1 kb homologous sequence flanking the target gene is required in the case of filamentous fungi[16]. Recently, some new techniques such as RNA interference (RNAi)[17] and Clustered Regularly Interspaced Palindromic Repeats (CRISPR)[18] are greatly expanding the application of gene disruption. However, the methods mentioned above should go through trial and error in each fungus host, and may suffer setbacks if the production yield is too low to observe any changes.

2) For some silent biosynthetic gene clusters, manipulating transcription factors allows activation of a specific BGC[15]. The production of secondary metabolites in the fungal host is always directly associated with the expression level of corresponding BGCs. The coordinated transcriptions of biosynthetic genes are sometimes controlled by transcription factors. These can be BGC-specific regulators or global regulators that control a wide range of genes beyond the BGC to respond to environmental cues, such as carbon and nitrogen source, temperatures and PH[19]. Overexpression or deletion of BGC-specific regulators may stimulate the expression of whole BGC and produce a corresponding natural products[15]. The pioneering work was reported by Sebastian Bergmann *et al* who successful induced a silent metabolic pathway in *Aspergillus nidulans* and led to the discovery of novel PKS-NRPS hybrid metabolites aspyridones A and B by overexpressing the BGC

transcription factor[20].

3) Heterologous expression is to express some or all of the genes on the BGC in a heterologous host such as *E. coli*, yeast and so on[15]. Once a host strain for heterologous expression is established, target compounds are expected to be biosynthesized in the transformants harboring biosynthetic genes under mandatory expression. Heterologous expression system has gained great attentions in the fungal biosynthetic studies due to its big successes over the recent years. Details will be discussed in 1-4.

1-4. Heterologous expression of biosynthetic genes in filamentous fungi.

Heterologous expression requires a suitable heterologous host which can be cultured in standard culture conditions and gives a limited natural metabolic profile[15]. *E. coli* and yeast, for example, have been long been established as heterologous expression hosts for BGCs from bacteria and eukaryotes[21,22]. Besides them, new hosts have been developed, including the filamentous fungi for more appropriate expression for fungal genes. In 1996, Fujii group introduced a function-unknown polyketide synthase (PKS) gene named *atX* from *Aspergillus terreus* into *Aspergillus nidulans*' genome. The transformant produced significant amount of 6-methylsalicylic acid, demonstrating that the *atX* gene encodes a 6-methylsalicylic acid synthase (MSAS)[23]. This is the first example the filamentous fungal biosynthetic gene was transferred into a different species and the corresponding product was produced. In 1999, following the same strategy, Hutchinson group introduced lovastatin synthase gene *lovB* and enoyl reductase gene *lovC* into *A. nidulans.* The transformant produced dihydromonacolin L and the iterative PKS/tranER system in the biosynthesis of lovastatin was characterized *in vivo*[24].

Following these pioneering works, more and more successful examples of heterologous expression in *A. nidulans* and *A. oryzae* have been reported[25, 26]. One thing to be noted is that, in these examples, the biosynthetic genes from original fungal host genomes were inserted into *A. nidulans* and *A. oryzae* without considering exon or intron issues. On the contrary, for *E. coli* and yeast, the introduced genes from filamentous fungi should contain no introns. Usually we obtain such intron-less fungal genes by cloning from cDNA of original host[22]. Thus, compared to *E. coli* and yeast, heterologous expression of biosynthetic genes in filamentous fungi such as *A. nidulans* and *A. oryzae* is preferred for the genome mining of fungal secondary metabolites.

1-5. *Aspergillus oryzae* heterologous expression system

Dr. Eiji Ichishima of Tohoku University called the *A. oryzae* (kōji fungus) a "national fungus" in the journal of the Brewing Society of Japan, because of its importance for production of sake, miso, soy sauce, and a range of other traditional Japanese foods. His proposal was approved at the society's annual meeting in 2006[27]. The most representative enzyme produced by *A. oryzae* is amylase, the yield of which can be as high as gram level in 1 L culturing scale. This high amylase production ability was attributed to the strong promoter PamyB in the upstream of amylase gene. Maltose and starch were found to activate PamyB and glucose to inhibit it[28]. This strong promoter was thus used in various plasmids to activate the downstream target genes after the plasmids was introduced into *A. oryzae.*

To introduce the PamyB and target gene into *A. oryzae*, plasmids with various markers and their applicable *A. oryzae* strains were developed (Figure 1-3). The pTAex3 plasmid was the early example for *A. oryzae* transformation[29]. Carrying the arginine biosynthetic gene *argB* as the marker, the plasmid was introduced into *A. oryzae argB* deletion mutant (Δ*argB*) for screening the plasmid integrated strains.

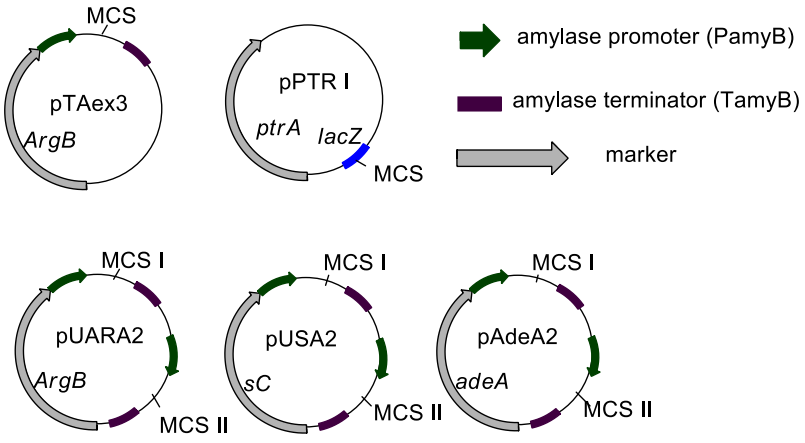

Figure 1-3. Expression vectors for heterologous expression in *A. oryzae*.

Another plasmid pPTRI carrying the pyrithiamine resistant marker (*ptrA*) was later developed, making the spontaneous expression of multiple biosynthetic genes possible. Ebizuka group reconstituted the biosynthetic pathway of a fungal meroterpenoid pyripyropene A in *A. oryzae* involving 5 genes[30]. Cox group also used the same strategy to firstly reconstitute the fungal biosynthetic multigene cluster (containing 4 genes) in *A. oryzae* and achieved the total biosynthesis of tenellin[31]. To enable multiple plasmids introduction, *A. oryzae* NSAR1 strain with 4 nutrition deficiency ($\Delta argB$, sC^-, $adeA^-$, $niaD^-$) was developed by Kitamoto group. Together with *ptrA,* 5 plasmids with different marker genes can be introduced to NSAR1 strain[32]. To make it further, our collaborator Gomi group modified the plasmids to contain 2 multiple cutting sites (e.g. pUARA2, pUSA2, pAdeA2), enabling us to introduce multiple genes into NSAR1 strain. On the other hand, our group has used two pUARA2 plasmids to introduce 4 genes into *A. oryzae* in a single transformation (Scheme 1-1)[33].

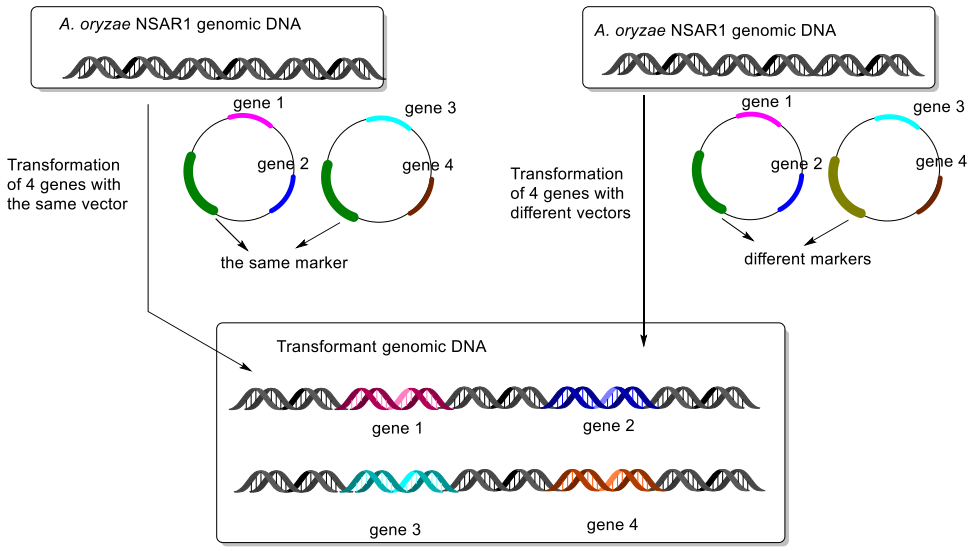

Scheme 1-1. Introduction of multiple genes into *A. oryzae*

Flexible uses of these plasmids greatly increased the capacity of *A. oryzae* to express heterologous genes, and more and more successful examples of their application has proven that *A. oryzae* has been a powerful and reliable system for the biosynthetic study of natural products. These include

the reconstitution of biosynthesis of fungal natural products: aphidicolin (Scheme 1-2 A), betaenone B (Scheme 1-2 B), didymellamide B (Scheme 1-2 C) and penitrem A (Scheme 1-2 D)[34].

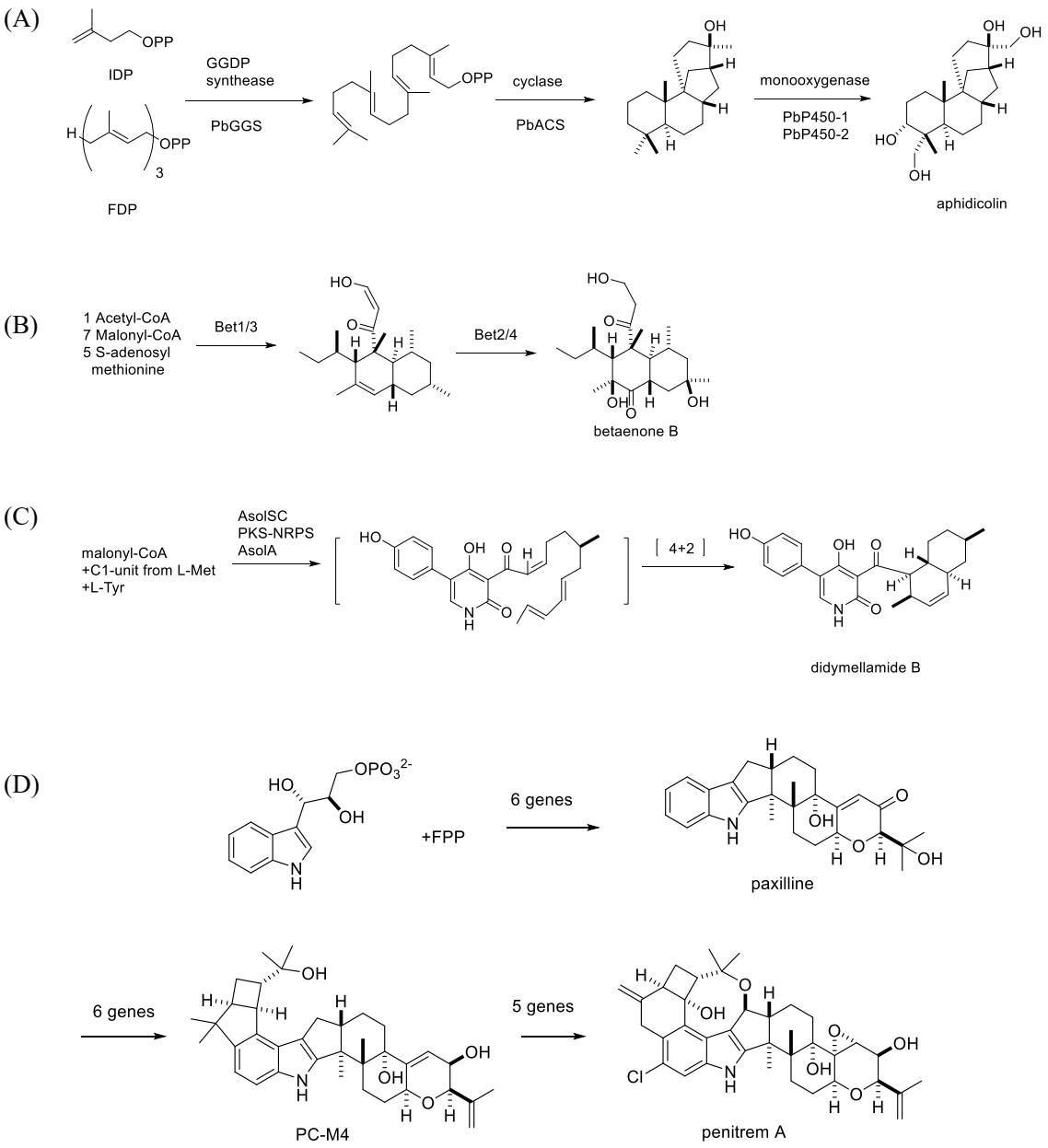

Scheme 1-2. Reconstitution of biosynthesis of fungal natural products; (A) aphidicolin (B) betaenone B (C) didymellamide B (D) penitrem A

Among them, 17 genes on the BGC of penitrem A has been introduced into *A. oryzae*. This is up to now the largest record of gene numbers heterologously expressed in *A. oryzae*. Considering most fungal BGCs contains less than 17 genes[35], *A. oryzae* heterologous expression system has shown its

great potential to study the biosynthetic pathway of almost all fungal secondary metabolites.

Holding such a powerful heterologous expression host, my work started with genome mining of bifunctional terpene synthases using *A. oryzae* as a screening system of functional terpene synthases. On my second and third topic, *A. oryzae* was firstly used to heterologously produce fungal RiPPs, a relatively new family of natural products with more and more attentions focusing on them[36].

Chapter 2. Genome mining for sesterterpenes using *A. oryzae* heterologous expression system

2-1. Bifunctional terpene synthases

Terpenes are biosynthetically derived from isoprene units (C5). According to the number of the isoprene units, the final products can be classified into monoterpene (C10), sesquiterpene (C15), diterpene (C20), sesterterpene (C25), triterpene (C30), tetraterpene (C40) and so on. Scheme 2-1 gave an outline of biosynthetic pathway to afford artemisinin[37] and taxol[38], two famous clinic drugs to treat malaria and cancers respectively.

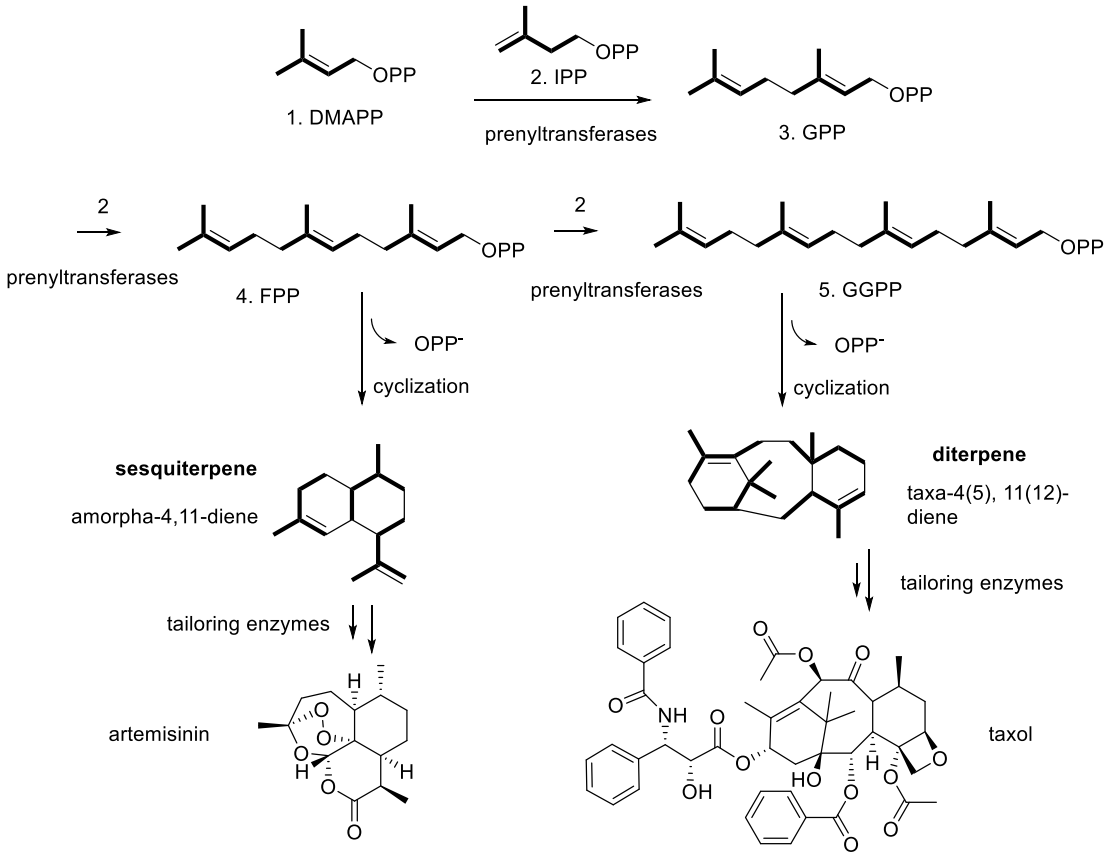

Scheme 2-1. Overall biosynthetic scheme of terpenoids. C5 isoprene unit is shown in bold.

Dimethylallyl pyrophosphate (DMAPP) and isopentenyl pyrophosphate (IPP) are the common precursors of basically all the terpene biosynthesis. They are biosynthesized through two pathways: mevalonate pathway (MVA) pathway and 2-C-methyl-D-erythritol 4-phosphate (MEP) pathway (Scheme 2-2).

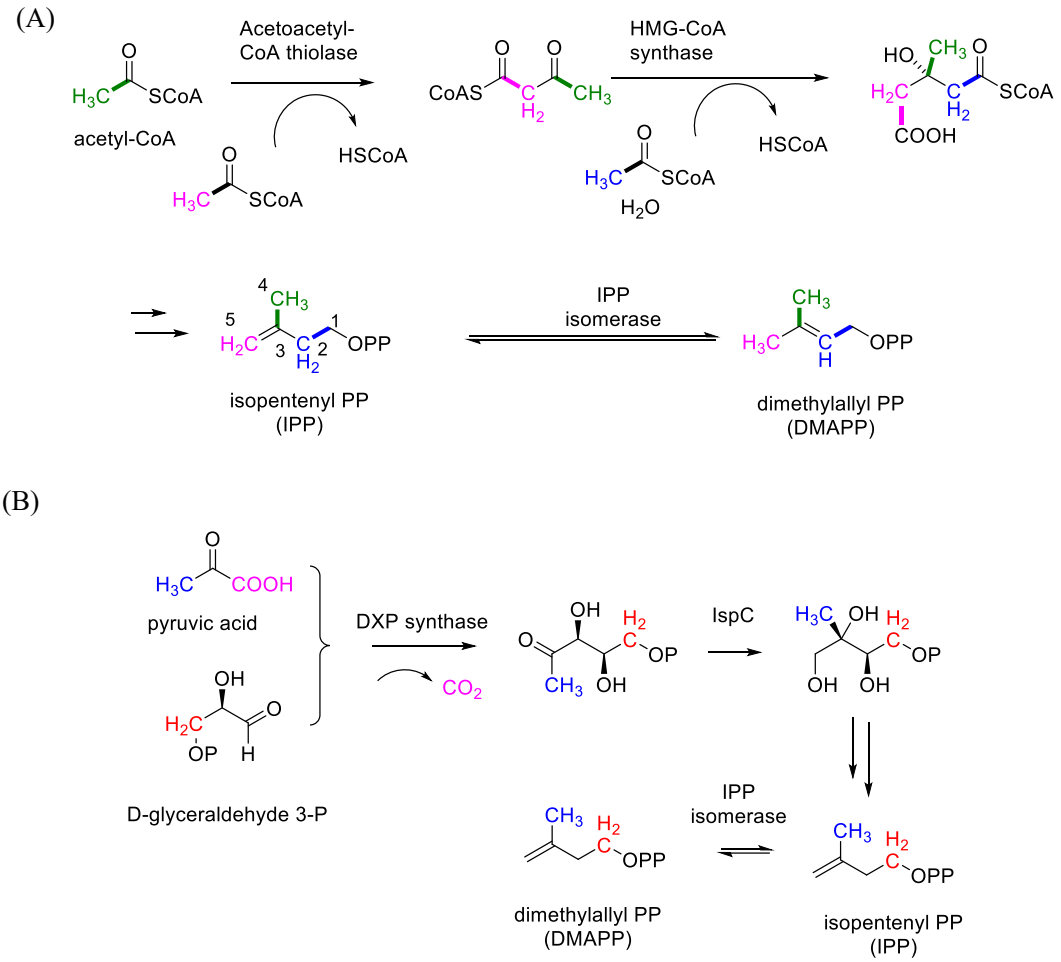

Scheme 2-2. Biosynthesis of IPP and DMAPP through A) Mevalonate pathway. The acetate unit is shown in bold line.

B) MEP pathway

Most bacteria utilize the MEP pathway of isoprenoid biosynthesis whereas all eukaryotes, archaea, and some bacterial utilize the mevalonate pathway[39]. In MVA pathway (Scheme 2-2 A), IPP and DMAPP are assembled by acetyl-CoA, with their methyl groups incorporated into C3, C4 and C5 of the products. On the other hand, MEP pathway uses the staring material of pyruvic acid and D-glyceraldehyde 3-P, with their methyl groups assembled into C1 and C4 of IPP/DMAPP. Based on this difference, the feeding experiments using ^{13}C labeled staring material (1-^{13}C acetate, for example) is a reliable method to determine whether the MVA or MEP pathway supplies isoprene units[40].

The chain length of naturally occurring linear isoprenoids ranges from C10 (GPP) to $C_{>100000}$ (natural rubber). This diversity is attributed to the prenyltransferase (PT) which mediates the sequential condensation of IPP and allylic diphosphates. According to the chain length and the stereochemistry of the chain elongation products, the prenyltransferases can be classified as shown in Figure 2-1. The *trans*- or *(E)*-prenyltransferases condenses IPP with *(E)*-configuration, and *cis*-

or (*Z*)-prenyltransferases condenses with *(Z)*-configuration.

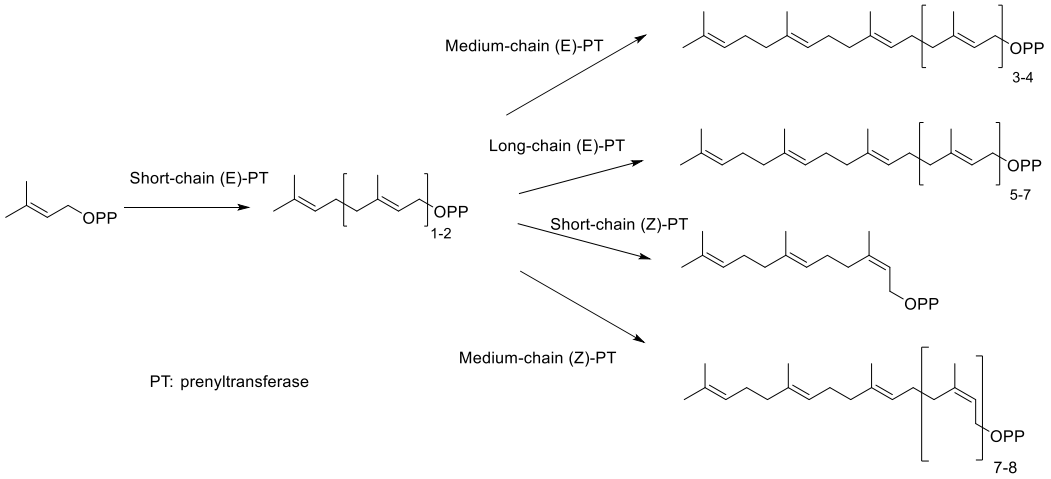

Figure 2-1. Prenyl chain elongation reactions catalyzed by prenyltransferases

As the precursor of diterpenes, GGPP is synthesized by the prenyltransferase denoted GGPP synthase. The mechanism involves the dephosphorylation of FPP, nucleophilic attack from IPP, and stereospecific deprotonation (Scheme 2-3). GGPP synthases across bacterial, eukaryotes and human conserve the DDxxD motif in their primary amino acid sequences[41]. GFPP further condenses an IPP unit to give geranylfarnesyl diphosphate (GFPP) in an analogous manner.

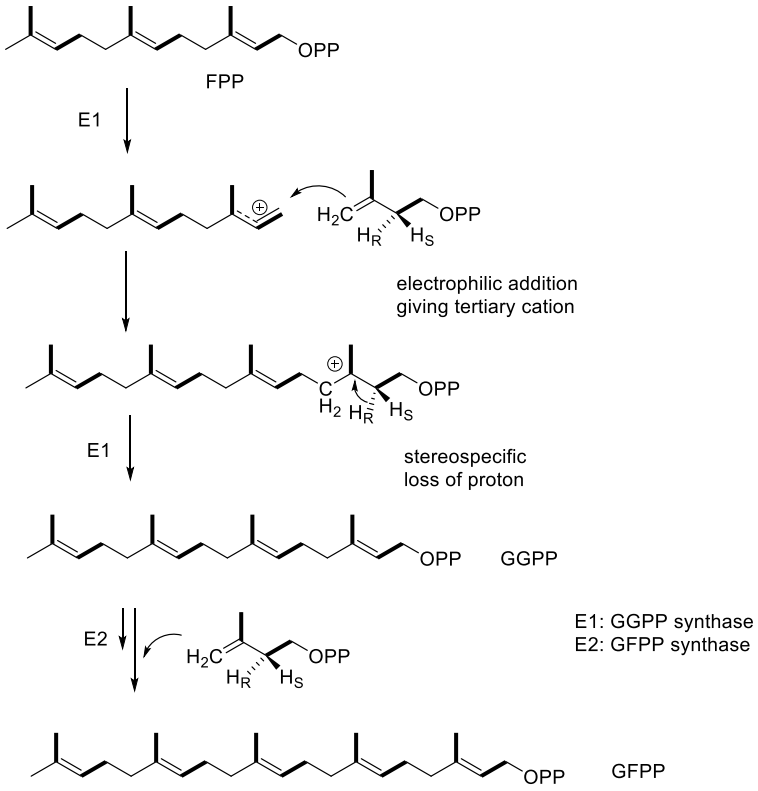

Scheme 2-3 Reaction mechanism of GGPP and GFPP synthases. Acetate unit is shown in bold line.

Diterpene cyclases catalyzed the stereospecific cyclization of linear GGPP to afford an amazing

diversity of cyclized diterpenes. MacMillan and Beale[42] described the classification of diterpene cyclases: Class I cyclization is initiated by the ionization of the diphosphate of GGPP, and Class II cyclization is initiated by the protonation of 14, 15-double bond of GGPP.

Both classes required the aspartate/glutamate rich motif in their active sites. Class I cyclases retain the DDxxD motif which coordinate with Mg^{2+} to stabilize the GGPP derived carbocation. Among them, casbene synthase catalyzes the dephosphorylation-initiated cyclization to afford casbene (Figure 2-2 A). Class II cyclase retains DxDD motif and utilized one of the aspartate as the acid for protonation of GGPP double bond. As an example of this class, *ent*-copalyl diphosphate synthases containing DxDD motif catalyzed the protonation of GGPP to afford *ent*-CPP (Figure 2-2 B). Notably, pbACS catalyzing the formation of aphidicolin-16β-ol possesses both DxDD and DDxxD motifs and promoted a two-step converstion: 1) class II cyclization to afford *syn*-CPP and 2) class I cyclization to give aphidicolin-16β-ol(Figure 2-2 C).

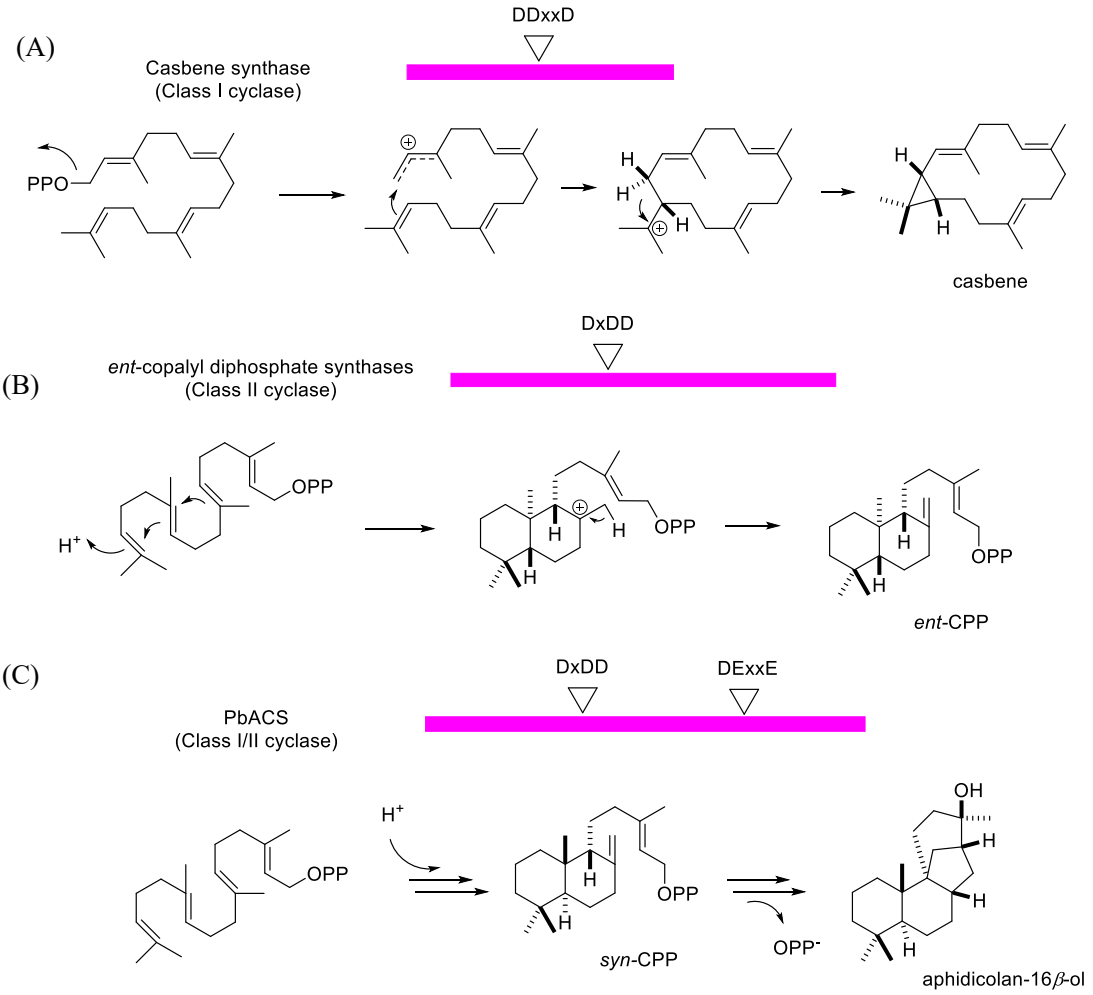

Figure 2-2. Representative diterpene cyclases and their reaction mechanism: A) Class I cyclase: *ent*-copalyl diphosphate synthase. B) Class II cyclase casbene synthase; C) Class I/II cyclase; PbACS. The triangles indicate the D(E) rich motifs.

Of various diterpene cyclases, an unusual diterpene cyclase named PaFS was firstly reported as a bifunctional diterpene synthase[43]. It contains both the prenyltransferase (PT) domain at C terminal and cyclase domain at N terminal (Figure 2-3). The PT domain of PaFS contains the DDxxD domain as observed in other prenyltransferases, and the cyclase domain possesses a DDxxD domain indicating it to be a class I cyclase.

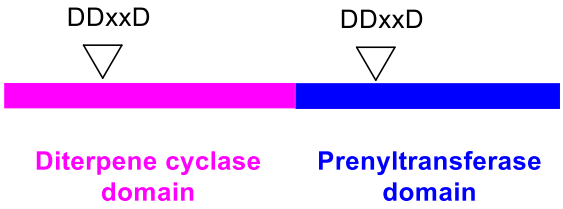

Figure 2-3. Primary structure of PaFS. Pink region: cyclases domain; Blue region: PT domain. The triangles indicate the D(E) rich motifs.

PaFS catalyzed the formation of fusicoccadiene which possesses a unique 5-8-5 tricyclic system (Scheme 2-4). It was hypothesized that the homologues of PaFS can also produce structurally unique diterpenes. Based on this prediction, Oikawa group used *A. oryzae* as an expression/screening system for genome mining of PaFS-like bifunctional terpene synthases and identified the first sesterterpene synthase named AcOS[44]. AcOS firstly synthesized the linear C25 unit GFPP through which a unique 5-8-5 tricyclic ring compound ophiobolin was produced (Scheme 2-4). This successful example showed genome mining of terpene synthases can be a promising strategy to discover novel terpene synthases and di/sesterterpenes.

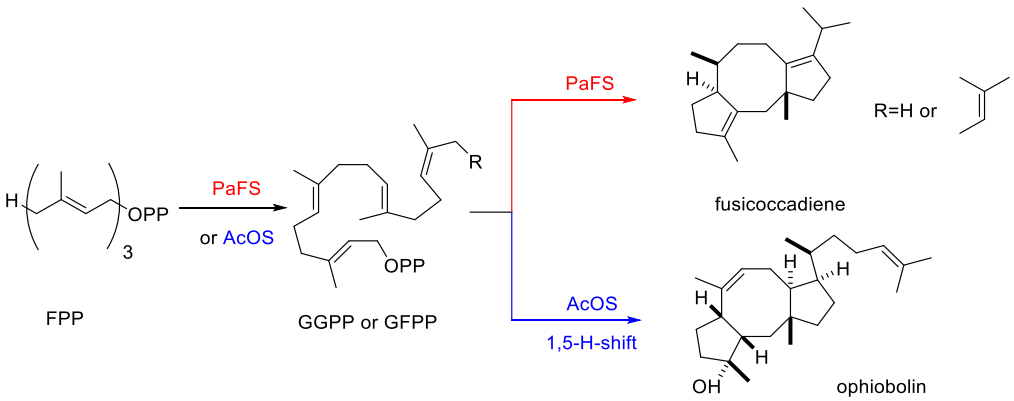

Scheme 2-4. Cyclization mechanisms of bifunctional terpene synthase PaFS and AcOS

2-2. Heterologous expression of various bifunctional terpene synthases using *A. oryzae* host.

2-2-1. Selection of bifunctional terpene synthases using phylogenetic analysis.

The N terminal cyclase domain of AcOS was used as a query sequence and 15 bifunctional terpene synthases were identified from five deposited fungal genomes (*Aspergillus nidulans*, *Aspergilus flavus, Aspergillus oryzae, Neosartorya fisheri, Aspergillus clavatus*). Four of them PaFS[43], AbFS[45], PaPs[46] and AcOS[44] have been previously characterized as bifunctional di/sesterterpene synthases. A phylogenetic analysis of 15 candidates (Figure 2-4) suggested that they could be classified into 5 clades (A~E). One thing to be noted is that the above-mentioned four known synthases fall into the clade B, while the other clades have never been explored. Furthermore, as far as is known, no terpenoids have been isolated from *Neosartorya fisheri* and *Aspergillus oryzae* suggesting the terpene synthases in these two species may be not expressed under normal culture conditions. These encouraged us to choose 4 genes from *N. fisheri* and *A. oryzae* for the first round of screening: NFIA_41470 (*NfTS1*), NFIA_55500 (*NfTS2*), and NFIA_62390 (*NfTS3*) from *N. fischeri*; AOR_1_1216074 (*AoTS1*) from *A. oryzae*.

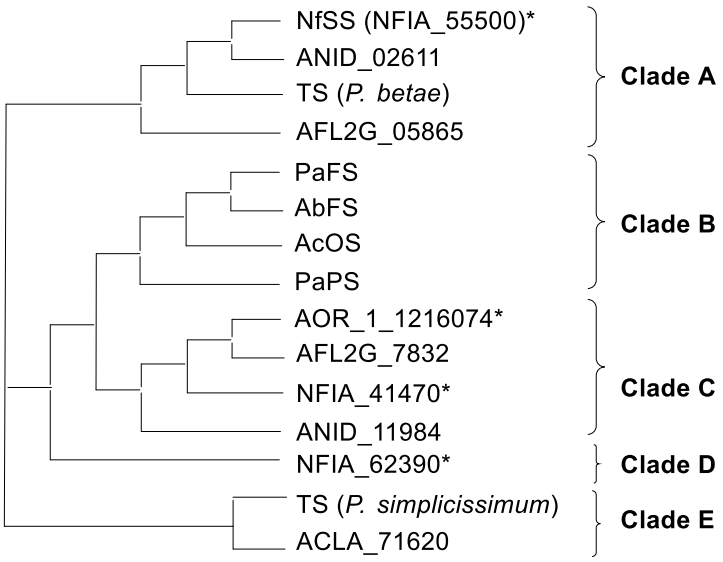

Figure 2-4. Phylogenetic analysis of terpene cyclase domain of bifunctional terpene synthases. * shows terpene synthases which have mutation in DDxxD motif.

2-2-2 Plasmid construction

To introduce the one biosynthetic gene into *A. oryzae* and obtain the corresponding metabolites, usually a month is needed (Scheme 2-5).

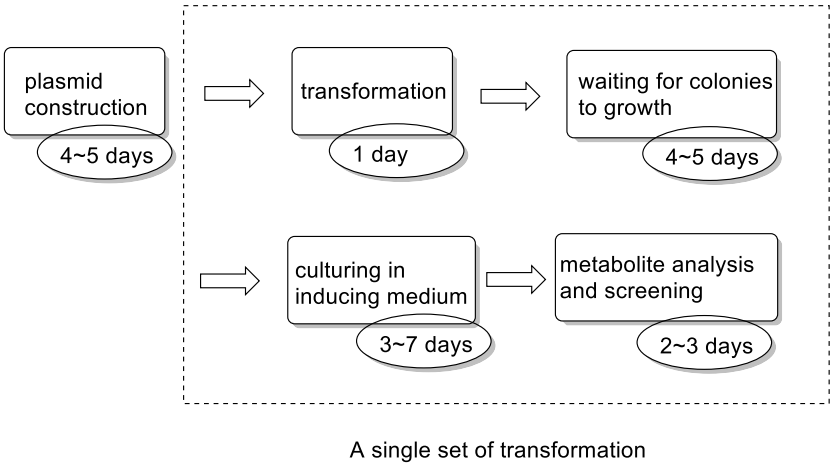

Scheme 2-5. Process and time of transformation and screening in *A. oryzae*

To make the screening process more rapid, an efficient transformation method to introduce multiple candidate genes was required. The author constructed plasmids pUARA2-*NfTS1/NfTS3* and pUARA2-*NfTS2/AoTS1* using infusion method (Scheme 2-6), and introduced them in a single transformation tandemly (Scheme 2-7)[47].

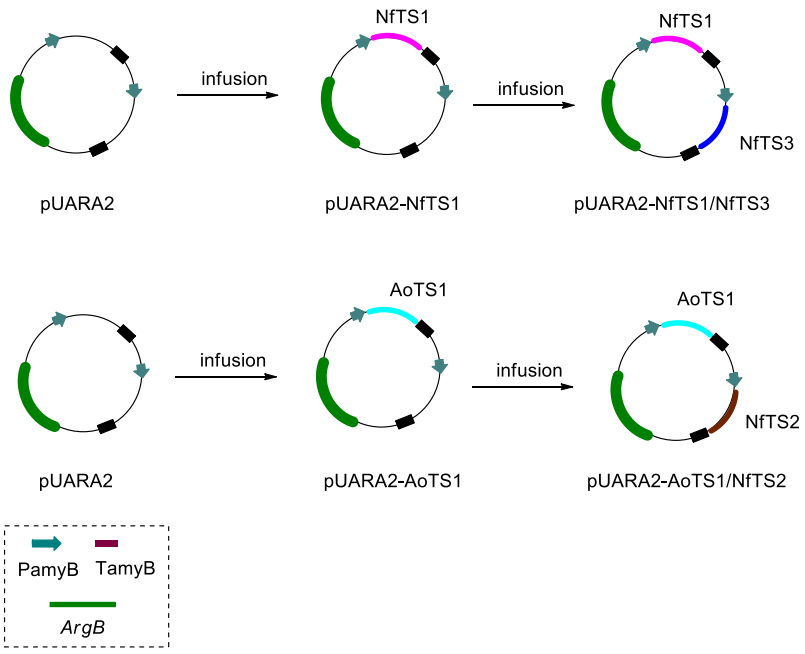

Scheme 2-6. Construction of plasmids containing 4 candidate genes

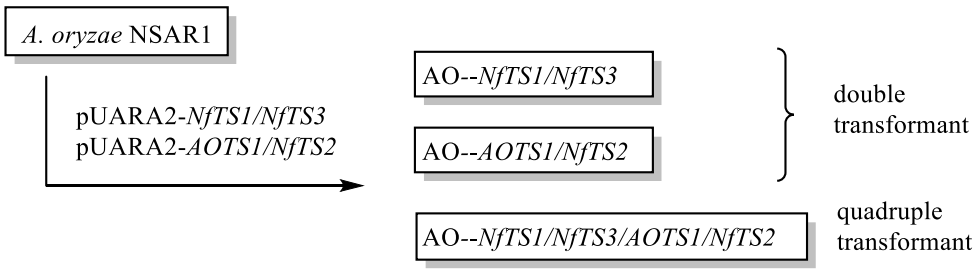

Scheme 2-7. Tandem transformation of 4 candidate genes

In tandem transformation method, two plasmids are randomly integrated into the genome of *A. oryzae*, giving double and quadruple transformants.

2-2-3. Transformants harvest and metabolites analysis

After transformation of *A. oryzae* with two plasmids containing four terpene synthase genes, thirteen colonies were obtained and cultured in rice medium for a week. The EtOAc extracts of these transformants were analyzed by GC-MS (Figure 2-5). GC-MS showed the new peak with *m/z* 358, suggesting that it is a sesterterpene alcohol. To narrow down and specify the terpene synthase that produced this new metabolite, *A. oryzae* transformants containing one or two candidate genes were also constructed using the available plasmids (Scheme 2-6), and the results were shown in the Table 2-1. GC-MS analysis of these transformants allowed the author to identify the one carrying *NfTS2* that produced the new metabolite.

(A)

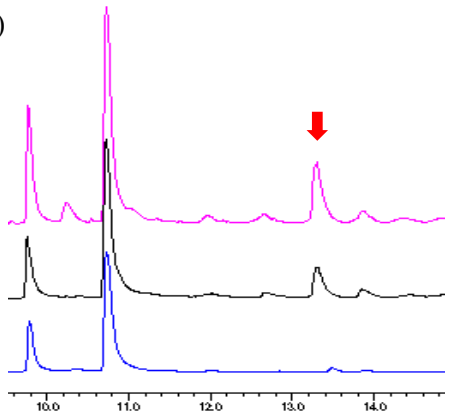

AO- *AOTS1/NfTS2*

AO-*NfTS1/NfTS3/NfTS2/AOTS1*

AO-*AOTS1*

(B)

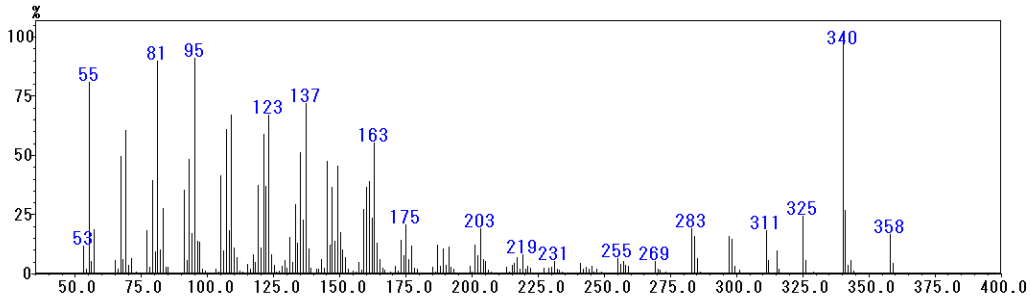

Figure 2-5. GC-MS profiles of metabolites produced by different transformants. (A) Chromatograph of GC-MS. Red arrow points to new peak (B) MS spectrum of new peak.

Table 2-1: Production screening of each transformant

Transformant	Plasmid	Total colonies obtained	Colonies producing **1**
AO-*NfTS1/NfTS3/NfTS2/AOTS1*	pUARA2-*NfTS1/NfTS3* pUARA2-*AOTS1/NfTS2*	13	9
AO-*NfTS1/NfTS3*	pUARA2-*NfTS1/NfTS3*	5	0
AO- *AOTS1/NfTS2*	pUARA2-*AOTS1/NfTS2*	5	3
AO-*NfTS1*	pUARA2-*NfTS1*	5	0
AO-*AOTS1*	pUARA2- *AOTS1*	5	0

The result confirmed that terpene synthase NfTS2 produced the new metabolite.

Among the colonies that produced the new metabolite, the highest producing colony was chosen for large scale rice fermentation. Large scale incubation (1 Kg rice) yielded 50 mg of **1**.

The HR-MS analysis of **1** ($[M]^+$ *m/z* 358.3243) indicated the molecular formula to be $C_{25}H_{42}O$. ^1H NMR and ^{13}C NMR data (Figure 2-6) showed the presence of one double bond (143.1, 133.0 ppm) and one oxygenated quaternary carbon (78.5 ppm) can be observed. Based on these data and five degree of unsaturation, the author speculated that **1** to be a tetracyclic sesterterpene alcohol. However, only 21 identifiable signals were observed on the ^{13}C NMR, indicating that several carbon signals (later determined to be C1, C3, C4, C20) were severally broadening. Similar examples was reported in NMR analysis of ciguatoxin in which the carbons signals on the nine-membered ether

ring were also missing[48]. Thus the author speculated that the highly strained middle-sized unsaturated ring structure might be the cause of carbon signal broadening. This hypothesis was supported by the observation that **1** was slowly epoxidized to **3** when dissolved in hexane and exposed to air for a week. Epoxidation of **1** with *m*-chloroperoxybenzoic acid quickly gave **3** in less than 1 min at 0℃ (Scheme 2-8).

In the ^{13}C NMR spectrum of **3** all 25 carbons were observed. Extensive 2D NMR analysis allowed the author to determine the planer structure of **1** and **3**.

(A)

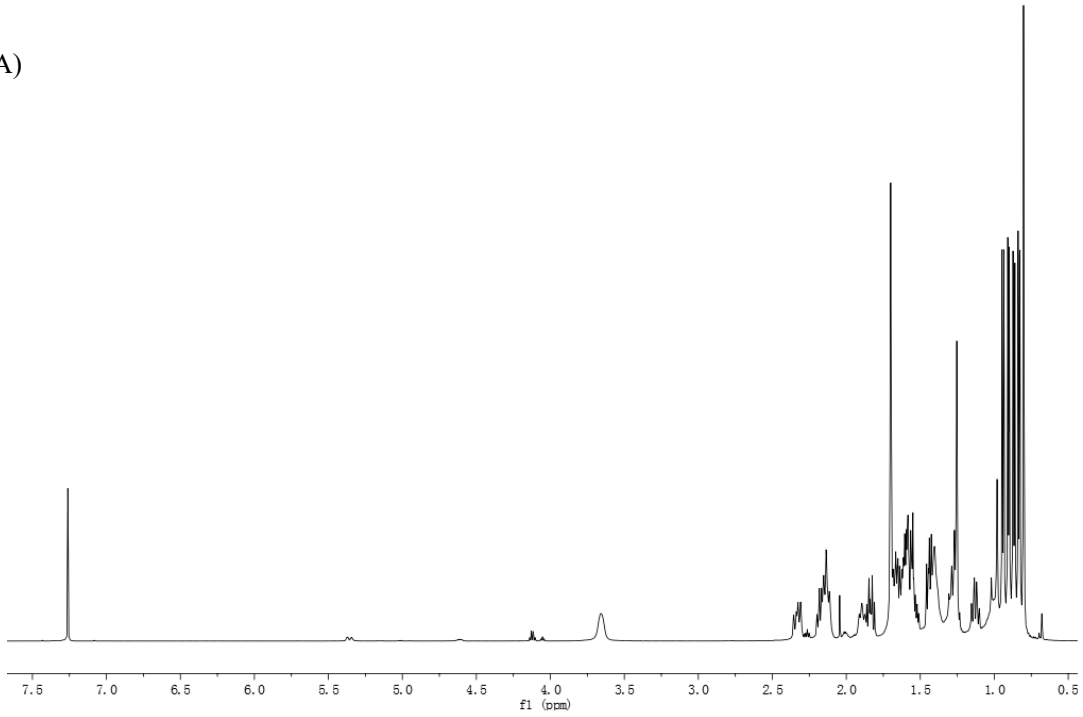

(B)

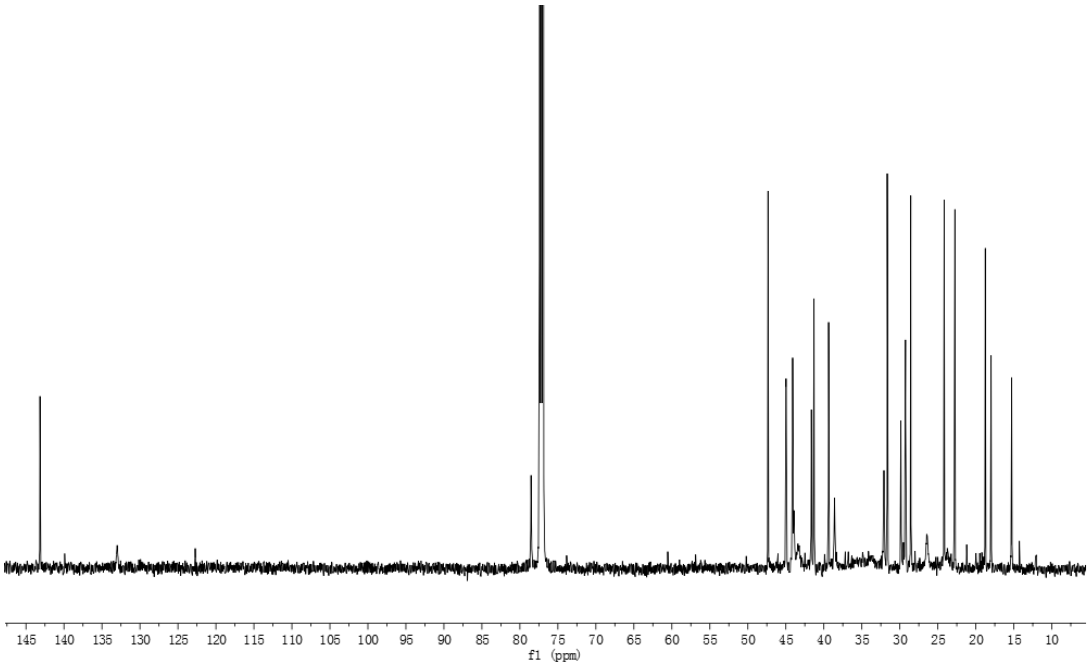

Figure 2-6. (A) ^{1}H NMR and (B) ^{13}C NMR of **1**.

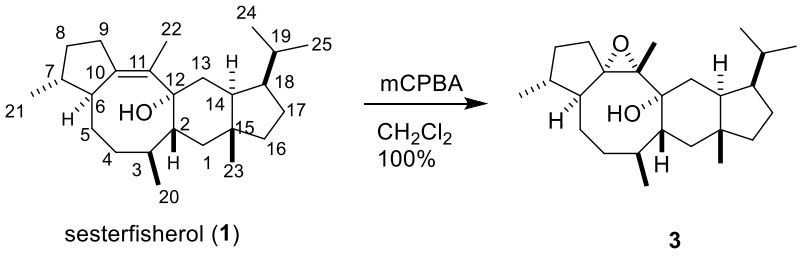

sesterfisherol (**1**) **3**

Scheme 2-8. Epoxidation reaction of **1** and the product **3**

NOESY analysis of **4** provided data for all the relative configuration of **1** and **3** except the C7 stereochemistry (Figure 2-7 A). On beta face of **3**, correlation peaks can be observed between H20-H1β, H22-H13β, H23–H2, H23–H19, H23– H13β. Later, **4** (a derivative of **1** obtained from section 2-2-4) gave a significant correlation between H21 and H6, making C7 relative configuration clarified (Figure 2-7 B).

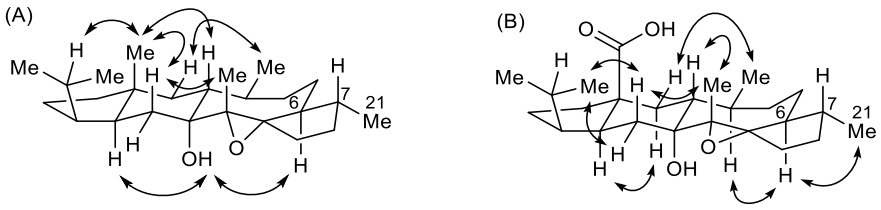

Figure 2-7. NOE correlation of A) **3** and B) **4**

The absolute configuration of **3** was determined by Prof. Monde and co-workers using the density functional theory (DFT) calculation combined with density functional theory (VCD) measurement [49]. From the DFT calculation, five confomers with lowest energy were chosen from all the possible models, and their Boltzmann-averaged VCD spectra were in good agreement with the experimental spectrum of compound **3** (Figure 2-8). The five conformers indicated that the absolute configuration of **3** was *2R, 3S, 6S, 7R, 10S, 11R, 12R, 14S, 15R* and *18R*. In this way, the structure of **1** was determined using epoxide **3** derived from **1**.

This novel compound **1** was named as sesterfisherol. Its structure was similar to nitidasin isolated from plant *Gentianella nitida*[50] except the oxidation state and the C7 stereochemistry. NFIA_55500

(*NfTS2*) encoded enzyme that produced sesterfisherol *in vivo* was later confirmed by *in vitro* experiments, and was named as *N. fischeri* sesterfisherol synthase (NfSS).

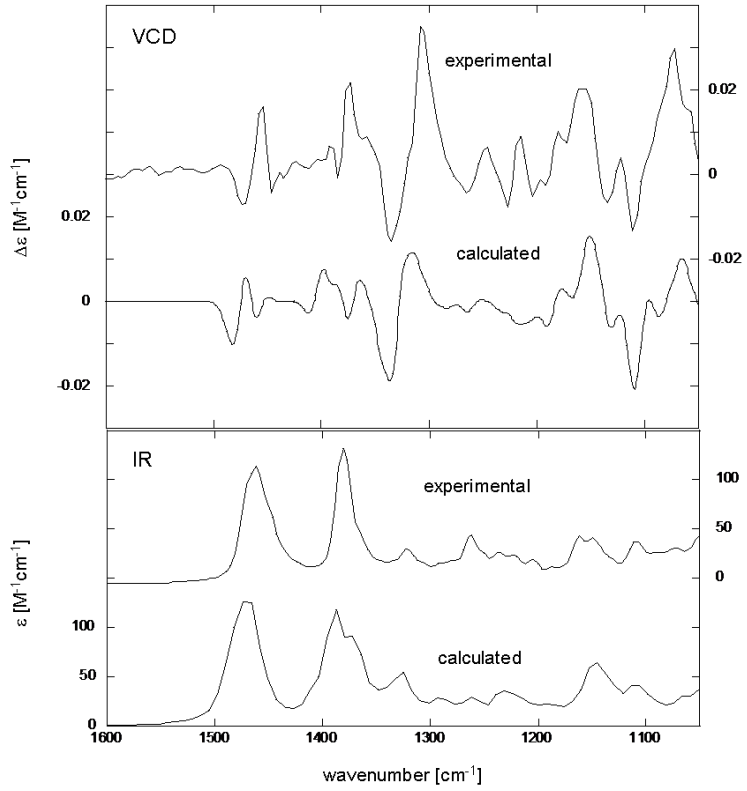

Figure 2-8. Vibrational circular dichroism and infrared spectra of **3** measured in $CDCl_3$ (c = 0.2 M, l = 100 mm) and calculated by B3LYP/TZVP with the polarized continuum model (PCM) for $CHCl_3$.

2-2-4. Identification of a biosynthetic gene cluster for sesterfisheric acid

When examining the genes close to *NfSS* on the *N. fischeri* genome, a cytochrome p450 family gene deposited as NFIA_55490 was found on the upstream of *NfSS*. Except for it, there are no other modification enzyme genes adjacent to the *NfSS* gene (Figure 2-9 A). It was hypothesized that this p450 enzyme would modify sesterfisherol to an oxidized compound. However, initial transformation of NFIA_55490 into AO-*NfSS* did not give any new product. The author rechecked the amino acid sequence of NFIA_55490 and found that this deposited sequence does not have transmembrane region predicted by TMHMM server[51]. Considering fungal p450s usually retain transmembrane region for localization to the endoplasmic reticulum membrane, the author speculated that N terminal sequence of NFIA_55490 was wrongly annotated in database. Indeed,

154 bp upstream from the NFIA_55490 old start codon, a new start codon was found (Figure 2-9 B). The new NFIA_55490 named NfP450 contains a N terminal hydrophobic transmembrane region (Figure 2-9 C) and was transformed into AO-*NfSS*. Analysis of metabolite from the AO-*NfSS/NfP450* enabled the author to find a new product **2** (Figure 2-10). From the HR-MS data ([M – H]$^-$ *m/z* 387.2919) of **2**, its molecular formula was deduced to be $C_{25}H_{40}O_3$. In the ^{13}C NMR spectrum of **2**, several C signals were missing due to signal broadening. As in the case of **1**, epoxidation of **2** allowed us to determine the structure: ^{13}C NMR showed a signal at 182.18 ppm, indicating the presence of carboxylic acid group. ^1H NMR showed disappearing of the signal belonging to H23 in **1**. These results revealed that 23-methyl group in **1** was oxidized to carboxylic acid group in **2**, which was thus named sesterfisheric acid (Figure 2-11).

(A)

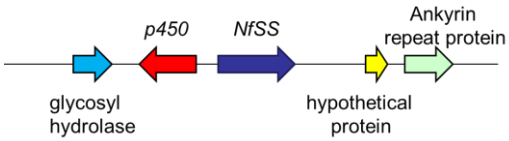

(B)

```
Nf-P450□ MDAQHLMTMSGISLEQVAIMGCSLGTGLLVSMIIYNYFFHPLARVPGPCTGAIFPFWSMS
NFIA_55490□ ------------------------------MIIYNYFFHPLARVPGPCTGAIFPFWSMS
                                           ****************************

Nf-P450□ SLYRRRLNPDLAELHKKYGQILSLLSGYGGLLMCPRNTGPIVRVGPNQLSFATVEAQKMI
NFIA_55490□ SLYRRRLNPDLAELHKKYGQILSLLSGYGGLLMCPRNTGPIVRVGPNQLSFATVEAQKMI
            ************************************************************
```

(C)

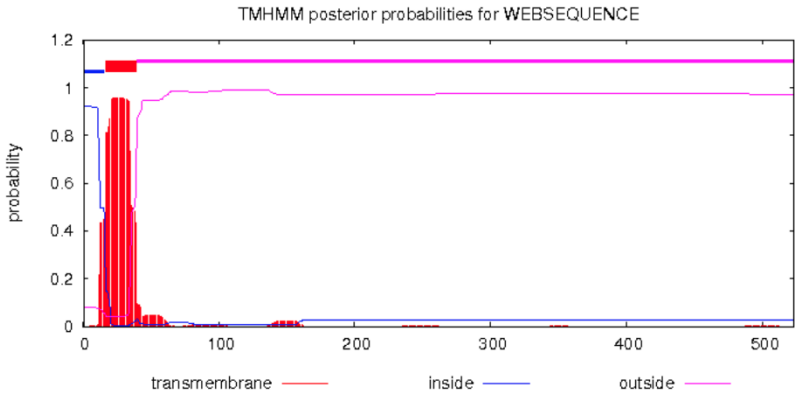

Figure 2-9. (A) *NfSS* and genes close to it on the *N. fischeri* genome. (B) N terminal amino acid sequences of NfP450 and original NFIA_55490. Amino acid sequences enclosed by red box shows additional membrane-binding region. (C) Membrane-binding region of NfP450. The prediction was examined by TMHMM Server ver.2.

(http://www.cbs.dtu.dk/services/TMHMM/).

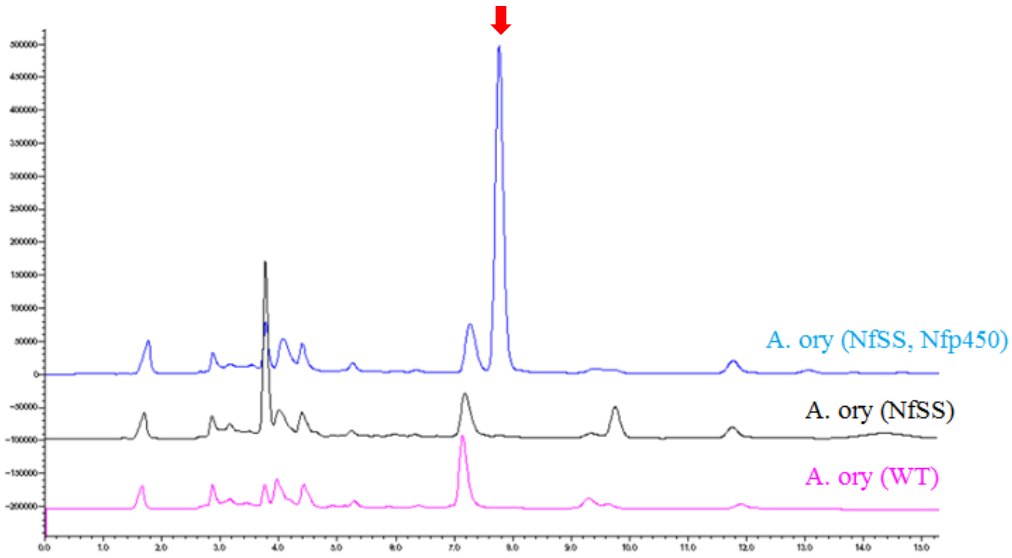

Figure 2-10. HPLC profile of metabolite analysis of AO-*NfSS/NfP450*.

Sesterfisheric acid showed activity against production of cholesteryl ester (data not shown), the accumulation of which is associated with atherosclerosis[52]. The bioactivity of sesterfisherol remains unknown. Bioactive fungal metabolites afforded by oxidative modifications of di/sesterterpenes are commonly observed (Scheme 2-10, 2-11), for example, a diterpenoid named conidiogenone from *Penicillium cyclopium* is a potent inducer of conidiogenesis[53].

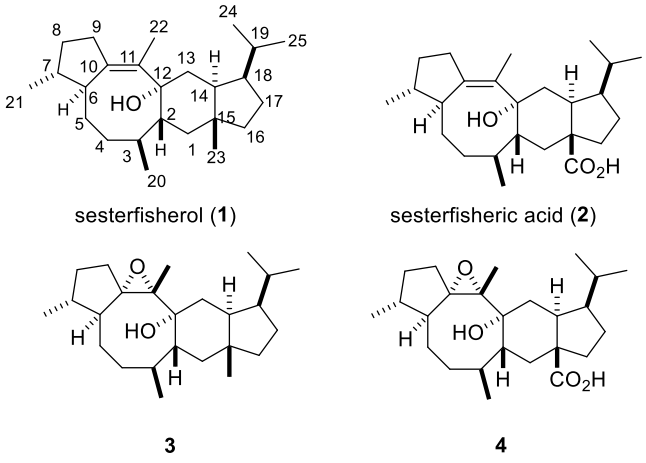

Figure 2-11. Sesterfisherol **1** and its derivatives.

2-3. Sesterfisherol synthase cyclization mechanism study

2-3-1. *In vivo* labeling experiments

The C1-C19 carbon framework of **1** is essentially the same as that in GFPP, including the positions of the branching methyl groups. This implies that cyclization of GFPP into **1** involves no backbone rearrangements but does a series of hydride shifts. As exemplified in the biosynthetic study of structurally complex steroids, labeling with [1-^{13}C,^{2}H3] acetate provided important evidence on the hydride shifts[54]. Therefore, *in vivo* isotopic labeling experiments with [1-^{13}C,^{2}H3] acetate were then conducted. The author fed [1-^{13}C,$^{2}H_3$] acetate to the sesterfisherol producing medium of AO-*NfSS* and isolated the ^{13}C and ^{2}H labeled sesterfisherol. To avoid NMR signal missing, epoxidation was again conducted to obtain labeled **3**. The ^{13}C labeling pattern was the same with that of GFPP biosynthesized through mevalonate pathway (Scheme 2-9 A, also described in section 2-1), providing clear evidence that no carbon rearrangement occurred during cyclization. Hydride shifts pattern could be analyzed by the ^{13}C NMR spectrum of labeled product: when deuterium is substituted for hydrogen at position β to the ^{13}C labeled carbons, the upfield shifts of ^{13}C signals could be observed. ^{13}C NMR spectrum (Figure 2-12, Table 2-2) shows that the C3 (number of upfield-shifted signals 3), C7 (3), C11 (3), C13 (1), C15 (3), C17 (1), and C19 (3) gave upshifted signals, while no upshifted signals were observed in C1, 5, 9, indicating the neighboring deuterium on C2, C6 and C10 was lost probably through hydride shift. An early stage 1, 5 hydride shift at C12 was also proposed, as observed in cyclization mechanism of ophiobolin F[44] (Scheme 2-9 B).

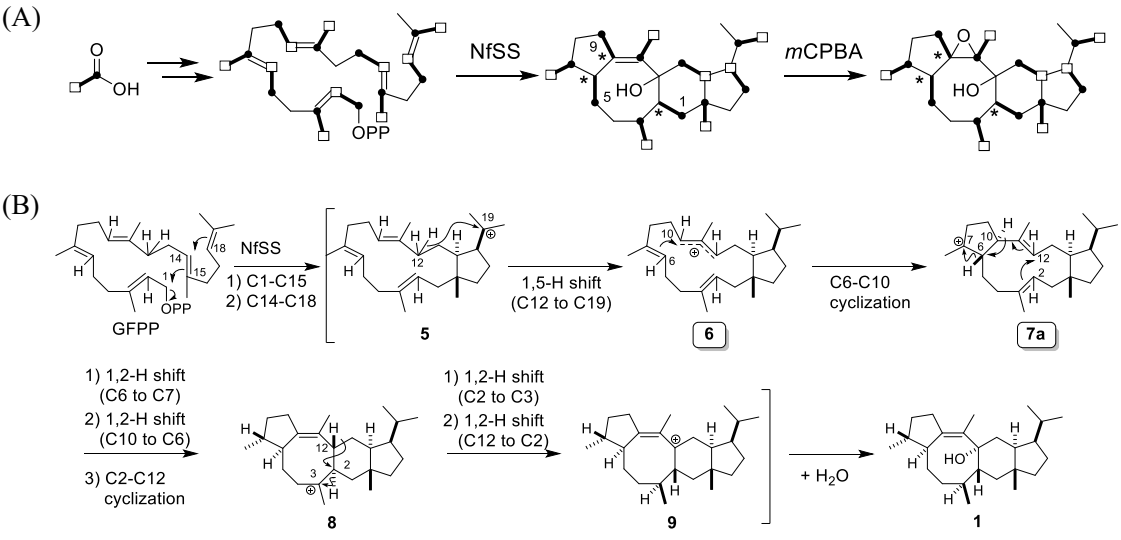

Scheme 2-9. (A) Summary of Feeding Experiments with [1-^{13}C,$^{2}H_3$] Acetate. Bold lines indicate acetate units. Black

circles and white squares show carbon-13 and deuterium atoms, respectively. Asterisks mark carbons from which deuterium labels were lost. (B) Proposed Cyclization Mechanism Catalyzed by NfSS

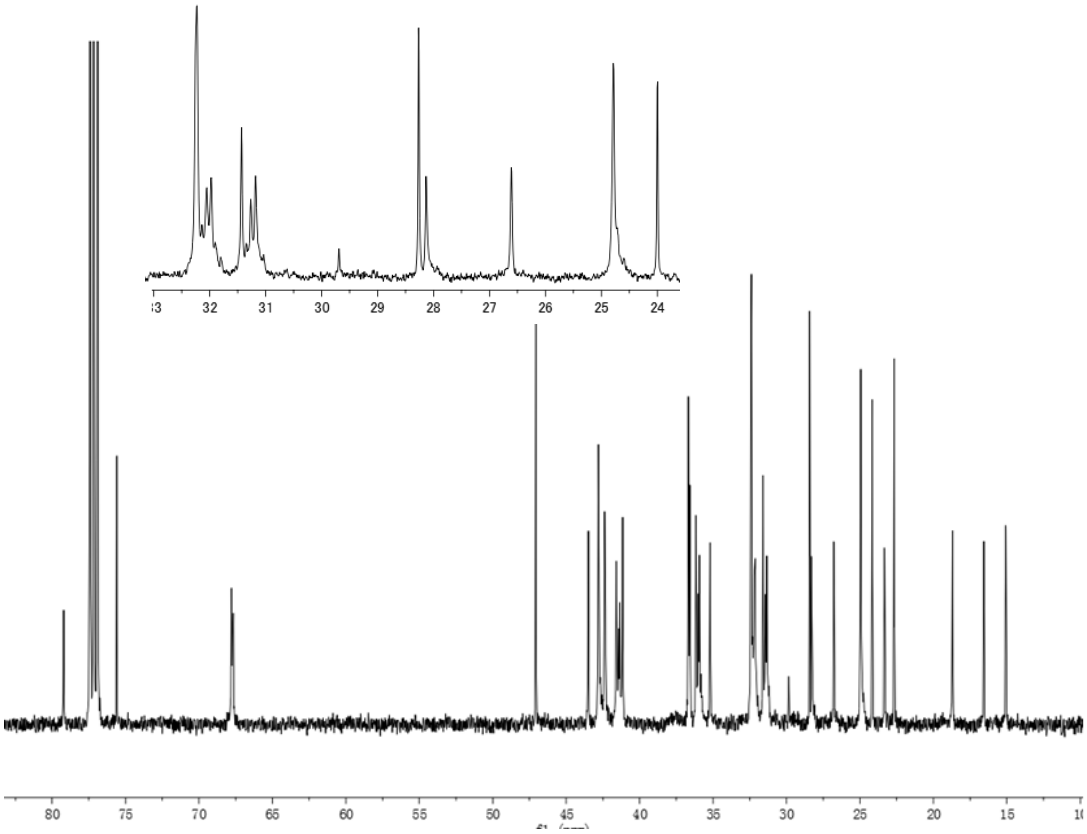

Figure 2-12. ^{13}C NMR of ^{13}C and ^{2}H labeled **3**

Table 2-2. 13C-NMR data of **3** prepared from labeled-**1**.

Carbon atom	δ_C	Enrichment	Isotope shift (ppm)
1	42.83	★	0
2	42.41		
3	32.4	★	0.093, 0.176,0.255
4	35.22		
5	24.96	★	0
6	42.35		
7	36.17	★	0.081, 0.160, 0.240
8	26.79		
9	32.45	★	0
10	79.22		
11	67.8	★	0.052, 0.090, 0.134
12	75.61		
13	36.69	★	0.099

14	43.51		
15	41.61	★	0.076, 0.158, 0.241
16	41.17		
17	28.43	★	0.134
18	47.09		
19	31.6	★	0.087, 0.165, 0.250
20	23.33		
21	15.07		
22	16.51		
23	18.71		
24	22.66		
25	24.16		

2-3-2. *In vitro* labelling experiments

To study the hydride shift on C12, we tried to conduct the *in vitro* reaction using recombinant NfSS expressed in *E. coli.* Initial trial of expressing His tagged NfSS was failed. However, fusion protein with maltose binding protein was obtained as soluble one as shown in figure 2-13.

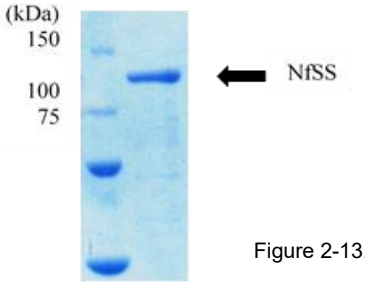

Figure 2-13. SDS-PAGE analysis of recombinant NfSS

Generally, bifunctional terpene synthases such as PaFS[43] and AcOS[44] utilize various allyl diphosphates (DMAPP, GPP, FPP and GGPP) as starter unit. Similarly, co-incubation of NfSS, GGPP and IPP gave a single peak corresponding to **1**, proving that NfSS synthesizes **1** through intermediate GFPP. Thus, NfSS catalyzed reaction with [8, 8-$^{2}H_{2}$] GGPP and IPP to afford the labeled **1**. Its epoxidized product (labeled **3**) was subjected to ^{1}H NMR and TOCSY analysis (Figure 2-14). In the ^{1}H NMR spectrum, doublet signals of 24, 25 methyl hydrogens of unlabeled **3** became two singlets in labeled **3**, indicating one deuterium was located at C19 after expected 1, 5 hydride shift from C12. TOCSY spectrum also supported this conclusion. The correlation peaks between H25 and H24 disappeared in labeled **3**. In the same way, the presence of the second deuterium was determined at C2 since the TOCSY correlation between H1-a and H3 disappeared in labeled **3**,

indicating deuterium was shifted from C2 to C12.

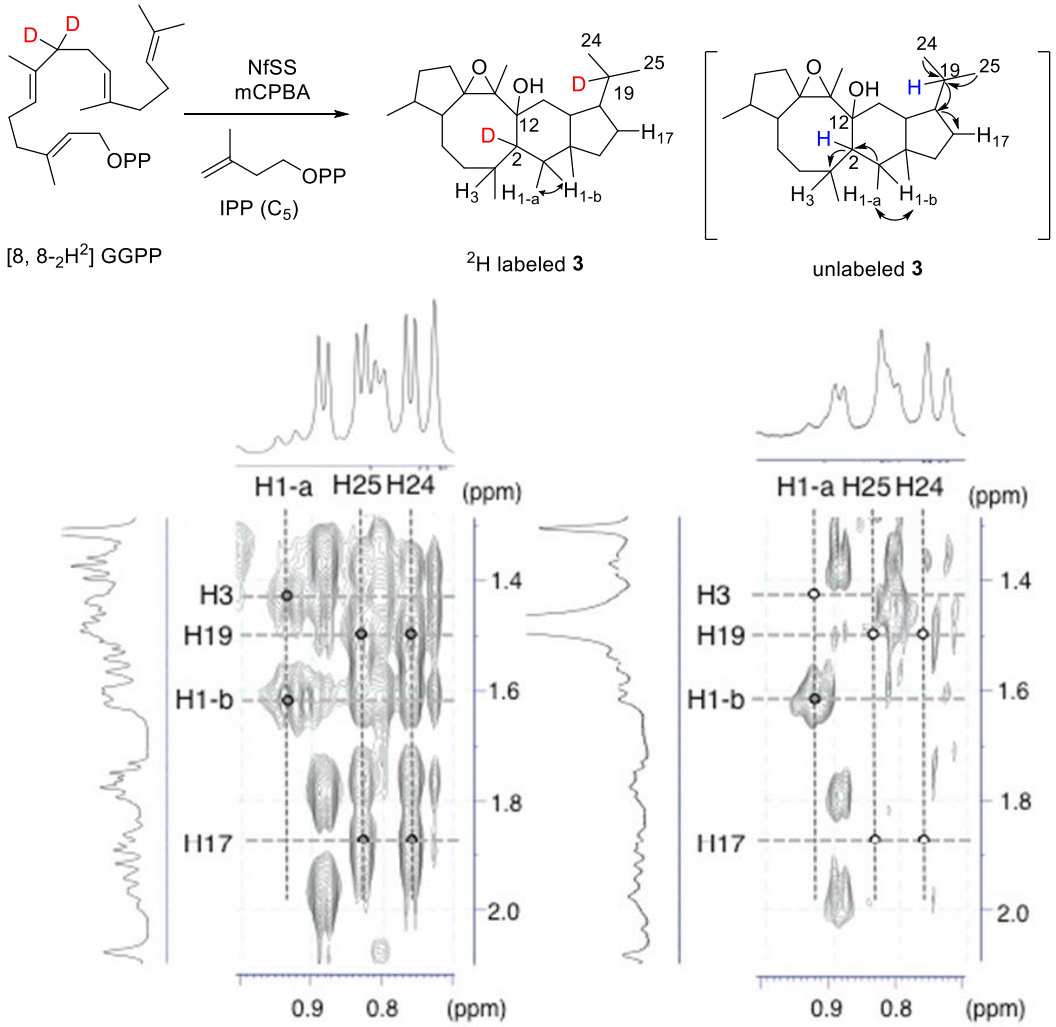

Figure 2-14. TOCSY spectra of (A, left) unlabeled and (B, right) deuterium-labeled **3**.

Combining results mentioned above, the cyclization mechanism is proposed as shown in Scheme 2-9. Reaction was initiated by the elimination of diphosphate group. Two successive cyclizations between C1-C15 and C14-C18 gave a bicyclic cation **5**. Next a 1, 5 hydride shift from C12 to C19 followed by another cyclization between C6-C10 formed the tricyclic cation **7a**. The resultant **7a** underwent two 1, 2 hydride shifts (C6 to C7, C10 to C6) and the forth cyclization between C2 and C12 to form tetracyclic cation **8**. A subsequent fourth and fifth hydride shifts (C2 to C3, C12 to C2) gave the cation **9**, which was quenched by water to afford the final product **1.** Altogether, NfSS catalyzed five hydride shifts, including the shifts of two hydrides from the same carbon at C12.

2-4 Unified biogenesis of sesterterpenes

Previous studies on cyclization mechanism of fusicoccin A[43] and ophiobolin A[44] revealed that their

cyclization formed a common bicyclic cation intermediate (Scheme 2-10 B): dolabelladien-15-yl (C20) or its C25 counterpart. This intermediate was formed by C1 cation-olefin III-olefin IV cyclization of GGPP or GFPP. The author classified this kind of initial cyclization as type B cyclization. Diterpenoids such as methyl phomopsenonate[46], fusicocccin A; sesterterpenoids such as mangicol A[55] and ophiobolin A are all formed by type B cyclization and are classified into group B di/sesterterpenoids. Alternatively, in this study, cyclization by C1-olefin IV-olefin V to afford fusaproliferan-19-yl cation can be proposed (Scheme 2-10 A). The author named this pattern of cyclization as type A cyclization. Similar cyclization might be involved in the biosynthesis of fusaproliferin[56] (bicyclic), variculanol[57] (tricyclic), sesterfisherol (tetracyclic), astellatol[58] (tetracyclic) and retigeranic acid[59] (pentacyclic) and several others, (alborosin[60], nitidasin[50], nitiol[61], YW3548[62], and YW3699[63]).

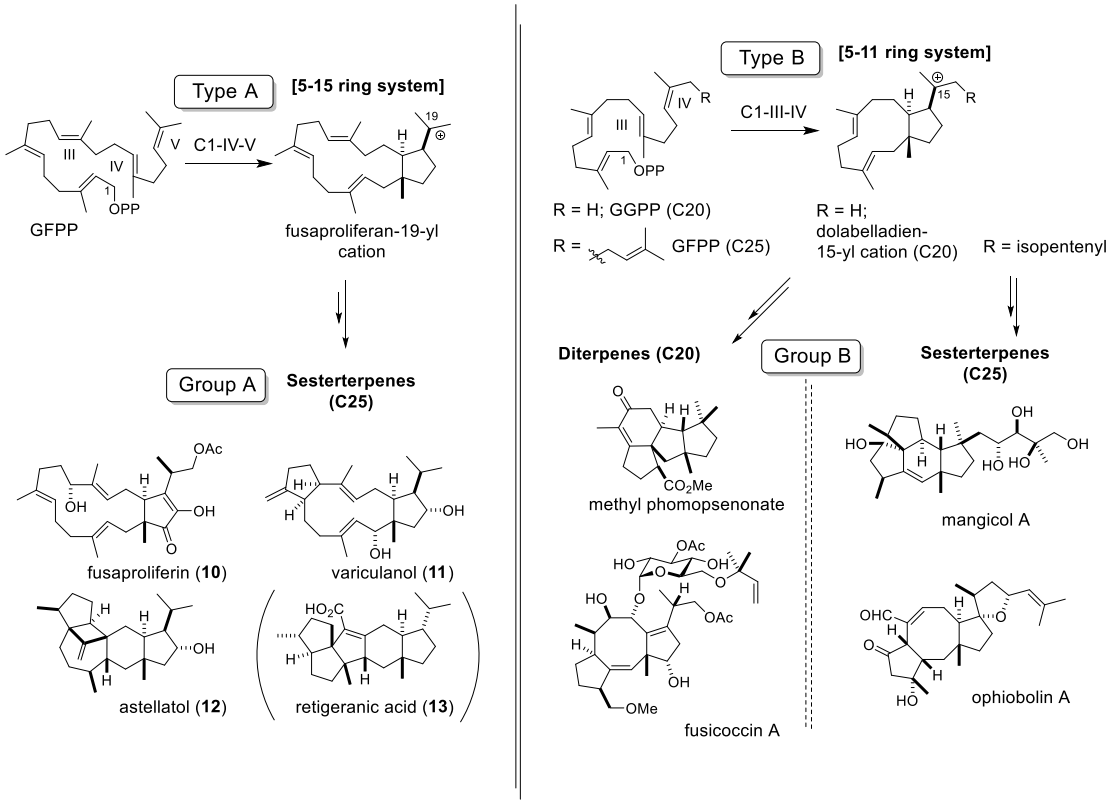

Scheme 2-10. Classification of Di/Sesterterpenes Based on Initial Cyclization: (A) Type A cyclization and Group A sesterterpenoids (B) Type B cyclization and Group B di/sesterterpenoids

Based on the mechanism, a unified biosynthesis of group A sesterterpenes was proposed (Scheme 2-11). Starting from GFPP, type A cyclization followed by 1, 5 hydride shift from C12 to C19 gives common cation intermediate **6.** If quenched by water, the fusaproliferin like bicyclic sesterterpenoid

is formed. In another route, **6** was further cyclized between C6 and C10 to form **7b** (the enantiomer of **7a)**, which is the precursor of variculanol and tetracyclic astellatol. The cation **7c**, similar to **7a/b**, would be a precursor to tetracyclic aleurodiscal and pantacyclic regigeranic acid. NfSS catalyzed reactions gave two key intermediates **6** and **7a** (Scheme 2-9) and formed the tetracyclic structure, thus serves as a model enzyme for studying the biosynthesis of group A sesterterpenes.

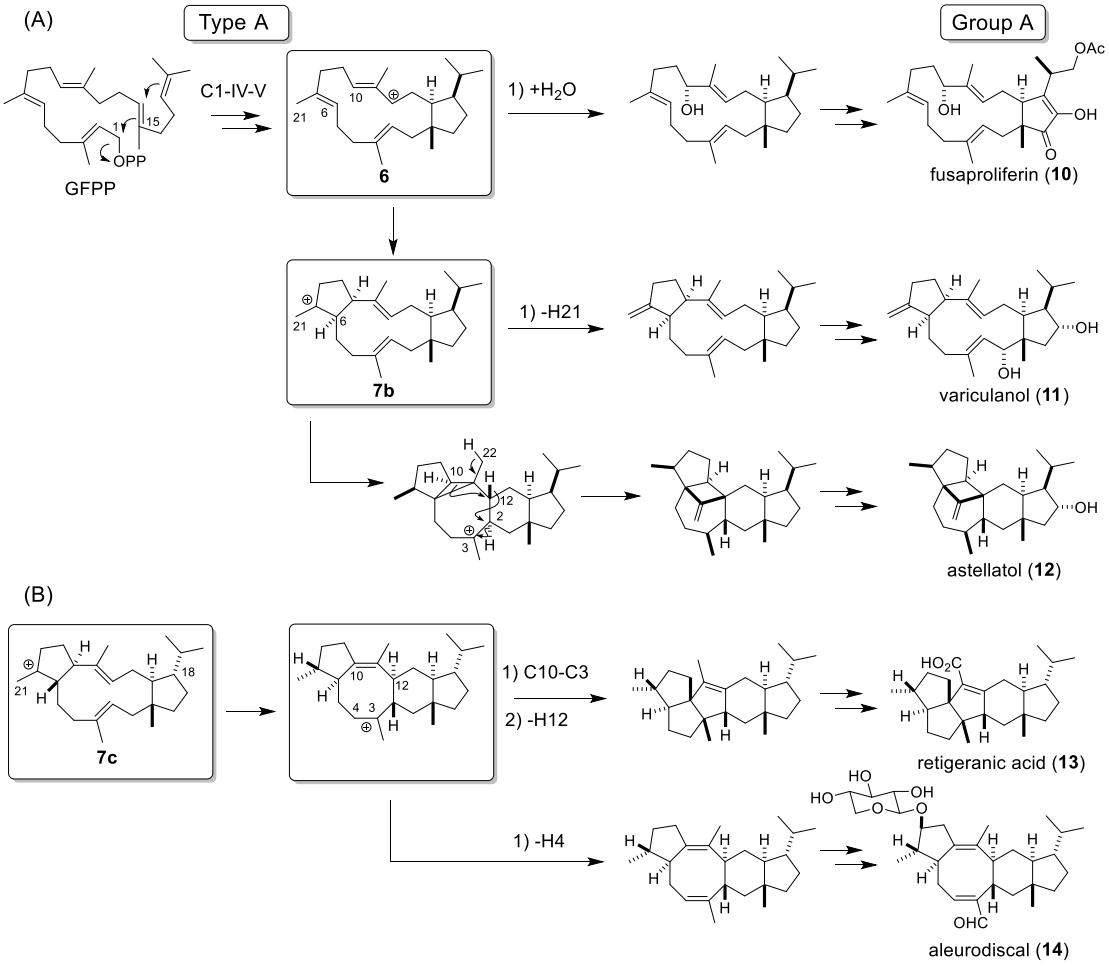

Scheme 2-11. Proposed Cyclization of Group I Sesterterpenes: (A) Cyclization Mechanism of **10**–**12** via Bicyclic Cation **6** and (B) Cyclization Mechanism of **13** and **14** via **7c**.

One interesting thing to notice is that the type of cyclization catalyzed by the di/sesterterpene synthases seems reflect the clade of those enzymes in the phylogenetic tree analysis. NfSS belongs to the clade A, and it catalyzed type A cyclization. On the other hand, PaFS, AbFs, PaPS and AcOS belong to the clade B, and they catalyzed type B cyclization. At this stage, it is reasonable to make a hypothesis that the phylogenetic classification of di/sesterterpene synthases could reflect the initial cyclization modes (C1–IV–V vs C1–III–IV). The connection between amino acid sequence and the

cyclization pattern might be explained by the amino acid residues in the cyclase active site that may guide the linear GFPP into different conformations. Recently the author's group conducted clade A specific genome mining using four sesterterpene synthases (manuscript in preparation). The results strongly supported this hypothesis. The biosynthetic proposal based on the author's study would play an important role in the future di\sesterterpene genome mining work guided by phylogenetic analysis.

Conclusion

In the study described in chapter 2, the author employed genome mining of novel sesterterpenes.

Achievements:

1) Based on the classification (clade A-E) by the phylogenetic analysis of putative bifunctional terpene synthases on the public database, the author chose four of them in different clades. Through heterologous expression of these genes in *A. oryzae*, the author found that one of them, named NfSS, generated a novel metabolite sesterfisherol, and the subsequent expression of modification gene *NfP450* yielded sesterfisheric acid.

2) To elucidate cyclization mechanism of tetracyclic sesterterpene core scaffold of sesterfisherol, the author performed a series of *in vivo* and *in vitro* transformations with labeled precursors, leading to a proposed mechanism of three step-cyclization via bicyclic, tricyclic and tetracyclic carbocation intermediates accompanied with five hydride shifts.

3) Based on cyclization mechanisms of NfSS (clade A) and PaFS/AcOS (clade B), the author classified known fungal di/sesterterterpenoids into two groups: A, metabolites including fusaproliferin, variculanol, astellatol and retigeranic acid; B, metabolites including methyl phomopsenonate, fusicoccin A, mangicol A, ophiobolin A. This classification (clade A and B) was closed related to the individual cyclization modes: A (C1-olefin IV-olefin V); B (C1-olefin III-olefin IV).

Although these results are promising, many unsolved questions and challenges are remained.

1. Among four candidate terpene synthases, only NfSS was obtained as a functional enzyme to produce sesterfisherol. The plausible reasons explaining why other three failed could be proposed as following. First, the premature-mRNAs of the other terpene synthases genes might not be correctly processed into mature mRNAs. Second, mutations of important residues that make terpene

synthases inactive might happen during the molecular evolution of these enzymes.

2. As proposed by this thesis, the phylogenetic analysis reflects the cyclization pattern of di/sesterterpene synthases. However, how the amino acid sequences of the enzymes control the cyclization mode remained a mystery. It's likely some key amino acid residues orient GGPP or GFPP into specific confirmations and determine the cyclization type. Further characterization of terpene synthases located at different clades are needed to get more information on the substrate binding in the active site. At the same time, mutation experiments and enzyme crystallization studies will provide deeper insight into this interesting issue.

Experimental

General: All reagents commercially supplied were used as received. Optical rotations were recorded on JASCO P-2200 digital polarimeter. Column chromatography was carried out on 60N silica gel (Kanto Chemicals), and PTLC was performed on PLC 60 F254 silica gel. ^{1}H- and ^{13}C-NMR spectra were recorded on Bruker AMX-500 spectrometer or JEOL-ECA600. NMR spectra were recorded in $CDCl_3$ (99.8 atom % enriched, Kanto). Mass spectra were obtained with a JEOL JMS-T100GCV (EI mode) or a JEOL JMS-T100LP (ESI mode). ^{1}H NMR chemical shifts were reported in δ value based on internal $CDCl_3$ (7.26 ppm) as a reference. ^{13}C chemical shifts were reported in δ value based on chloroform (77.1 ppm) as a reference. Data are reported as follows: chemical shift, multiplicity (s = singlet, d = doublet, t = triplet, q = quartet, m = multiplet, br = broad), coupling constant (Hz), and integration. GC-MS analyses were conducted with MS-2010 (Shimadzu), using a DB-1MS capillary column (0.32 mm x 30 m, 0.25 μm film thickness; J&W Scientific). The sample was injected into the column at 100°C in the splitless mode. After a 3-min isothermal hold at 100°C, the column temperature was increased at 14°C min^{-1} to 268°C, with a 4-min isothermal hold at 268°C. The flow rate of helium carrier gas was 0.66 mL min^{-1}. Oligonucleotides for polymerase chain reaction (PCR) were purchased from Hokkaido System Science Co., Ltd. Cell disruption was dealt with an ultrasonic disrupter UR-200P (TOMY SEIKO, Tokyo, Japan). Analysis of the samples during protein purification was performed using SDS-polyacrylamide gel electrophoresis, and the proteins were visualized by using coomassie brilliant blue staining. Protein concentration was determined by the bradford method with bovine serum albumin as a standard.

Strain and Culture Conditions

E. coli HST08 and *E. coli* DH5α were used for cloning, following standard recombinant DNA techniques. *E. coli* BL21-Gold(DE3) was used for protein expression. A fungal host strain used in this study was *A. oryzae* NSAR1, a quadruple auxotrophic mutant (*niaD*$^{-}$, *sC*$^{-}$, Δ*argB, adeA*$^{-}$) for fungal expression.

Genomic DNA preparation

Genomic DNA of *Neosartorya fischeri* JMC1740 was extracted according to the following method; the mycelia of fungus was collected by filtration, washed with water, and dried using paper towel. The dried mycelia were frozen in liquid nitrogen and crushed by SK-mill (Tokken). To the frozen powder was added extraction buffer (400 mM of Tris-HCl (pH 8.0), 500 mM of NaCl, 20 mM of ethylenediaminetetraacetic acid (EDTA) and 1% of sodium dodecyl sulfate) and the suspension was kept at room temperature for 5 min. To the suspension was added phenol:chloroform solution and the mixture was vortexed for 2 sec. After incubation at 65°C for 60 min, the reaction mixture was centrifuged at 12000 rpm for 5 min. The supernatant was then treated with RNase at 37°C for 90 min. To the reaction mixture was then added phenol:chloroform solution. After being vortexed for 2 sec, the mixture was centrifuged at 12000 rpm for 5 min. The supernatant was transferred to a new centrifuge tube and re-extracted twice with phenol:chloroform solution followed by chloroform. To the final supernatant was added cold-isopropanol and CH_3COONa solution and genomic DNA was recovered by centrifugation at 12000 rpm for 10 min. The pellet was then washed with 70% ethanol solution and dried for 15 min. Finally, the isolated DNA was resuspended in TE buffer (10 mM of Tris-HCl (pH 8.0) and 1mM of EDTA) and stored at -20°C for further use.

Preparation of Expression Plasmids

The NFIA_041470, Nf-P450, NfSS, NFIA_062390, and AOR_1_1216074 were amplified from genomic DNA with a primer set as shown in Table 2-3. Polymerase chain reactions (PCRs) were performed with the KOD-Plus-Neo (TOYOBO). Each PCR product was inserted into the appropriate restriction site (site 1 and/or site 2) of pUARA2 or pUSA2 using the In-Fusion Advantage PCR cloning kit (Clontech Laboratories) to construct expression plasmids.

Table 2-3. Oligonucleotides used for construction of *A. oryzae* expression plasmids.

Insert	Restriction site	Sequence 5'-3'	Size Vector
NFIA_41470	*Kpn*I	F: CGGAATTCGAGCTCGATGGAGCGACAGCAAGATC	2.6 kb
		R: ACTACAGATCCCCGGTCAGACCTTCAATCTTTGCA	pUARA2
NfSS	*Nhe*I	F: ATCGATTTGAGCTAGATGGAGGTCTGGGAGCAT	2.5 kb
		R: TAGTGCGGCCGCTAGTTAATTCTCCTTCACACTCAG	pUARA2
NFIA_62390	*Nhe*I	F: ATCGATTTGAGCTAGATGGAAGGACAGAGGCGC	2.4 kb
		R: TAGTGCGGCCGCTAGTCAATTCATCGACCTCCAAG	pUARA2
AOR_1_1216074	*Kpn*I	F: CGGAATTCGAGCTCGATGGAACAGACAATCTCGAA	2.6 kb
		R: ACTACAGATCCCCGGTTAAACTCGCAGTCGTGTC	pUARA2
NFIA_55490	*Nhe*I	F: ATCGATTTGAGCTAGATGATCATCTATAACTACTTTTT	1.8 kb
		R: TAGTGCGGCCGCTAGCTAAGTCAGGCGCTCTTG	pUSA2
NfP450	*Nhe*I	F: ATCGATTTGAGCTAGATGGACGCACAGCACCTC	2.0 kb
		R: TAGTGCGGCCGCTAGCTAAGTCAGGCGCTCTTG	pUSA2

Transformation of *Aspergillus oryzae*.

A spore suspension of *A. oryzae* NSAR1 or transformant (1.0 x 10^8 cells) were inoculated into DPY (dextrin-polypeptone-yeast extract: 2% dextrin, 1% polypeptone, 0.5% yeast extract, 100 mL) medium supplemented with appropriate nutrients. After 3 days' incubation at 30°C, mycelia was collected by filtration and washed with water. Protoplasting was performed using Yatalase (Takara; 5.0 mg mL^{-1}) in Solution 1 (0.8 mM of NaCl, 10 mM of NaH_2PO_4, pH 6.0) at 30°C for 2 h. Protoplasts were centrifuged at 2,000 rpm (Beckman JLA10.500) for 5 min and washed with 0.8 M of NaCl solution. Then, protoplasts were adjusted to 2.0 x 10^8 cells/mL by adding Solution 2 (0.8 M of NaCl, 10 mM of $CaCl_2$, 10 mM of Tris-HCl, pH 8.0) and Solution 3 (40% (w/v) of PEG4000, 50 mM of $CaCl_2$, 50 mM of Tris-HCl, pH 8.0) in 4/1 volume ratio. To the protoplast solution (200 μL) was added appropriate plasmid (13 μg). The aliquot was incubated on ice for 20 min and then Solution 3 (1 mL) added to the aliquot. After 20 min incubation at room temperature, Solution 2 (10 mL) added to the mixtures and the mixture was centrifuged at 2,000 rpm (Beckman JLA10.500) for 5 min. The transformation mixture was poured onto the Czapek-Dox (3.5%) agar plate supplemented with 0.8 M of NaCl and appropriate nutrients and then overlaid with the soft-top agar

(1.2 M of sorbitol, 3.5% of Czapek-Dox, 0.6% of agar). The plates were incubated at 30°C for 3-7 days.

To construct transformants harboring terpene synthase genes, three plasmids, pUARA2-*NfTS1*/*NfTS3*, pUARA2-*NfTS2*/*AoTS1*, and pUARA2-*AoTS1*, were used for the transformation. The transformant with *NfSS* was further transformed with pUSA2-*NfP450* to construct *AO*-NfSS/NfP450.

Extraction of Metabolites

Mycelia of *A. oryzae* transformants were inoculated into a solid medium containing polished rice (100 g) and adenine (10 mg) in 500 mL Erlenmeyer flasks. Each culture was incubated at 30 °C for 2 weeks. After extraction with ethyl acetate, the extract was then concentrated in vacuo and the residues were extracted with ethyl acetate (100 mL × 2). The combined organic layers were washed with brine, dried over Na_2SO_4, and concentrated in vacuo to afford crude extracts.

Analysis of the Metabolites

After partial purification of the crude extracts, the metabolites were analyzed by GC–MS with a DB-1 MS capillary column (0.32 mm × 30 m, 0.25 mm film thickness; J&W Scientific) or LC–MS with a ZORBAX XDB-C18 column (50 mm × 2.1 mm) at the following conditions.

GC conditions to analyze sesterfisherol (**1**): Each sample was injected into the column at 100 °C in the splitless mode. After a 3min isothermal hold at 100 °C, the column temperature was increased at 14°C min^{-1} to 268 °C, with a 4min isothermal hold at 268°C. The flow rate of helium carrier gas was 0.66 mL min^{-1}.

LC conditions to analyze sesterfisheric acid (**2**): 95% acetonitrile for 15 min at a flow rate of 0.2 mL/min with 210 nm detection.

Sesterfisherol (1)

Isolation yield: 52.5 mg from 1 kg of rice medium. $[\alpha]_D^{24}$ −48.3 (*c* 1.5, $CHCl_3$). HR-EIMS analysis (positive): *m*/*z* calcd for $C_{25}H_{42}O$ $[M]^+$ 358.3230, found 358.3243. ^1H NMR and ^{13}C NMR data are summarized in Table 2-4.

Table 2-4. NMR spectral data of sesterfisherol (**1**) and 9,10-epoxysesterfisherol (**3**)

	sesterfisherol (**1**)		9,10-epoxysesterfisherol (**3**)	
	δ_C	δ_H (multiplicity, *J* in Hz)	δ_C	δ_H (multiplicity, *J* in Hz)
1	*	*	42.83	1.68 (m)
		*		0.99 (m)
2	44.97	1.40 (m)	42.41	1.49 (m)
3	*	*	32.4	1.5 (m)
4	*	*	35.22	1.30 (m)
		*		1.28 (m)
5	26.42	1.41 (m)	24.96	1.41 (m)
		1.00 (m)		1.1 (m)
6	43.93	3.66 (bs)	42.35	2.48 (m)
7	38.59	2.12 (m)	36.17	2.37 (m)
8	29.25	1.68 (m)	26.79	1.85 (m)
		1.27 (m)		1.25 (m)
9	32.09	2.33 (m)	32.45	2.05 (m)
		2.16 (m)		1.45 (m)
10	143.15	-	79.22	-
11	133	-	67.8	-
12	78.53	-	75.61	-
13	39.37	2.13 (m)	36.69	1.98 (m)
		1.57 (m)		1.62 (m)
14	44.1	1.89 (m)	43.51	1.94 (m)
15	41.64	-	41.61	-
16	41.29	1.44 (m)	41.17	1.44 (m)
		1.13 (m)		1.14 (m)
17	28.56	1.83 (m)	28.43	1.82 (m)
		1.54 (m)		1.53 (m)
18	47.34	1.65 (m)	47.09	1.67 (m)
19	31.66	1.58 (m)	31.6	1.57 (m)
20	*	0.87 (Me, d, 7.2)	23.33	0.87 (Me, d, 6.6)
21	15.28	0.94 (Me, d, 6.6)	15.07	0.95 (Me, d, 7.2)
22	17.99	1.70 (Me, s)	16.51	1.38 (Me, s)
23	18.75	0.80 (Me, s)	18.71	0.79 (Me, s)
24	22.75	0.83 (Me, d, 6.0)	22.66	0.83 (Me, d, 6.0)
25	24.17	0.90 (Me, d, 6.0)	24.16	0.9 (Me, d, 6.6)

.

Sesterfisheric Acid (2)

Isolation yield: 20.0 mg from 1 kg of rice medium. $[\alpha]_D^{25}$ −11.1 (*c* 0.3, C_6H_6). HR-ESIMS analysis

(negative): *m/z* calcd for $C_{25}H_{39}O_3$ $[M–H]^-$ 387.2905, found 387.2919. ^1H NMR and ^{13}C NMR data are summarized in Table 2-5.

Epoxidation of Sesterterpene

To a solution of **1** (5.0 mg, 14.0 mmol) in CH_2Cl_2 (1.0 mL) was added *m*CPBA (4.9 mg, 28.4 mmol for **1** or 4.0 mg, 23.2 mmol for **2**) at 0 °C, and the mixture was stirred for 10 min. After addition of a satd Na_2SO_3 solution, the reaction mixture was extracted with EtOAc. The combined organic extracts were washed with satd $NaHCO_3$, dried over anhydrous Na_2SO_4, and concentrated in vacuo. The 10,11-epoxysesterfisherol (**3**) (4.8 mg from **1**) was directly used for NMR analysis. The same procedure was applied for the epoxidation of **2** (2.4 mg, 6.2 mmol) to afford 10,11-epoxysesterfisheric acid (**4**) (2.6 mg from **2**).

10,11-Epoxysesterfisherol (3)

$[\alpha]_D^{24}$ 1.3 (*c* 0.4, $CHCl_3$). HR-ESIMS analysis (positive): *m/z* calcd for $C_{25}H_{43}O_2$ $[M + H]^+$ 375.3258, found 375.3302. ^1H NMR and ^{13}C NMR data are summarized in Table 2-4.

10,11-Epoxysesterfisheric Acid (4)

$[\alpha]_D^{26}$ 0.2 (*c* 0.4, $CHCl_3$). HR-ESIMS analysis (negative): *m/z* calcd for $C_{25}H_{39}O_4$ $[M – H]^-$ 403.2854, found 403.2902. ^1H NMR and ^{13}C NMR data are summarized in Table 2-5.

Table 2-5. NMR spectral data of sesterfisheric acid (**2**) and epoxidized sesterfisheric acid (**4**)

	Sesterfisheric acid (**2**)		9,10-epoxysesterfisheric acid (**4**)	
	δ_C	δ_H (multiplicity, J in Hz)	δ_C	δ_H (multiplicity, J in Hz)
1	*	*	38.27	2.27 (m)
				1.16 (m)
2	46.33	1.41 (m)	43.52	1.51 (m)
3	*	*	32.4	1.51 (m)
4			35.01	1.28 (m)
				1.28 (m)
5	26.20	1.4 (m)	24.94	1.4 (m)
		1.03 (m)		1.09 (m)
6	44.12	3.59 (bs)	42.27	2.45 (m)
7	38.75	2.12 (m)	36.17	2.37 (m)
8	29.23	1.68 (m)	26.73	1.85 (m)

		1.29 (m)		1.24 (m)
9	32.18	2.32 (m)	32.4	2.01 (m)
		2.16 (m)		1.42 (m)
10	143.20	-	79.26	-
11	133.0	-	67.81	-
12	78.33	-	75.34	-
13	39.74	2.92 (t, 13.5)	36.85	2.78 (t, 13.5)
		1.56 m		1.62 (m)
14	44.60	2.21	44.49	2. 17 (m)
15	53.77	-	53.3	-
16	37.92	2.19 (m)	37.83	2.2 (m)
		1.27 (m)		1.24 (m)
17	29.98	1.92 (m)	29.57	1.9 (m)
		1.44 (m)		1.44 (m)
18	47.08	1.7 (m)	46.82	1.7 (m)
19	30.99	1.77 m	30.81	1.68 (m)
20	*	0.88 (Me, d, 7.5)	23.27	0.89 (Me, bd)
21	15.32	0.95 (Me, d, 6.0)	15.06	0.95 (Me, d, 6.5)
22	17.96	1.67 (Me, s)	16.4	1.35 (Me, s)
23	182.18	-	182.77	-
24	22.66	0.78 ((Me, d, 6.5)	22.47	0.78 (Me, d, 6.0)
25	23.81	0.93 (Me, d, 5.5)	23.79	0.92 (Me, d, 5.5)

Spectral Measurements

This experiment was conducted by our collaborator Doc. Attila Mandi. IR and VCD spectra were measured on a BioTools Chiral*ir*-2X at a resolution of ca. 8 cm^{-1}under ambient temperature for 32 and 13504 scans, respectively. The sample was dissolved in $CDCl_3$ at a concentration of 0.2 M, and the solution was placed in a 100 mm CaF_2 cell. All spectral data were corrected by a solvent spectrum obtained under identical experimental conditions.

Computational details.

This experiment was conducted by our collaborator Doc. Attila Mandi. Conformational search was carried out by means of the Conflex software at MMFF94S level.1 Geometry reoptimizations, VCD and OR calculations were performed with the Gaussian 09 package.2 X-ray geometry was optimized at B3LYP/TZVP level in vacuo and OR calculations were performed with various functionals (B3LYP, BH&HLYP, PBE0) and TZVP basis set in vacuo. For the solution conformers geometry

reoptimizations and VCD calculations were carried out at B3LYP/TZVP level with PCM solvent model for $CHCl_3$ while for OR calculations B3LYP, BH&HLYP and PBE0 functionals and TZVP basis set with PCM solvent model for $CHCl_3$ was applied. VCD spectra were generated as the sum of Gaussians with 10 cm^{-1} half-height width. Computed VCD - S3 - and IR data were scaled by a factor of 0.975. Boltzmann distributions were estimated from the B3LYP/TZVP energies of the low-energy conformers. The MOLEKEL3 software package was used for visualization of the results.

Feeding Experiments with Isotopically Labeled Acetate

Mycelia of the *A. oryzae* transformant were inoculated into MPY medium (maltose–polypeptone–yeast extract; 3% maltose, 1% polypeptone, 0.5% yeast extract; final volume 100 mL) containing 8 mg of [1-^{13}C,$^{2}H_3$] acetate in 500 mL Erlenmeyer flasks (two flasks) for 4 days at 200 rpm. After extraction with acetone, the extract was then concentrated in vacuo and the residues were extracted with ethyl acetate (100 mL × 2). The combined organic layers were washed with water, concentrated in vacuo, and partitioned between *n*-hexane and $CHCl_3$. The *n*-hexane layer was purified by silica gel chromatography (cyclohexane/$CHCl_3$ = 10/1) to give labeled **1** (3.2 mg). Epoxidation of **1** gave **3** (3.0 mg).

NfSS Cloning and Expression in *E. coli*

To generate the overexpression construct for *NfSS*, *NfSS* was amplified using the codon-optimized synthetic DNA of the *A. oryzae* transformant using the following primer sets: NfSS-F (5′-**GATGACGATGACAAG**ATGGAAGTTTGGGAACATAG-3′; bold characters indicate the complementary sequence for the In-Fusion reaction), NfSS-R (5′-**AGGATCCGAATTCCG**TTAGTTTTCTTTAACGCTCAG-3′; bold characters indicate the complementary sequence for the In-Fusion reaction). The PCR products were directly inserted into the *Kpn*I-digested pMALc4E to generate pMALc4E-*NfSS*. pMalc4E-*NfSS* was separately introduced into *E. coli* BL21-Gold(DE3) for overexpression. The transformant was grown at 37 °C at an OD_{600} of ~0.6 in a 500 mL flask. After the culture was cooled at 4 °C, isopropyl β-d-thiogalactopyranoside (0.1 mM) was added to it. After incubation at 20 °C for 18 h, the cells were harvested by centrifugation at 4000 rpm. The harvested cells were resuspended in disruption buffer (50 mM Tris–HCl (pH 7.5), 200 mM NaCl) and disrupted by sonication. After centrifugation, the

supernatant was applied to an amylose column to purify the expressed protein.

NfSS Assay

Typical conditions are as follows: A reaction mixture (50 μL of Tris–HCl buffer (pH 7.5)) containing GGPP (220 μM), IPP (660 μM), $MgCl_2$ (5 mM), DTT (2 mM), and NfSS (10 μM) was incubated at 30 °C for 3 h. The reaction was quenched by the addition of EtOAc (50 μL), and the resultant mixture was vortexed and centrifuged at 12000 rpm. The upper EtOAc layer was collected and analyzed by GC–MS with the same GC conditions used to analyze **1**.

Chapter 3. Fungal RiPP ustiloxin B biosynthesis study

3-1. Background of RiPPs biosynthesis.

Ribosomally synthesized and post-translationally modified peptides (RiPPs) have been widely discovered in bacteria[64], archaea[65] and eukaryota[66], and their extensive post-translational modifications involving double bond formation, oxidation, cyclization render these family of peptides of significant structure diversity and wide range of bioactivities[67,68,69,70]. Several examples are shown in Figure 3-1. Bacterial RiPPs family such as lanthipeptides, cyanobactins and thiopeptides are characteristics of their heterocyclic moieties and exo-olefins from seryl, cysteinyl or threonyl residues. α-amanitin isolated from mushroom is featured with the hydroxylated amino acid sidechains. Macrocyclizations are frequently observed in RiPPs to increase their stability to peptidases or to decrease their conformational flexibility[36].

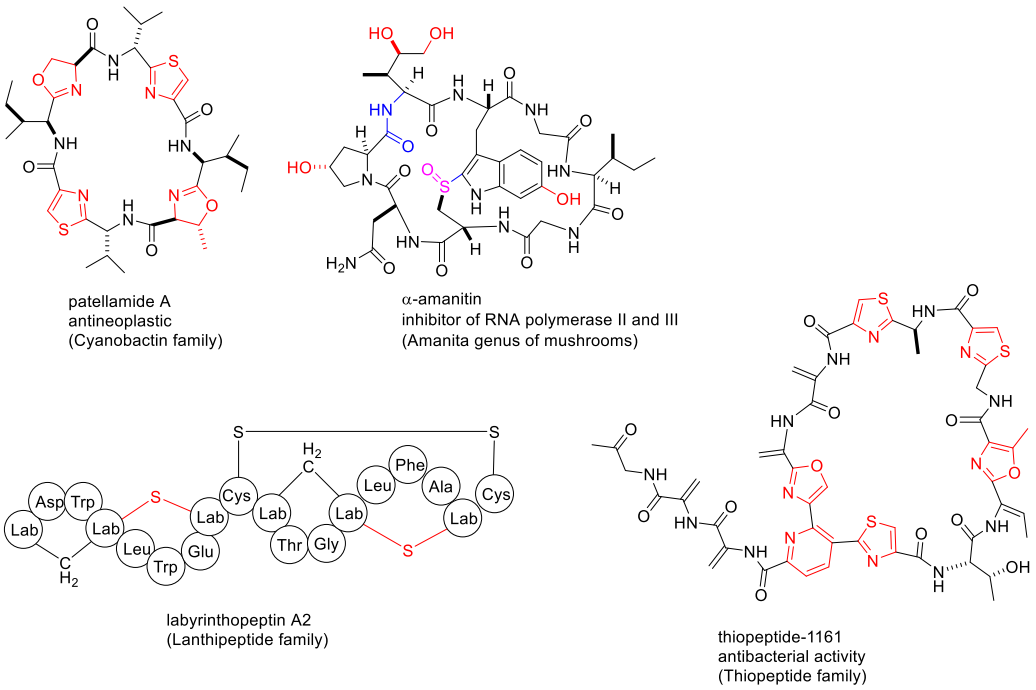

Figure 3-1. RiPPs structures

The biosynthesis of RiPPs usually follows the common scheme[71] (scheme 3-1). The precursor peptide organized with three regions (leader peptide, core peptide, follower peptide) is firstly synthesized by ribosome. The leader peptide region usually locates at the N terminal, serving as a recognition site of modifying enzymes or transporters[72]. It is digested at certain stage and not present

in the final product[73]. The core peptide region is the part to become the mature product after the post-translational modifications. Sometimes follower peptide exists in the C terminal region, involved in the cyclization or excision[74,64]. The precursor peptide undergoes modifications such as oxidation, phosphorylation, cyclization catalyzed by relevant biosynthetic genes, some of which are novel enzymes through unprecedented mechanisms[75,76,77]

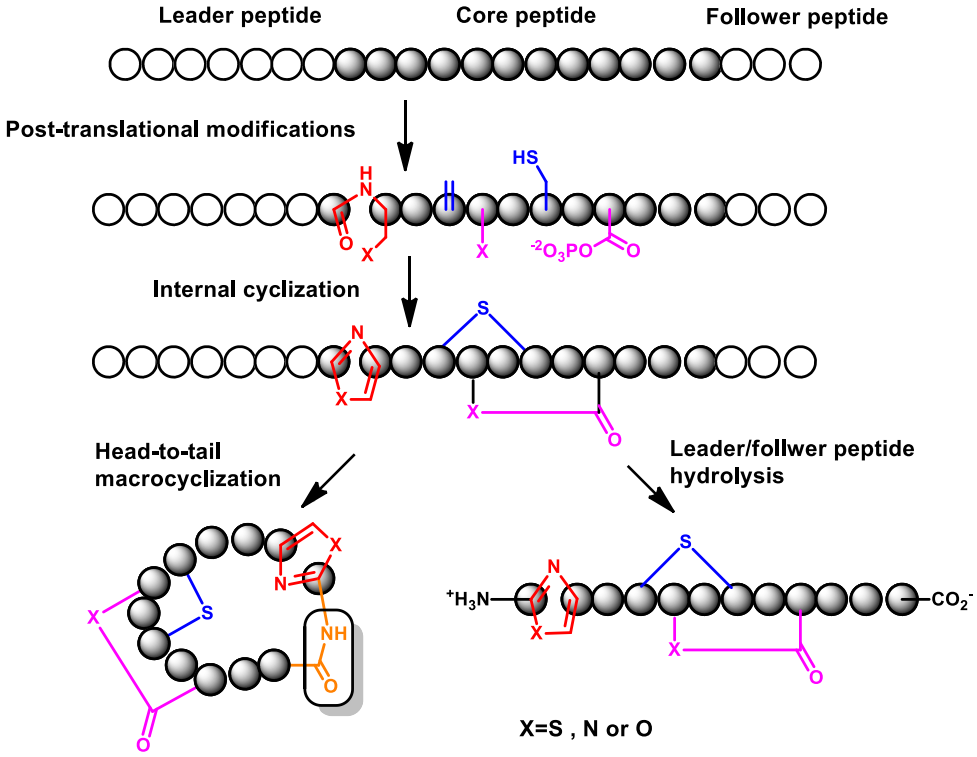

Scheme 3-1. General scheme for bacterial RiPPs biosynthesis

Although in the last two decades, the biosynthesis of many bacterial RiPPs have been elucidated in detail, the fungal RiPPs biosynthetic gene clusters have rarely been reported. Amanitin is the first fungal example whose precursor peptide gene was discovered from mushroom genome[66]. Recently, Umemura *et al* reported the biosynthetic gene cluster for ustiloxin B in *Aspergillus flavus* using MIDDAS-M, an algorithm that predicts secondary metabolite biosynthetic (SMB) gene clusters based on the concurrent expression of contiguous genes in the genome rather than relying on the presence of core genes for secondary metabolism production, such as PKS or NRPS[78]. This is the first example of RiPPs BGC from filamentous fungi. Ustiloxin B was originally isolated from *Ustilaginoidea virens* and possesses potent antimitotic activity[79]. On this cluster, a precursor peptide protein UstA encodes a protein with repeated YAIG motif that exactly matches the core scaffold of ustiloxin B (Figure 3-2). Since this breakthrough, the BGCs from three other compounds, phomopsin[80], asperipin-2a[10] and epichloëcyclin[10] from filamentous fungi have also been identified belonging to RiPPs (Figure 3-3). Although ribosomal origins of precursor peptide were proven in several cases, post-translational modifications in fungal RiPPs has not been studied in detail. Therefore, the author performed studies on the elucidating the biosynthetic pathway of ustiloxin B.

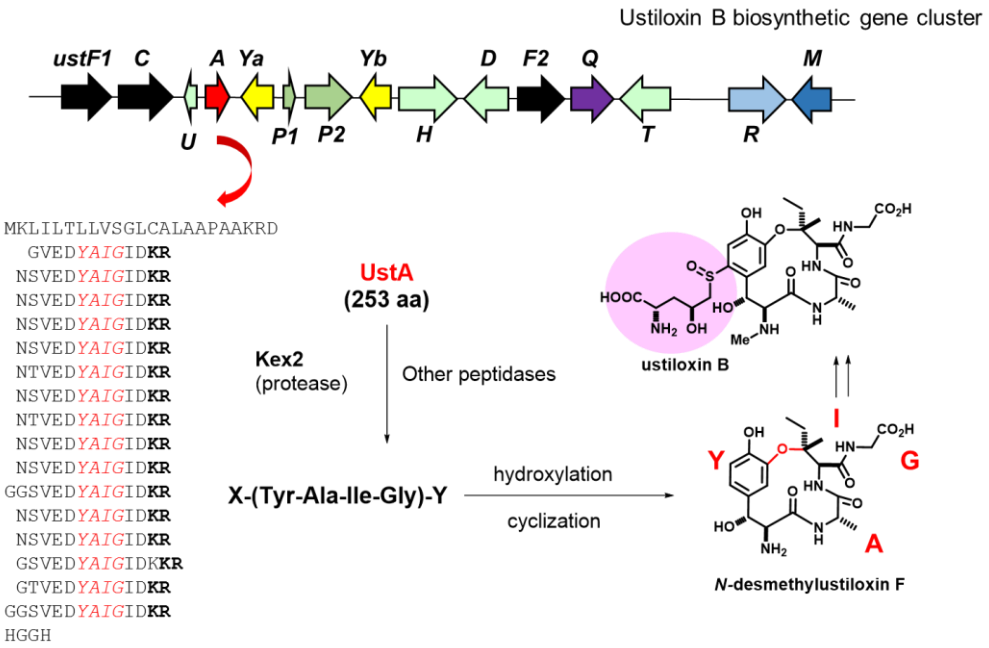

Figure 3-2. Biosynthetic gene cluster of ustilxin B and proposed general biosynthetic pathway

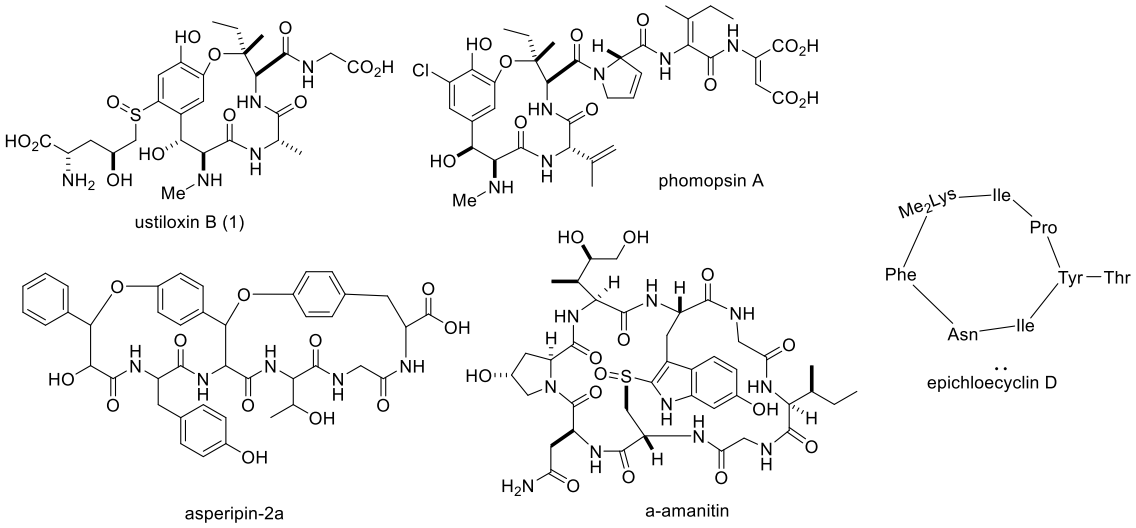

Figure 3-3. Representative fungal RiPPs whose precursor peptides have been identified.

3-2. Prediction of ustiloxin B biosynthetic pathway.

Umemura *et al* identified the biosynthetic gene clusters and performed gene deletion experiments to characterize the function of each gene on the cluster. *A. flavus* deletion muatants *ΔustM, ΔustC, ΔustF1, ΔustF2, and ΔustD* were constructed, and their metabolites were analyzed by LC-MS (Figure 3-4). Five ustiloxin derivatives **2**~**6** were accumulated in the mutants, which showed characteristic UV spectrum (Figure 3-5).

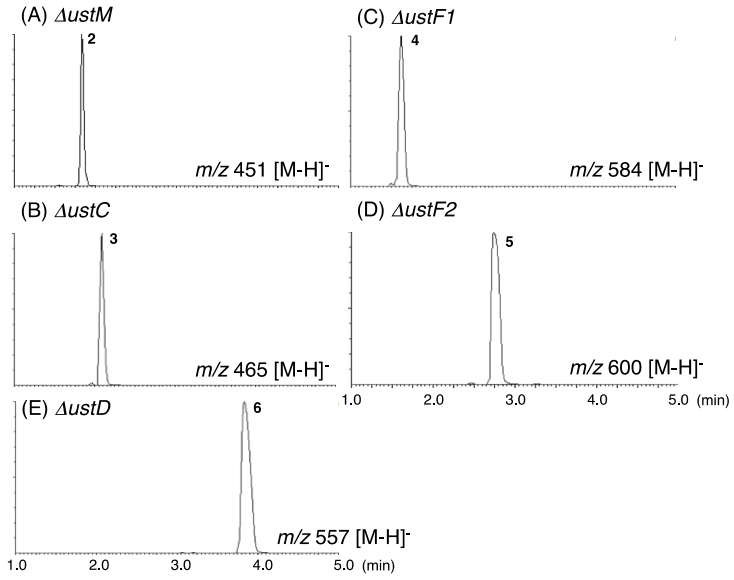

Figure 3-4. LC-MS profiles of the ustiloxin derivatives: (A) **2** produced by *ΔustM*, (B) **3** produced by *ΔustC*, (C) **4** produced by *ΔustF1*, (D) **5** produced by *ΔustF2*, (E) **6** produced by *ΔustD*.

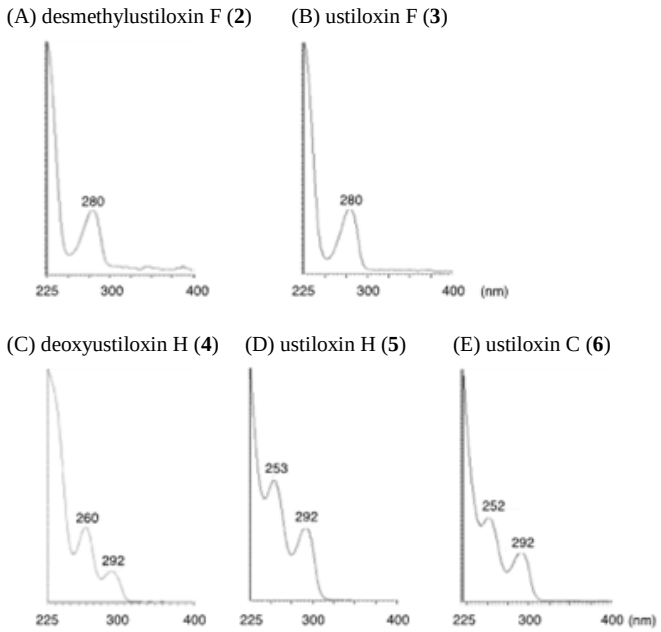

Figure 3-5. UV spectra of ustiloxin derivatives

From the HR-MS data, the molecular formulae of these derivatives were deduced to be **2**: $C_{20}H_{28}N_4O_8$, **3**: $C_{21}H_{30}N_4O_8$, **4**: $C_{24}H_{35}N_5O_{10}S$, **5**: $C_{24}H_{35}N_5O_{11}S$, and **6**: $C_{23}H_{34}N_4O_{10}S$. Compounds **3** and **6** were determined to be ustiloxin F and ustiloxin C by comparing with reported data[81,79]. Compound **2** gave similar ^{1}H NMR spectrum similar to that of **3**, except for lack of *N*-CH_3 signal observed in **3**, indicating **2** was *N*-desmethylustiloxin F. For compounds **4** and **5**, data provided by Umemura and co-workders contained small amount of impurities. To elucidate their structures, the author purified **4** and **5** from the extracts of large scale fermentation of the mutants. **4** showed a 119 mass unit shift from that of **3**, corresponding to addition of a cysteine residue. One of the aromatic protons in **3** was lost in **4**, revealing that the cysteine is added to **4**'s tyrosine aromatic ring. **5** has similar UV and ^{1}H NMR spectrum with those of **4**. Signals of the cysteine β-CH_2 of **4** and **5** (**4**: δ_H 3.43, 3.61 (CH_2); 5: δ_H 3.15, 3.71 (CH_2)) as well as that of the aromatic protons (**4**: δ_H 7.14, 7.27; **5**: δ_H 7.63, 7.42) indicating that **5** is the sulfoxide derivative of **4**. Compounds **2**, **4**, **5** were further analyzed by ^{13}C NMR, H-H COSY, HSQC, HMBC, and their structures were elucidated. Taken together with the predicted gene functions by the sequence analysis (Table 3-1), a biosynthetic pathway was proposed as shown in Scheme 3-2:

Table 3-1. Gene functions related in deletion experiments.

Gene ID in NCBI	Gene name	Predicted function	Accumulated compound
AFLA_094950	*ustF1*	Flavin-containing monooxygenase	**4**
AFLA_094960	*ustC*	Cytochrome P450	**3**
AFLA_094980	*ustA*	Precursor peptide protein	-
AFLA_094990	*ustYa*	Uncharacterized protein	-
AFLA_095020	*ustYb*	Uncharacterized protein	-
AFLA_095040	*ustD*	Cysteine desulfurase	**6**
AFLA_095050	*ustF2*	Flavin-containing monooxygenase	**5**
AFLA_095060	*ustQ*	Tyrosinase	-
AFLA_095070	*ustT*	MFS multidrug transporter	**2**
AFLA_095100	*ustM*	SAM-dependent methyltransferases	**2**

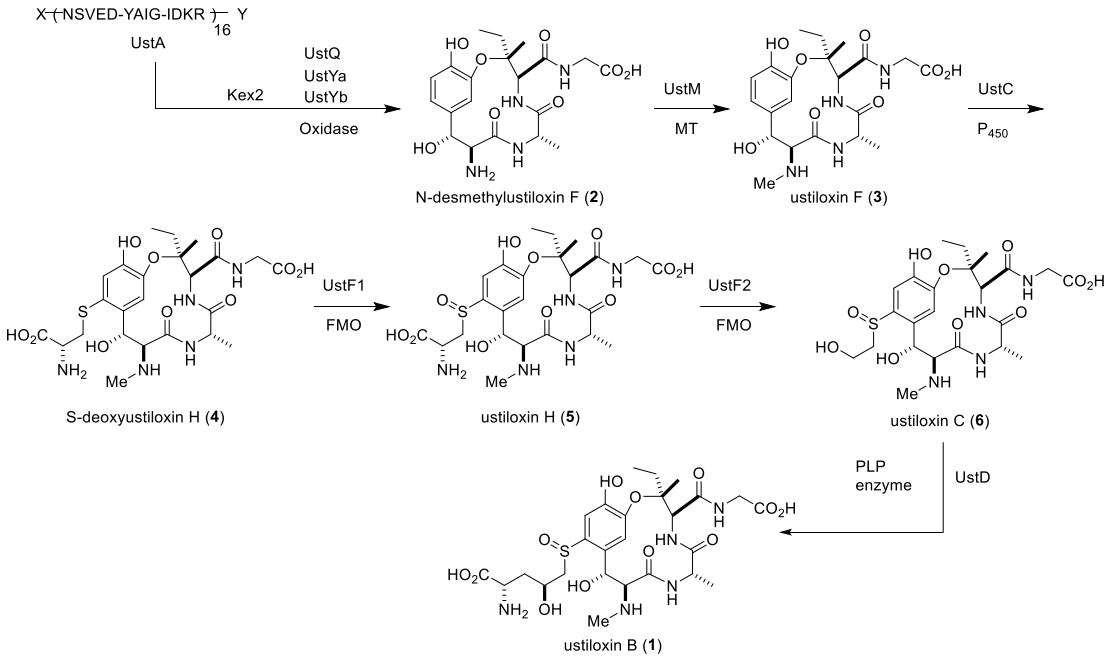

Scheme 3-2. Proposed biosynthetic pathway of ustiloxin B based on gene deletion experiments

3-3. Heterologous expression of ustiloxin B biosynthetic genes in *A. oryzae*.

The macrocyclic ether ring is commonly observed in fungal RiPPs ustiloxin, phomopsin derivatives and asperipin-2a. Although oxidative cyclization(s) is required to form this ether ring, no characterization of such reactions has been reported. Therefore, the author focused on the formation of **2** which was the first intermediate to be isolated. In the gene deletion experiments, it was discovered that deletion of any of these four genes *ustAQYaYb* resulted in the abolishment of any ustiloxin derivatives. It suggested that besides the precursor peptide, the three genes *ustQYaYb* are necessary for the oxidative cyclization.

Bioinformatics analysis suggested that tyrosinase UstQ may be responsible for hydroxylation of tyrosine aromatic ring[82]. UstYa and UstYb are homologues showing 30% sequence identity to each other and conserve a domain of unknown function (DUF) 3328. To characterize these three enzymes, *A. oryzae* heterologous expression of them was examined.

3-3-1 Plasmid preparation and transformation of *ustYaYbQ*.

As shown in Scheme 3-3, plasmids pUARA2 and pAdeA2 containing *ustYa* or *ustYb* or both were constructed by infusion method. Plasmid pUSA2-*ustAQ* was constructed using a rapid construction method called Gibson assembly[83].

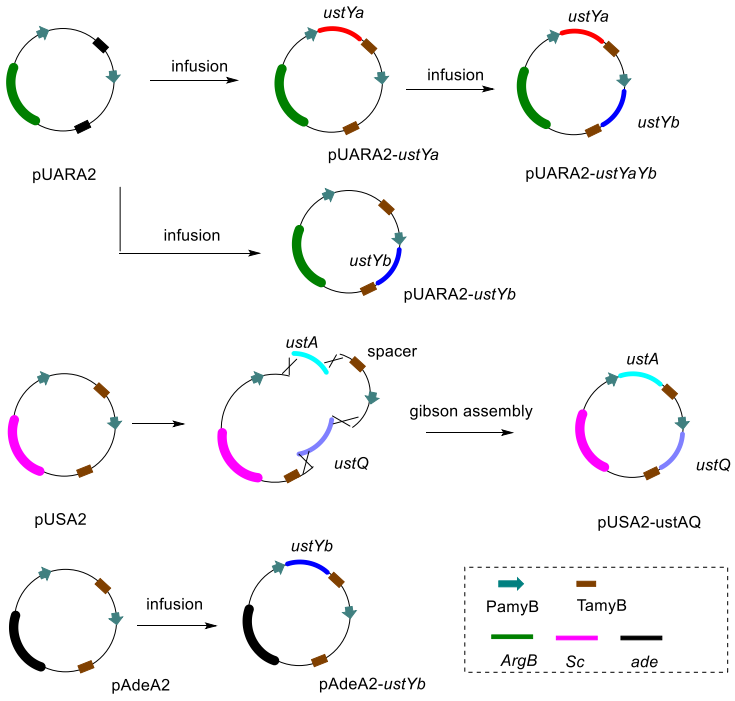

Scheme 3-3. Plasmid construction for *ustAQYaYb*

Transformation of these plasmids into *A. oryzae* NSAR1 was conducted according to Scheme 3-4. Four kinds of transformants: AO-*ustAQYa*, AO-*ustAQYb*, AO-*ustAQYaYb* and AO-*ustAQYa+Yb* were obtained.

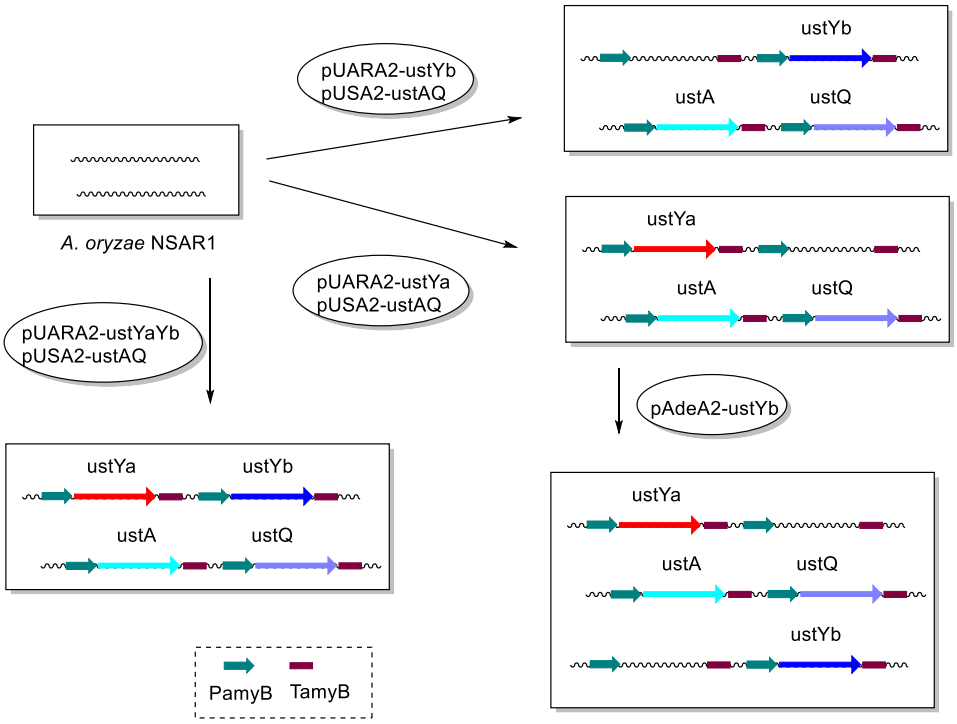

Scheme 3-4. *A. oryzae* transformation of *ustAQYaYb*

3-3-2. Analysis of metabolites from ustiloxin gene transformants.

After the transformations, following transformant strains were obtained as shown in Table 3-2.

Table 3-2 Transformation result of ustAQYaYb introduction

Transformant	Total colonies obtained	Colonies producing **2**
AO-*ustAQYaYb*	7	4
AO-*ustAQYa*	10	0
AO-*ustAQYb*	10	0
AO-*ustAQYa+Yb*	6	5

Each transformant was cultured in 20 g rice medium and the metabolite was extracted with 70% acetone water solution. After removing the acetone, the water layer was analyzed by UPLC-MS (Figure 3-6). Compared to WT, the AO-*ustAQYaYb* transformant produced a new peak. This new

metabolite was isolated and all data including various NMR spectra were identical to those of **2**. This was the first example of the heterologous production of fungal RiPP in *A. oryzae.* While AO-*ustAQYa* or AO-*ustAQYb* did not produce **2**, transformant derived from introduction of *ustYb* into AO-*ustAQYa* produced **2**. These results gave solid evidence that precursor peptide UstA and three enzymes UstQYaYb are indispensable to produce the first cyclized intermediate **2**. Although the UstYaYb show 30% sequence identity to each other, their function is not redundant. As a starting material, UstA was proposed to be digested by Kex2 protease at KR sites to give 16 trideca-/tetradecapeptides. To be further hydrolyzed to tetrapeptide, the N and C terminal peptides should be cleaved by peptidases from *A. oryzae.* However, there is no information on the peptidases and their timing of cleavage.

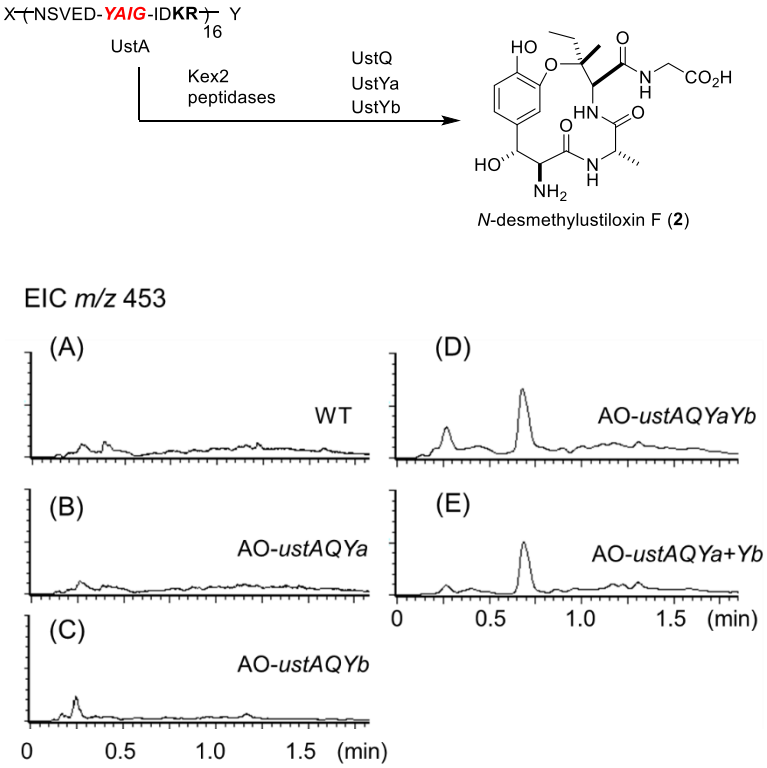

Figure 3-6. LC-MS profiles of extracts from transformants: (A) WT strain, (B) AO-*ustAQYa*, (C) AO-*ustAQYb*, (D) AO-*ustAQYaYb* (co-transformation), and (E) AO-*ustAQYaYb* (stepwise incorporation).

The author further constructed plasmid pAdeA2-*ustM* to be transformed into AO-*ustAQYaYb* (Figure 3-7). As expected, the AO-*ustAQYaYbM* produced a new peak corresponding to ustiloxin F (**3**). However, the production of **3** was not efficient with significant amount of precursor **2** remained. Since *ΔustT* accumulated **2** , UstT, a putative transporter, was postulated to improve the production

of **3**[84]. Indeed, after introduction of *ustT,* AO-*ustAQYaYbMT* obviously gave improved yield of **3** by three times. Given the fact that ustiloxin F retains activity against tubulin polymerization[81], its production might inhibit the cell proliferation. UstT belongs to MFS multidrug transporter which is closely related to extrusion of toxic substances from fungal cells[85]. Based on the results mentioned above, it was postulated that UstT transports cytotoxic ustiloxin F to the outside of the cell, thus allows the heterologous host to produce more **3**.

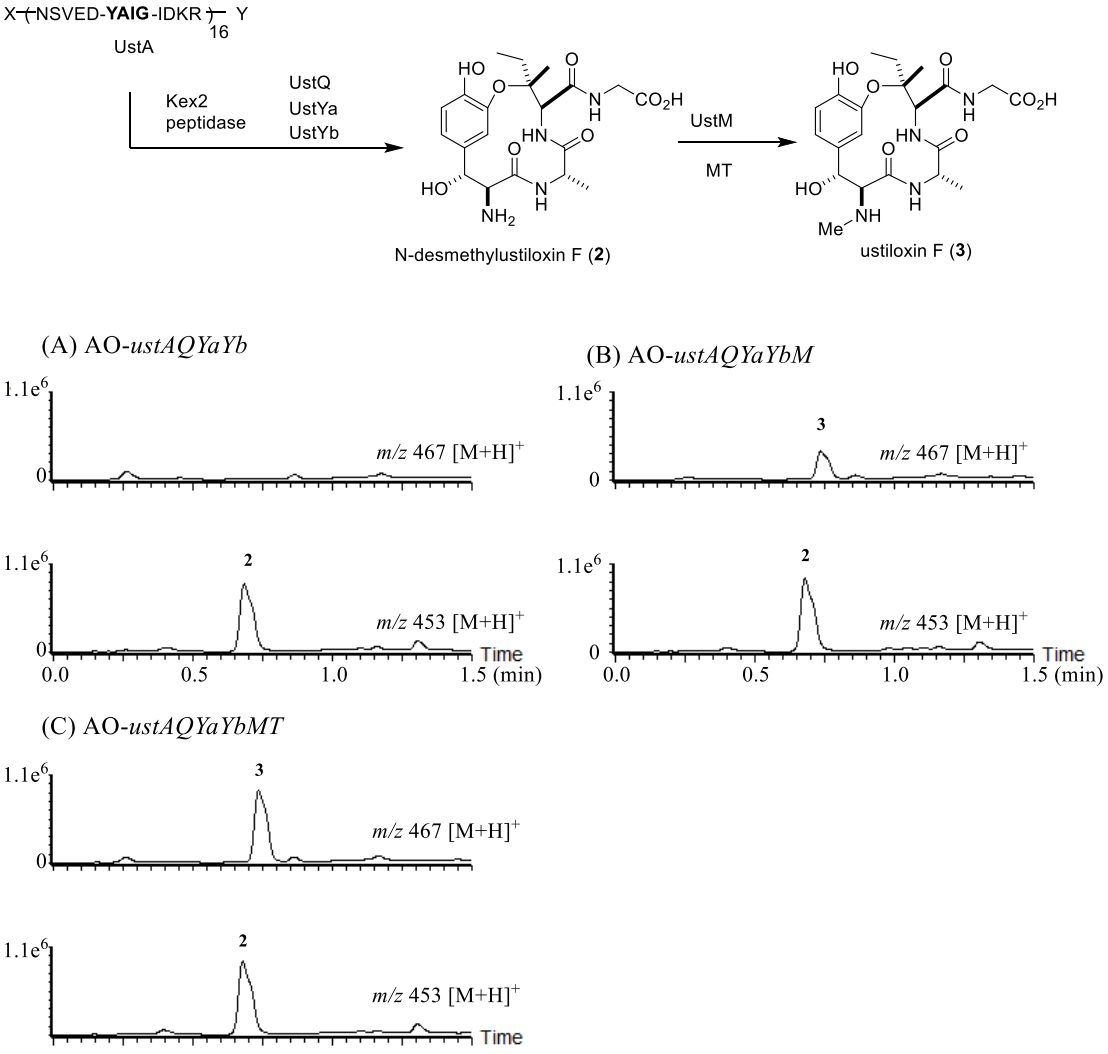

Figure 3-7. LC-MS profiles of extracts from transformants: (A) AO-u*stAQYaYb*.

(B) AO-*ustAQYaYbM*, (C) AO-*ustAQYaYbMT*.

3-3-3. Proposed mechanism for oxidative cyclization

From linear YAIG to cyclized **2**, three oxidation reactions are involved: (1) a hydroxylation at either the aromatic ring of Tyr or β-position of Ile. (2) a hydroxylation at the benzylic position and (3) an

oxidative cyclization. We proposed a reaction mechanism as shown in Scheme 3-5

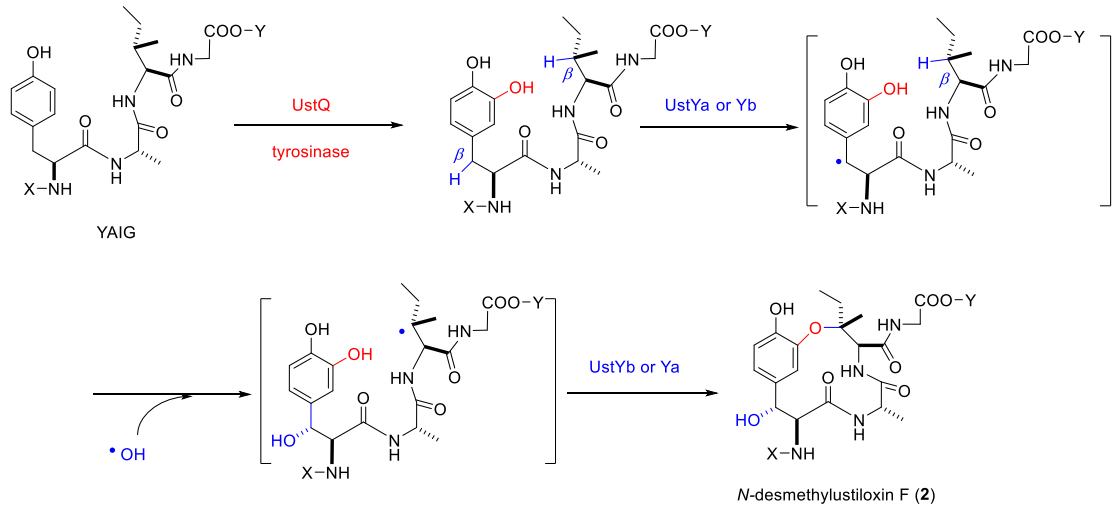

Scheme 3-5. Proposed cyclization mechanism of UstYaYb

Sequence analysis revealed that UstQ is a putative tyrosinase which usually catalyzes hydroxylation of a phenol, as in the case of oxidizing tyrosine into L-DOPA[82]. Similarly, UstQ introduced a hydroxy group on the tyrosine aromatic ring. UstYa (or Yb) abstracts a β hydrogen from tyrosine residue, leaving a radical species quenched by a possible "rebound oxygen"[86] to afford the benzylic hydroxy group. Similar oxidation at β carbon of isoleucine followed by cyclization with phenol hydroxyl group afforded *N*-desmethylustiloxin F. UstYaYb homologues conserved 5 histidines and 5 cysteines in their sequences (described at section 4-4) which may be involved in binding to metal cofactors. Usually enzymes catalyzing C-H functionalization requires metal cofactors, such as radical *S*-adenosylmethionine enzymes[87], mononuclear non-heme iron enzymes[88]. Thus UstY homologues are postulated here as metal binding oxidases that catalyzes the amino acid β C-H functionalization.

The heterologous production of **2** in *A. oryzae* is an encouraging starting point from which large numbers of RiPPs hidden in the fugal genomes might be discovered through genome mining using *A. oryzae* expression system.

3-4. *In vitro* enzymatic assays of tyrosine residue side chain modifications.

Besides the oxidative cyclization, the tyrosine side chain modifications on ustiloxin B also might involve unique chemical transformations: from cysteine residue of **4** to the 4-hydroxy-5-sulfinyl-L-

norvaline residue of **1**, three enzymes UstF1F2D were predicted to be involved according to the gene deletion experiments. UstF1F2 with a 50% sequence identity between each other belong to flavoprotein monooxygenases family requiring a flavin as cofactor[89]. UstD belongs to Aminotransferase class-V family requiring pyridoxal phosphate (PLP) cofactor[90]. Based on these information, we decided to conduct *in vitro* assays to reconstitute the final stage of the ustiloxin B biosynthetic pathway.

3-4-1. Functional analysis of UstF2.

UstF1F2 were overexpressed in *E. coli*. Purified MBP-UstF1F2 showed yellow color and clear UV absorption at 450 nm (Figure 3-8), indicating that flavin was still attached to these purified proteins[89].

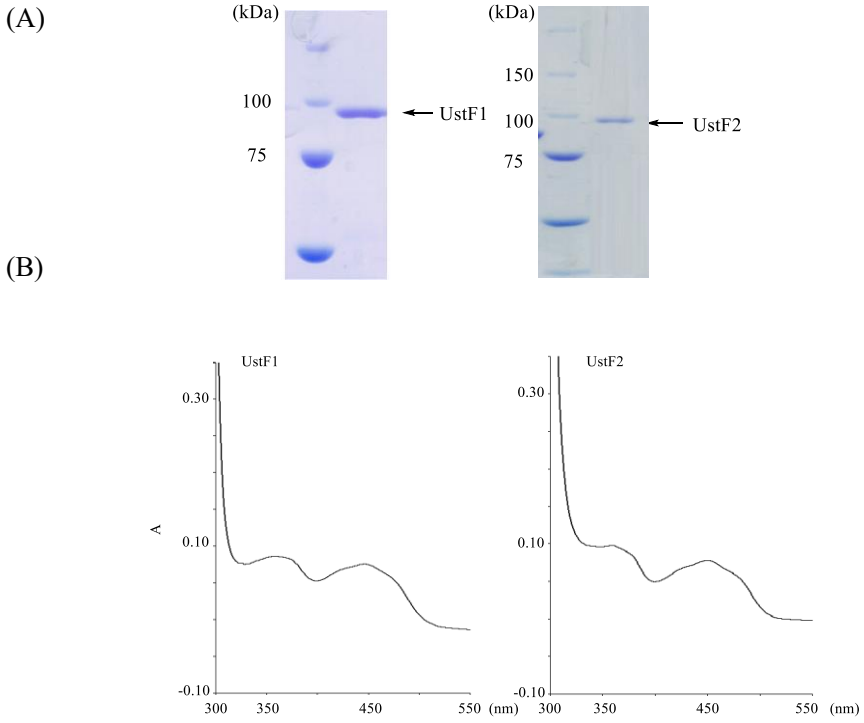

Figure 3-8. (A) SDS-PAGE analysis of UstF1F2. (B) UV spectrum of UstF1F2

MBP-UstF1 was purified and characterized *in vitro* in the author's lab[91]. The result showed that UstF1 catalyzed the oxidation to the sulfoxide **5** (Scheme 3-6), agreeing with the gene deletion experiment.

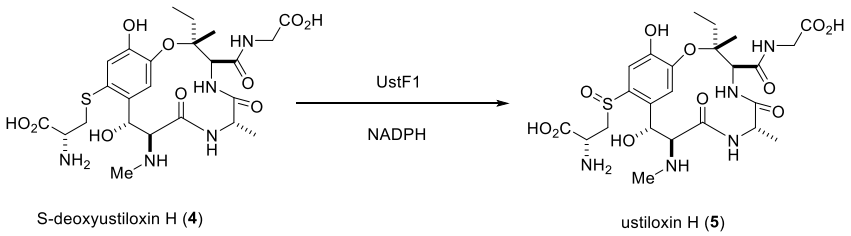

S-deoxyustiloxin H (**4**) ustiloxin H (**5**)

Scheme 3-6. S oxidation catalyzed by UstF1

To characterize UstF2, the *in vitro* enzymatic assay was conducted using ustiloxin H as the substrate and NADPH as the cofactor.

The assay result showed that the substrate ustiloxin H (**5**) was completely consumed within 2 min, and a new peak appeared (Figure 3-9). Milligram scale enzymatic reaction allowed us to isolate this product **7**.

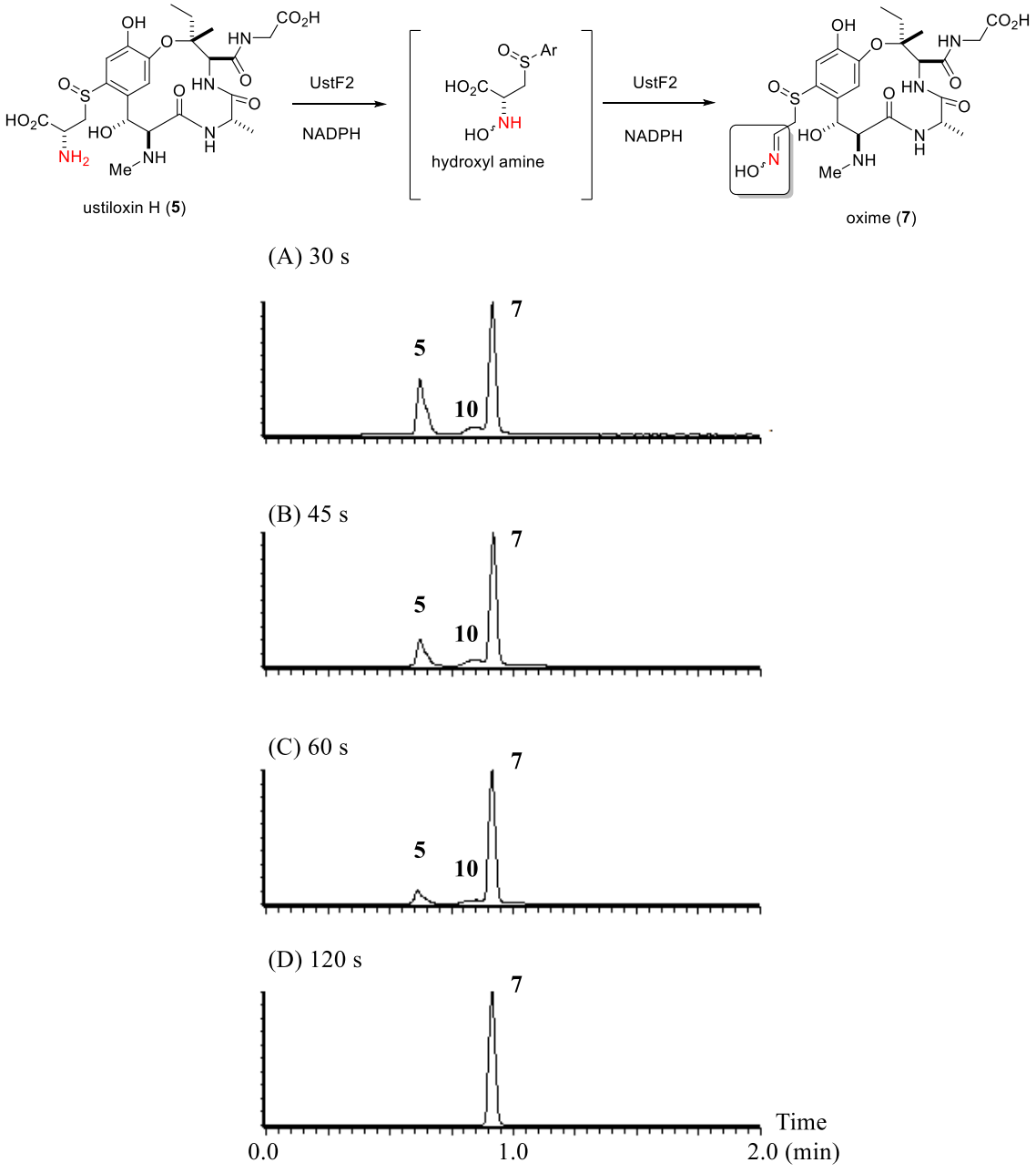

Figure 3-9. Time course analysis of the UstF2 reaction mixture

The molecular formula of this product was determined to be $C_{23}H_{34}N_5O_{10}S$ by HR-MS analysis. For

the ^{1}H NMR (Figure 3-10), the signals of the cysteine α-H of **5** disappeared. Instead, signals of isomeric oxime methine protons (hollow arrow) appeared (major isomer: δ_H 7.43, minor isomer: δ_H 6.96). Also the ortho aromatic proton (filled arrow) appeared as a pair of *E/Z* mixture. Thus the product of UstF2 reaction was determined to be the *E/Z* mixture of oxime **7**.

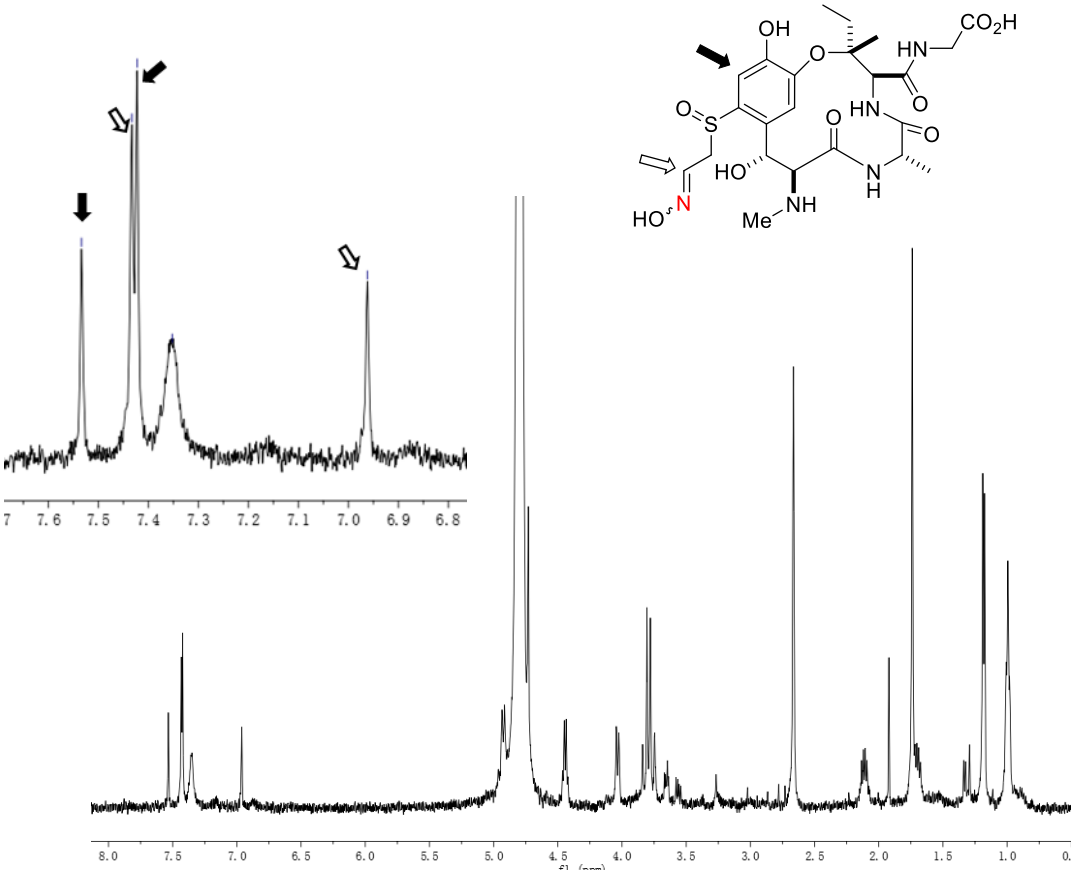

Figure 3-10. NMR spectrum of E/Z mixture of ustiloxin oxime (**7**). The proton signals with hollow arrows indicate oxime methine protons, and those with filled arrows indicate aromatic ortho protons.

Next the UstF2 catalytic mechanism was focused on. Time course UstF2 reaction was monitored in short internals (Figure 3-9) and the new peak **10** was observed with *m/z* 618 $[M+H]^+$, 16 mass unit larger than that of **5** (*m/z* 602 $[M+H]^+$). It disappeared in 2 min with starting material, strongly suggesting that **10** was the *N*-monohydroxylamine intermediate of UstF2 reaction.

Taken the results in consideration, the reaction mechanism of oxime formation was proposed (Scheme 3-7). UstF2 firstly catalyzed *N*-hydroxylation forming intermediate **10**, and further

oxidation formed *N*-dihydroxy intermediate which quickly underwent decarboxylative dehydration to form oxime **7**. Similar oxime formation catalyzed by FAD enzyme CrmH was reported in biosynthesis of caerulomycin A[92]. The uniqueness of UstF2 compared to CrmH was these two points: 1) UstF2 catalyzed dehydration was accompanied by decarboxylation. 2) UstF2 does not need flavin reductase to reduce FAD cofactor, that is, UstF2 is a bifunctional enzyme that catalyzed both amino group oxidation and FAD reduction (Scheme 3-8). Interesting, although UstF1 and UstF2 possesses 50% sequence identity, they are oxidizing different heteroatoms S and N on the cysteine residue.

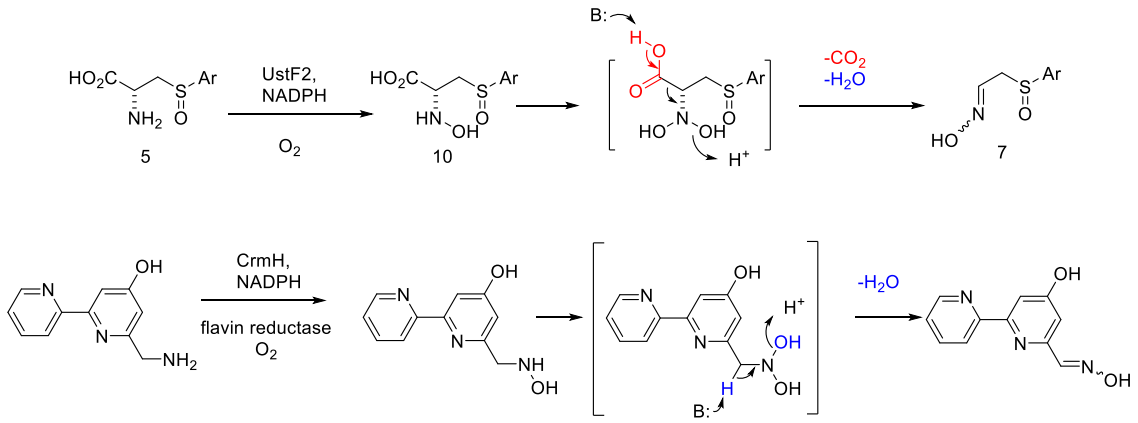

Scheme 3-7. Proposed mechanism of (A) decarboxylative dehydration catalyzed by UsfF2 and (B) oxime formation catalyzed oxime formation

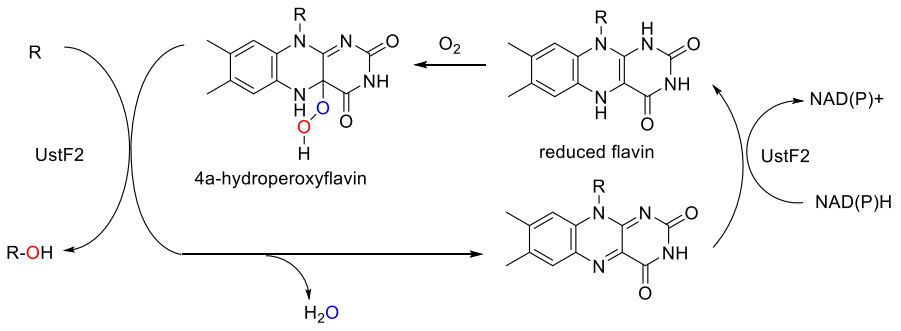

Scheme 3-8. UstF2 is a bifunctional enzyme that catalyzes oxygenation reaction and FAD reduction

In the process of HPLC purification of **7** using solvent system containing 0.1% TFA, it was found that the oxime was slowly converted to another compound **9** in the acid solutions (Figure 3-11A). The TFA treatment of **7** in larger scale enabled the author to isolate **9**. ^{1}H NMR analysis showed that the signals of oxime methine on **7** disappeared, instead, a geminal diol proton signal could be

observed at 5.48 ppm (Figure 3-11B), revealing that **9** was geminal diol, the hydrated form of aldehyde. The dominant formation of geminal diol over aldehyde may be explained by the hydrogen bond between hydroxy proton and sulfoxide oxygen.

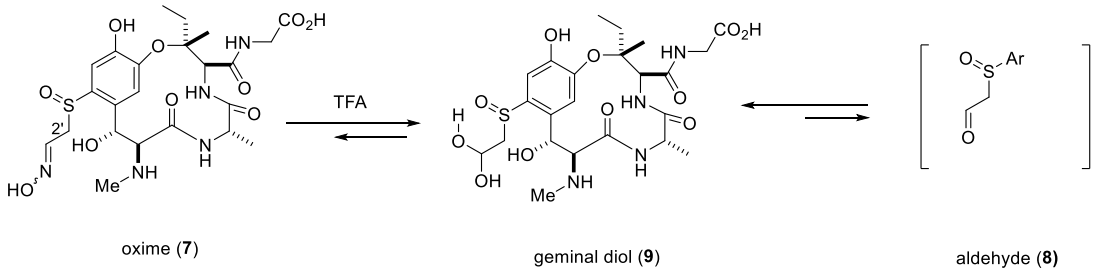

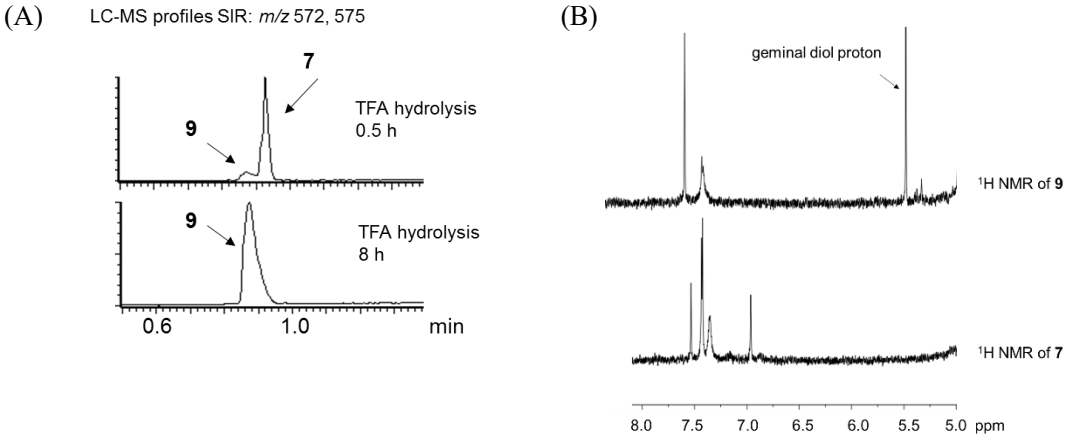

Figure 3-11. Conversion of oxime **7** to geninal diol **9** in TFA solutions. A) LC-MS profile B) Selected region of ^{1}H NMR of **9** and **7**

In the ^{1}H NMR analysis of **7** and **9**, we noticed that the α proton signal on the C2' was slowly diminished and totally disappeared when these compounds were left in the D_2O overnight. (Figure 3-12 A, black arrows pointed to proposed signal of C2'). We reasoned that the α protons of imine and aldehyde has enough acidity for D/H exchange. This was further supported by MS analysis of **7** immediately recovered from D_2O (Figure 3-12 B) which showed 2 mass unit increase.

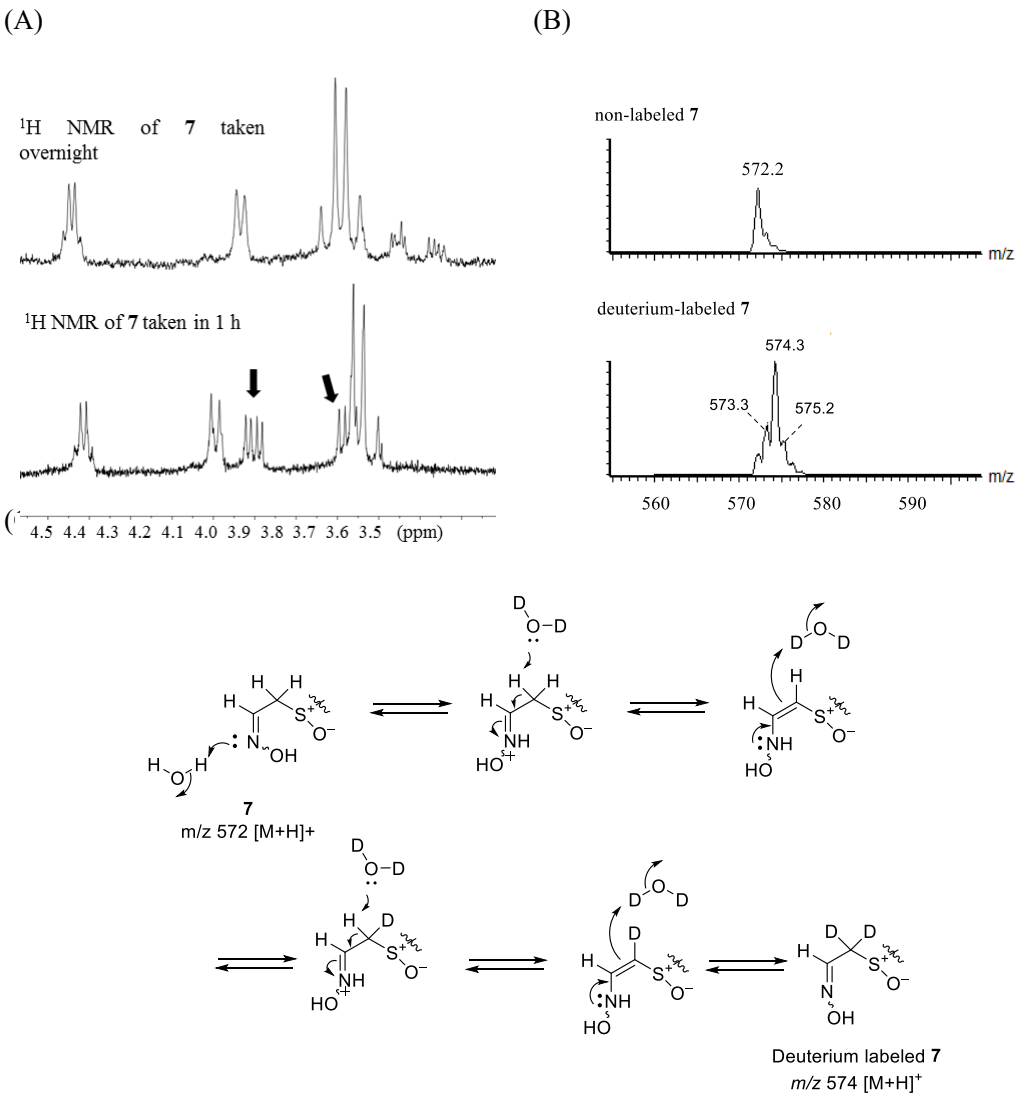

Figure 3-12. (A) selected region of ^{1}H NMR of **7**. up: taken in 24 h. down; taken in 1 h. (B) MS spectra of up: non-labeled **7** and down: deuterium-labeled **7** after D_2O treatment. (C) proposed mechanism of H/D exchange on α protons of oxime

As has been shown above, UstF2 *in vitro* reaction afforded oxime **7** which could be further hydrolyzed into geminal diol **9**. Although both of them were not observed in gene deletion experiments, they shed the light on the exact pathway of final stage of ustiloxin B biosynthesis. Firstly, ustiloxin C accumulated in UstD deletion strain was probably a shunt product reduced from **9** by unknown reductases in *A. flavus*. Indeed, after we isolated geminal diol **9** and reduced with $NaBH_4$, ustiloxin C was produced (Figure 3-13), giving more evidence ustiloxin C was a shunt product in this pathway.

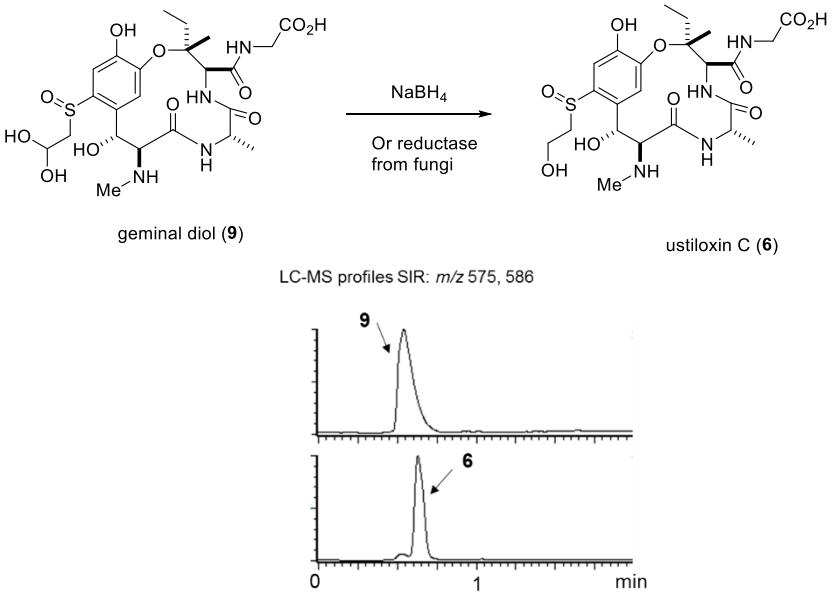

Figure 3-13. LC-MS profiles of $NaBH_4$ reduction of **9** and the production of ustiloxin C

Secondly, **9** was speculated to be the substrate of UstD. As the hydrate form of aldehyde **8**, it is predicted to be condensed with a C3 unit to give ustiloxin B.

3-4-2. Functional analysis of UstD.

UstD is a PLP dependent enzyme catalyzing the final step of ustiloxin B biosynthesis. For the reasons mentioned in 3-4-1, hydrate form **9** was used as substrate for UstD *in vitro* reaction.

Another point we could not ignore was where the elongated C3 carbon units comes from. Considering reported examples in condensing amino acids with other compounds through C-C bond formation[90, 93], it was speculated the C3 unit comes from amino acids.

UstD *in vitro* assays were conducted with UstD, PLP, geminal diol, and amino acids (Figure 3-14). LC-MS analysis showed that a new peak corresponding to ustiloxin B was detected in the presence of aspartate, but not in the case of alanine. Exogenous PLP is not necessary, indicating that PLP has a relatively tight binding with purified UstD.

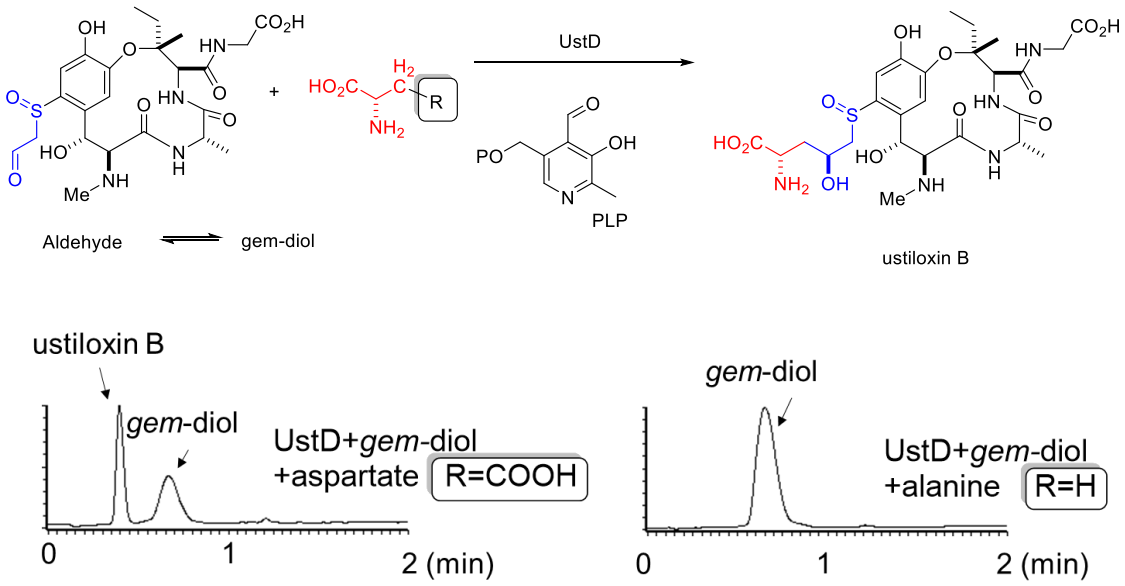

Figure 3-14. LC-MS profiles of enzymatic reaction of UstD

In the conversion from aspartate to C3 nucleophile, a decarboxylation reaction was expected. PLP dependent decarboxylase has long been reported with established mechanism[94](Scheme 3-9).

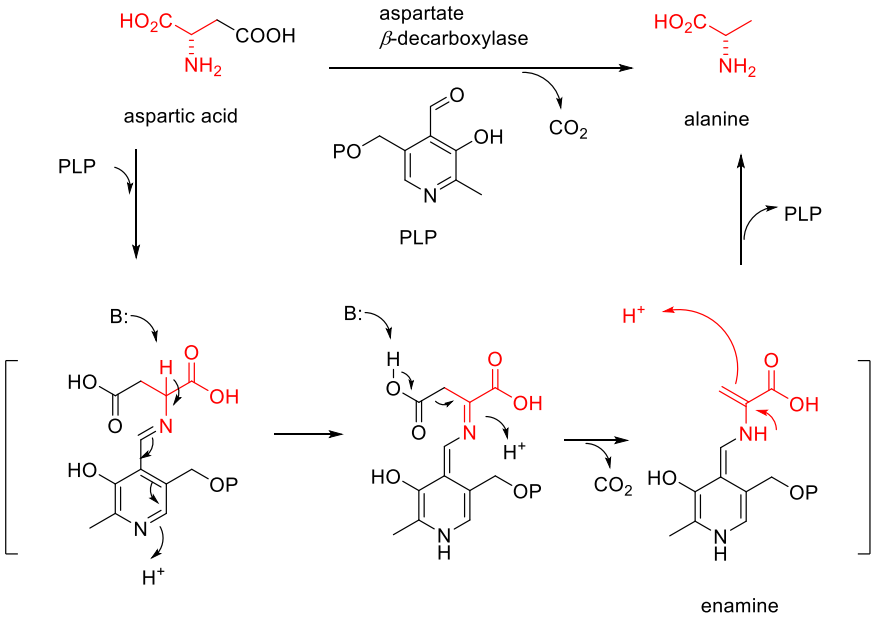

Scheme 3-9. Mechanism of PLP enzyme catalyzed decarboxylation reaction

In order to prove UstD can also catalyze decarboxylation of aspartate, we conducted *in vitro* assay with UstD and aspartate in the absence of geminal diol. Dansyl derivatives of the reaction products were analyzed by LC-MS (Figure 3-15).

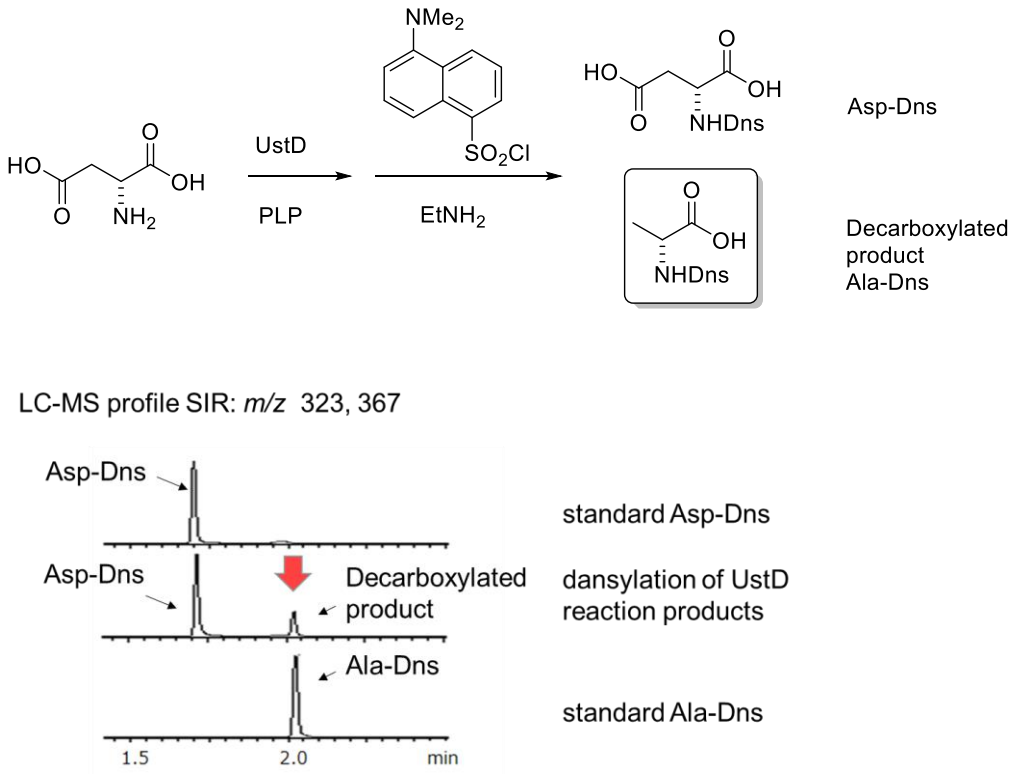

Figure 3-15. LC-MS profiles of UstD catalyzed decarboxylation reaction

Results showed that Ala-Dns was detected in reaction mixture, indicating that decarboxylation occurred. As shown in Schemes 3-9, decarboxylation reaction of UstD gives an enamine intermediate. In the absence of ustiloxin aldehyde, enamine would readily be hydrolyzed to afford alanine. On the other hand, when ustiloxin aldehyde was present in the active site of UstD, enamine would readily serve as a nucleophile to attack the aldehyde (Scheme 3-10). This highly unique decarboxylative condensation reaction catalyzed by UstD was unprecedented. In this way, we successfully biosynthesized ustiloxin B *in vitro*.

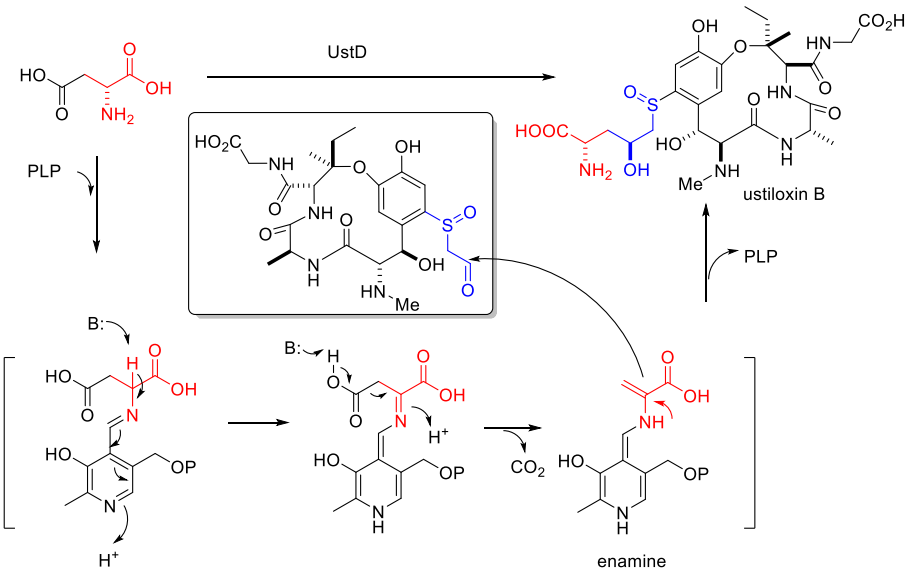

Scheme 3-10. Proposed mechanism of UstD catalyzed decarboxylative condensation reaction

Conclusion

Through gene deletion experiments, *A. oryzae* heterologous expression and *in vitro* enzymatic assays, the author unveiled the whole biosynthetic pathway of ustiloxin B, whose biosynthetic gene cluster was the first example of a RiPP from filamentous fungi. Specifically:

1. Based on the gene deletion experiments, 4 genes *ustAQYaYb* were shown to be involved in oxidative cyclization to form *N*-desmethylustiloxin F (**2**). Heterologous expression of them in *A. oryzae* successfully produced **2** and proved that UstQYaYb are essential to synthesize the first cyclized intermediate. UstY homologues containing DUF 3328 were firstly characterized *in vivo* to be a family of novel oxidative cyclases.

2. UstF2 and UstD were characterized *in vitro* as unique enzymes catalyzing the modifications on the tyrosine residue sidechain. FAD dependent UstF2 catalyzed two rounds of hydroxylation on amino group followed by decarboxylative dehydration to form oxime. While UstD catalyzed a decarboxylative C-C bond formation to produce ustiloxin B *in vitro*.

Although the author elucidated the functions of most enzymes on the ustiloxin BGC, there are still many unsolved questions:

1. How are the peptides on the terminals of YAIG cleaved? Although *in vivo* formation of cyclized YAIG needs only UstA and three enzymes UstQYaYb, obviously Kex2 and endogenous peptidases

were required to digest UstA and release the YAIG or its cyclized form from NSVEDYAIGIDKR repeating motif. However, to elucidate the timing of cleavages are currently difficult because no linear or cyclized intermediates were isolated containing residues longer than YAIG. Interestingly, in phomopsin's case, the core skeleton was YVIPID derived from GEAVEDYVIPIDKR repeating motif. It is likely that the double bonds on the last Pro, Ile and Asp prevents the peptidase from hydrolyzing those residues.

2. How is it to reconstitute the UstY enzyme *in vitro*? *In vivo* UstY homologues showed novel activity of oxidative cyclization, probably involving a radical reaction mechanism. However, initial trial to obtain soluble UstY enzyme in *E. coli* turned out to be challenging. In addition, no cofactor information is available from sequence analysis, making the *in vitro* reconstitution difficult. More effort is needed to search for suitable method to isolate the functional enzymes and narrow down the candidates of cofactors.

Bioinformatics have revealed that many potential RiPPs BGCs containing both precursor peptides and UstY homologues exist in fungal genomes[10]. This study proves *A. oryzae* is a powerful tool for expression of genes responsible for biosynthesis of fungal RiPPs, and more and more novel RiPPs with their BGCs would be discovered by genome mining.

Experimental

General. All reagents commercially supplied were used as received. Optical rotations were recorded on JASCO P-2200 digital polarimeter. ^{1}H- and ^{13}C-NMR spectra were recorded on Bruker AMX-500 spectrometer or Bruker DRX-500. NMR spectra were recorded in D_2O (99.9 atom % enriched, CIL). ^{1}H chemical shifts were reported in δ value relative to water: δH 4.79 ppm). Data are reported as follows: chemical shift, multiplicity (s = singlet, d = doublet, t = triplet, q = quartet, m = multiplet, br = broad), coupling constant (Hz), and integration. Mass spectra were obtained with a Xevo G2-S QTof (Waters) or JEOL JMS-T100LP. Column chromatography was carried out on C18 silica gel. (Wako 30~50 μm). Oligonucleotides for polymerase chain reaction (PCR) were purchased from Hokkaido System Science Co., Ltd. Cell disruption was dealt with an ultrasonic disrupter UR-200P (TOMY SEIKO, Tokyo, Japan). Analysis of the samples during protein purification was performed

using SDS-polyacrylamide gel electrophoresis, and the proteins were visualized by using coomassie brilliant blue staining. Protein concentration was determined by the bradford method with bovine serum albumin as a standard.

Strain and culture conditions. *Escherichia coli* HST08 and *E. coli* DH5α were used for cloning, following standard recombinant DNA techniques. *E. coli* BL21-Gold(DE3) was used for protein expression. Aspergillus flavus deletion mutants1 were used for isolation of ustiloxins. *Aspergillus oryzae* NSAR1, a quadruple auxotrophic mutant (*niaD*$^{-}$*, sC*$^{-}$*, ΔargB, adeA*$^{-}$), was used for the fungal expression.

Isolation of ustiloxin derivatives from *A. flavus* mutants

Mycelia of *A. flavus* deletion mutants were inoculated into a solid medium containing cracked maize (30 g) and uracil (30 mg) in 500 mL Erlenmeyer flasks for 1 week. The fungal mycelia were then extracted with 70% aqueous acetone (200 mL) for overnight at room temperature. After vaporizing the acetone, the water layer was washed with ethyl acetate and butanol and then subjected to C18 column chromatography eluted with stepwise gradient of CH3CN (0%, 5%, and 50%) with 0.1% TFA. The fraction containing ustiloxins was separated by HPLC (Shimazu Class VP system) equipped with Wakopak Navi C18-5 column (10 x 250 mm, A linear gradient from 5 to 20% of CH3CN with 0.1% TFA in water with 0.1% TFA over 10 min, and 20% CH3CN with 0.1% TFA for 10 min; flow rate of 3 mL/min). Further HPLC purification (Shimazu Class VP system) equipped with Wakopak Navi C18-5 column (10 x 250 mm): 5 to 10% CH3CN for 5 min and 10% CH3CN for 10 min, flow rate 3 mL/min) gave compounds as followed:

***N*-desmethylustiloxin F (2)** $[\alpha]_D^{25}$ -78.8 (c 0.65, H_2O), HR-ESIMS analysis (negative); calcd. for $C_{20}H_{27}N_4O_8$ $[M-H]^-$: 451.1834, found: 451.1829. The NMR data are shown on Table 3-3.

ustiloxin F (3) HR-ESIMS analysis (positive); calcd. for $C_{21}H_{31}N_4O_8$ $[M+H]^+$: 467.2136, found: 467.2180.

***S*-deoxyustiloxin H (4)** HR-ESIMS analysis (negative); calcd for $C_{24}H_{34}N_5O_{10}S$ $[M-H]^-$: 584.2032, found: 584.2030. The NMR data are shown on Table 3-3.

ustiloxin H (5) $[\alpha]_D^{25}$ -39.9 (c 0.34, H_2O), HR-ESIMS analysis (positive); calcd. for $C_{24}H_{35}N_5O_{11}S$ $[M+H]^+$: 602.2127, found: 602.2122. The NMR data are shown on Table 3-3.

ustiloxin C (6) HR-ESIMS analysis (positive); calcd. for $C_{23}H_{35}N_4O_{10}S$ $[M+H]^+$: 559.2068, found: 559.2108.

Table 3-3. NMR spectral data of **2**, **4**, **5**

	N-desmethylustiloxin F (**2**)		deoxyustiloxin H (**4**)		ustiloxin H (**5**)	
	δ_C	δ_H (multiplicity, *J* in Hz)	δ_C	δ_H (multiplicity, *J* in Hz)	δ_C	δ_H (multiplicity, *J* in Hz)
2	88.3	-	86.3	-	89.7	-
3	61.7	4.66 (s)	59.2	4.71 (s)	62.3	4.73 (s)
5	175.1	-	172.1	-	174.5	-
6	52.3	4.33 (q, 7.0)	49.6	4.43 (q, 7.0)	52.1	4.48 (q, 7.0)
8	169.9	-	166.2	-	168.3	-
9	62.5	3.90 (d, 9.5)	64.6	4.65 (d, 7.0)	68.7	4.20 (d, 10.3)
10	74.9	4.81 (d, 9.5)	73.8	4.98 (brs)	75.80	4.99 (d, 10.3)
11	133.3	-	129.1	-	130.6	-
12	125.5	7.26 (dd, 8.5, 2.0)	129.3	-	139.1	-
13	121.1	7.06 (d, 8.5)	119.2	7.14 (s)	116.0	7.63 s
14	153.3	-	151.2	-	154.6	-
15	144.7	-	141.4	-	148.5	-
16	126.5	7.41 brs	126.0	7.27 (brs)	126.4	7.43 brs
17	173.5	-	170.3	-	172.4	-
19 a	44.0	4.08 (d, 17.8)	43.3	3.88 (d, 17.0)	46.2	3.84 (d, 17.3)
19 b	-	4.00 (d, 17.8)	-	3.83 (d, 17.0)	-	3.78 (d, 17.3)
20	175.7	-	175.6	-	178.9	-
21	24.7	1.66 s	21.4	1.65 s	24.2	1.73 s
22 a	32.6	2.04 (dq 14.0, 7.5)	30.9	2.05 (dq 14.0, 5.5)	33.6	2.13 (dq, 13.5, 7.3)
22 b	-	1.72 (dq, 14.0, 7.0)	-	1.73 (dq, 14.0, 5.5)	-	1.70 (dq, 13.5, 7.3)
23	10.5	0.91 (t, 7.5)	7.7	0.98 (t, 7.5)	10.3	0.96 (t, 7.3)
24	18.1	1.18 (d, 7.5)	15.1	1.23 (d, 7.5)	17.8	1.18 (d, 7.0)
N-CH_3	-	-	32.1	2.78 s	34.2	2.76 s
2' a	-	-	35.2	3.61 (dd, 15.0, 6.5)	59.8	3.71 (dd, 13.7, 7.5)
2' b	-	-	-	3.43 (dd, 15.0, 6.0)	-	3.16 (dd, 13.7, 7.0)
3'	-	-	53.6	3.95 (t, 6.0)	53.8	4.27 (t, 7.3)
4'	-	-	172.7	-	174.2	-

Genomic DNA preparation

Genomic DNA was extracted from *A. flavus* CA14 according to the same method of chapter 1 experimental section.

Preparation of expression plasmids. The *ustA, ustQ, ustYa, ustYb, ustM*, and *ustT* were amplified

from genomic DNA of *A. flavus* with primer set as shown on Table 3-4. PCR reactions were performed with the KOD-Plus-Neo (TOYOBO). Each PCR product was inserted into appropriate restriction site (site 1 and/or site 2) of pUARA2, pUSA2, or pAdeA2 using In-Fusion Advantage PCR cloning kit (Clontech Laboratories) to construct expression plasmids.

Table 3-4. Oligonucleotides used for construction of *A. oryzae* expression plasmids

Insert	Restriction site	Sequence 5'-3'	Size vector
ustA	*Kpn*I	F: AATTCGAGCTCGGTACATGAAGCTTATTCTTACTCTACTCG R: TTAATGCCCTCCATGGCGCTTGTC	770 bp pUSA2
ustQ	*Nhe*I	F: ATGGCCGTGGAATATTTCCAGGAAAAACTA R: ACGACTACCCGGGTCACTAATACGTATAACATA	1350 bp pUSA2
ustYa	*Nhe*I	F: ATCGATTTGAGCTAGATGGCAGAGCGCTCATCT R: TAGTGCGGCCGCTAGTTAATGAATCCCATACGTCG	946 bp pUARA2
ustYb	*Kpn*I	F: CGGAATTCGAGCTCGATGTCGGATCTCTACGCAC R: ACTACAGATCCCCGGCTAATTATGCTTAGCATCCAC	974 bp pUARA2
ustM	*Nhe*I	F: ATCGATTTGAGCTAGATGGAAACAATCCTATCCAG R: TAGTGCGGCCGCTAGTCAAGCGCCCAGCTCCAG	891 bp pAdeA2
ustT	*Kpn*I	F: CGGAATTCGAGCTCGATGTCGGGCACCTCTCCA R: ACTACAGATCCCCGGTCAATACGACCTTGCTGCA	1791 bp pUARA2

Transformation of *Aspergillus oryzae*.

Transformation of *A. oryzae* NSAR1 or transformant (1.0 x 108 cells) were performed by the protoplast-polyethylene glycol method the same with chapter 1 experimental section. To construct transformants harboring ustiloxin B synthase genes, pUSA2-ustA/Q, pUARA2-ustYa/Yb, pUARA2-ustYa, pUARA2-ustYb, pAdeA2-ustYb, pAdeA2-ustYb/M, pUARA2-ustT were used for the transformation. The following transformants were obtained: AO-*ustAQYaYb* (co-transformation), AO-*ustAQYa*, AO-*ustAQYb*, AO-*ustAQYaYb* (stepwise incorporation), AO-*ustAQYaYbM*, AO-*ustAQYaYbMT*.

Extraction of metabolites.

Mycelia of *A. oryzae* transformants were inoculated into a solid medium containing polished rice (20 g) and adenine (10 mg). Each culture was incubated at 30°C for 7 days followed by extraction with 70% acetone/H_2O overnight. After centrifuge, 300 μL aqueous acetone supernatant was evaporated out of acetone and washed with an equal volume of ethyl acetate to give the analytical sample.

Analysis of the metabolites.

An 5 μL aliquot of each water extract was analyzed by UPLC (Waters ACQUITY UPLC H-Class system) equipped with a ACQUITY UPLC BEH C18 column (50 mm ×2.1 mm, 1.7 μm particle size) at the following conditions: Flow rate; 0. 7 mL/min, Solvent system: A linear gradient from 5 to 50% of HCOOH with 0.1% TFA in water with 0.1% HCOOH over 2 min.

Isolation of N-desmethylustiloxin F (2) from *A. oryzae* transformant AO-*ustAQYaYb*.

Mycelia of AO-*ustAQYaYb* was inoculated into a solid medium containing polished rice and adenine (10 mg) in 500 mL Erlenmeyer flasks for a week. The fungal mycelia were than extracted with 70% aqueous acetone (200 mL) for overnight at room temperature. After vaporizing the acetone, the water layer was washed with AcOEt and butanol and then subjected to C18 column chromatography. The fraction containing 2 was separated by HPLC (Shimazu Class VP system) equipped with Wakopak Navi C18-5 column (10 x 250 mm, a linear gradient from 5 to 20% of CH3CN with 0.1% TFA in water with 0.1% TFA over 10 min, and 20% CH3CN with 0.1% TFA for 10 min; flow rate of 3 mL/min). Further HPLC purification (Shimazu Class VP system) equipped with Wakopak Navi C18-5 column (10 x 250 mm): 5 to 10% CH_3CN for 5 min and 10% CH_3CN for 10 min, flow rate 3 mL/min) gave 2 (Yield: 3.5 mg/500 g rice).

mRNA preparation and cDNA synthesis of *A. flavus* strain CA14

mRNA preparation and cDNA synthesis of *A. flavus* strain CA14 was cultured in V8 juice media (100 mL in 500 mL Erlenmeyer flask) for 2 days at 30°C (200 rpm). Total RNA was extracted from each dried mycelia using TRIzol® Reagent (Invitrogen) according to the manufacturer's instructions. The total RNA treated with DNase I (Life Technologies) was used for reverse transcription. Complementary DNA (cDNA) was synthesized with PrimeScriptTM II 1st strand

cDNA synthesis kit (Takara) using the oligo dT primer according to the manufacturer's instructions.

Overexpression of UstF1, UstF2, and UstD in *E. coli.* The ustF1 (Conducted by Mr. Igarashi), ustF2 and ustD genes were PCR amplified from the cDNA of *A. flavus* CA14 using primers (Table 3-5). The PCR products were directly inserted into the BamHI or KpnI-digested pMALc4E to generate pMALc4E-ustF1, pMALc4E-ustF2, pMalc4E-ustD. These plasmids were separately introduced into E. coli BL21-Gold (DE3) for overexpression. The transformants was grown at 37°C at an OD600 of ~0.6 in a 500 mL flask. After the culture was cooled at 4°C, isopropyl β-D-thiogalactopyranoside (0.1 mM) was added to it. After incubation at 16°C for 18 h, the cells were harvested by centrifugation at 4000 rpm. The harvested cells were resuspended in disruption buffer (20 mM Tris–HCl (pH 7.4), 200 mM NaCl, EDTA 1 mM, DTT 1 mM) and disrupted by sonication. After centrifugation, the supernatant was applied to an amylose column to purify the expressed protein. The concentration of purified proteins was determined by Bradford method.

Table 3-5. Oligonucleotides used for construction of *E. coli* expression plasmids

Insert	Restriction site	Sequence 5'-3'	Size vector
ustF1	*BamH*I	F: ACCGGAATTCGGATCCATGACTGTTTCTCAGGTTCG R: GCTTGACGGTGTAGAATTAATCCTAGGAGATCTCAGCT	1515 bp pMalc4E
ustF2	*Kpn*I	F: GATGACGATGACAAGATGGCCAATCCTCAAACCA R: AGGATCCGAATTCCGCTACTTGTTAACTTGAGCCC	1428 bp pMalc4E
ustD	*Kpn*I	F: GATGACGATGACAAGATGAAATCGGTAGCAACCTC R: AGGATCCGAATTCCGCTAGGTATCCCGCGTGAC	1320 bp pMalc4E

UstF1 and UstF2 Assays. Typical conditions are as follows; a reaction mixture (40 μL of Tris-HCl buffer (pH 8.0)) containing 4 μM of the substrate, 2 mM NADPH, 5% glycerol, 0.6 μM of UstF1

or UstF2) was incubated at 30°C. The reaction was quenched by the addition of methanol (40 μL) and the resultant mixture was vortexed and centrifuged at 12,000 x g. The supernatant was directly analyzed UPLC (Waters ACQUITYTM UPLC H-Class system) equipped with a ACQUITYTM UPLC BEH C18 column (50 mm ×2.1 mm, 1.7 μm particle size) at the following conditions: Flow rate; 0. 7 mL/min, Solvent system: A linear gradient from 5 to 50% of CH3CN with 0.1% HCOOH in water with 0.1% HCOOH over 2 min. An ACQUITY QDa MS was used for detection.

Large scale reaction with UstF2

Large scale reaction of **5** (2.0 mg) with UstF2 yielded **7** (1.4 mg, 72.6%) as an isomeric mixture (*E/Z* = 2/1). $[\alpha]_D$ 27 21.6 (c 0.45, H_2O). HR-ESIMS analysis (positive); calcd. for $C_{23}H_{34}N_5O_{10}S$ $[M+H]^+$ 572.2021, found: 572.1983. NMR data is shown in Table 3-6.

UstD Assays.

Typical conditions are as follows; a reaction mixture (50 μL of Tris-HCl buffer (pH 7.4)) containing 100 μM of the substrate, 0.4 μM UstD, 400 μM aspartic acid was incubated at 30°C. The reaction was quenched by the addition of methanol (50 μL) and the resultant mixture was vortexed and centrifuged at 12,000 x g. The supernatant was directly analyzed UPLC (Waters ACQUITYTM UPLC H-Class system) equipped with a ACQUITYTM UPLC BEH C18 column (50 mm×2.1 mm, 1.7 μm particle size) at the following conditions: Flow rate; 0. 7 mL/min, Solvent system: a linear gradient from 5 to 50% of CH_3CN with 0.1% HCOOH in water with 0.1% HCOOH over 2 min. An ACQUITY QDa MS was used for detection.

Transformation of oxime into geminal diol in acidic condition.

To a solution of of **7** (0.9 mg, 1.5 μmol) in water (10 mL) was added TFA (20 μL, 0.26 mmol) and the mixture was sitrred at room temperature for overnight. The reaction mixture was directly subjected to 40C18 open column (Wakosil, 30~50 μm, MeCN/H_2O 5/95). The fraction containing **9** was concentrated in vacuo and further purified by HPLC (Shimazu Class VP system) equipped with Wakopak Navi C18-5 column (10 x 250 mm, A linear gradient from 5 to 20% of CH3CN with 0.1% TFA in water with 0.1% TFA over 10 min, and 20% CH3CN with 0.1% TFA for 10 min; flow rate of 3 mL/min; detection at 290 nm) to afford **9** (0.365 mg, 40%). $[\alpha]_D^{26}$ -7.2 (c 0.16, H_2O). HR-ESIMS analysis (positive); calcd. for $C_{23}H_{35}N_4O_{11}S$ $[M+H]^+$: 575.2018, found: 575.2004. NMR

data is shown in Table 3-6.

	7 (*E*/*Z* mixture)		**9**	
	δ_C	δ_H (multiplicity, *J* in Hz)	δ_C	δ_H (multiplicity, *J* in Hz)
2	89.1	-	89.5	-
3	62.2	4.73 (s)	62.0	4.70 (s)
5	174.5	-	174.6	-
6	51.9	4.42 (q, 7.0)	52.1	4.44 (q, 7.0)
8	169.8	-	168.2	-
9	69.6	4.04 (d, 11.0)	68.6	4.19 (d, 10.0)
10	76.3	4.92 (d, 11.0)	75.8	4.96 (d, 10.0)
11	130.9	-	130.4	-
12	136.8 (Major)	-	138.9	-
	137.6 (Minor)	-	-	-
13	117.2 (Major)	7.42, s	116.5	7.60, s
	116.6 (Minor)	7.53, s	-	-
14	154.3	-	154.7	-
15	148.4	-	148.1	-
16	126.6	7.35, brs	126.9	7.42, brs
17	172.5	-	173.0	-
19 a	46.2	3.82 (d, 17.0)	45.6	3.95 (brs)
19 b	-	3.76 (d, 17.0)	-	-
20	178.9	-	176.6	-
21	24.1	1.74, s	24.4	1.73, s
22 a	33.7	2.11 (dq, 14.3, 7.5)	33.4	2.10 (dq, 14.0, 6.5)
22 b	-	1.70 (dq, 14.3, 7.5)	-	1.69 (dq, 14.0, 6.5)
23	10.3	0.99 (t, 7.0)	10.4	0.96 (t, 7.0)
24	17.7	1.18 (d, 7.0)	17.9	1.19 (d, 7.0)
N-CH_3	34.7	2.66 (s)	34.3	2.75 (s)
2’ a	65.2	3.65 (dd, 12.0, 4.3)	*	*
2’ b	-	3.56 (dd, 12.0, 6.3)	-	*
3’	146.0 (Major)	7.43 (s)	88.9	5.48 (s)
	144.2 (Minor)	6.96 (s)	-	-

Table 3-6. NMR data of **7** and **9**

Reduction of 9 to give ustiloxin C (6)

To a solution of **9** (0.3 mg) in water (500 μL) was added $NaBH_4$ (2 mg, 248 μmol). After being stirred for 90 min at r.t., the reaction mixture was quenched by the addition 50 μL TFA. The mixture was concentrated in vacuo and purified by HPLC (Shimazu Class VP system) equipped with Wakopak Navi C18-5 column (10 x 250 mm). HPLC purification conditions: A linear gradient from **5** to 20% of CH_3CN with 0.1% TFA in water with 0.1% TFA over 10 min, and 20% CH3CN with 0.1% TFA for 10 min; flow rate of 3 mL/min; detection at 290 nm. Purified product (0.19 mg, 65%) was identified as ustiloxin C from the reported ^1H NMR data[95] .

Chapter 4. Fungal RiPP asperipin-2a biosynthesis study

4-1. Asperipin-2a and its biosynthetic gene cluster.

Ustiloxin B biosynthetic gene cluster is the first example of an RiPP from filamentous fungi[78], and its biosynthetic pathway has been elucidated as described in chapter 3. On its cluster, the most characteristic genes are *ustA* encoding the precursor peptide with repeated YAIG motif (Figure 4-1), and *ustYaYb* encoding novel oxidative cyclases.

Based on the features of precursor peptide protein (signal peptide, repeated motif, kex2-site), Nagano *et al* identified nearly 2000 precursor peptide candidates from fungal genomes. UstYa homologues search were also conducted by the same group. From 20 Aspergilli genomes, 244 UstYa/Yb homologues (242 UstYa and 191 UstYb homologues) were detected. To identify the gene clusters including both UstYa homologue and RiPPs precursor candidate genes, the region within 10 kbp of the UstYa homologue genes were analyzed. Results showed that nearly 100 sets of putative RiPPs gene clusters were found.

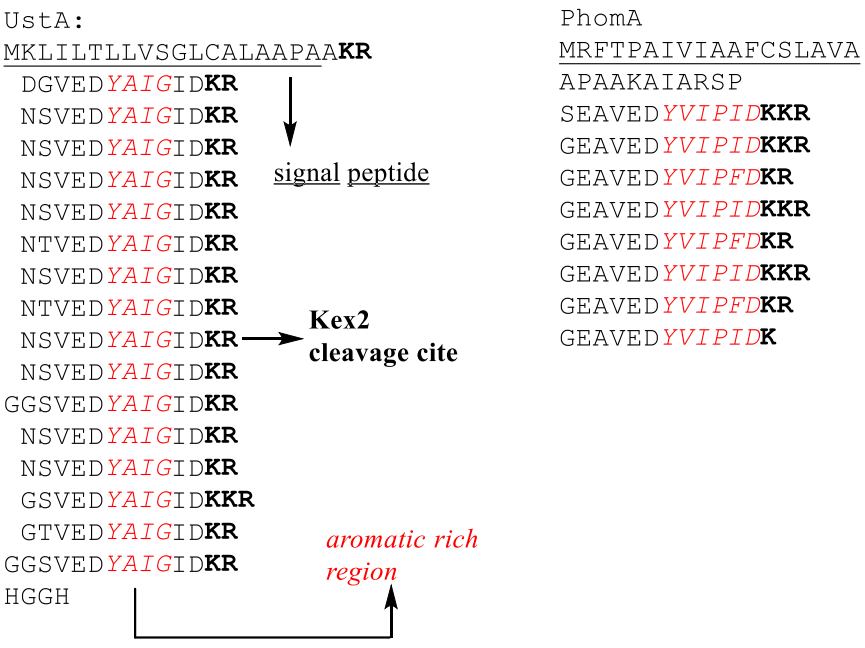

Figure 4-1. Precursor peptide protein sequences of UstA and PhomA

Among them, they found a simply gene cluster that consisted of four genes denoted here as *aprA* (RiPPs precursor candidate gene), *aprY* (encoding UstYa homologue), *aprT* (encoding MFS transporter) and *aprR* (encoding isoflavone reductasea) shown in Table 4-1.

Table 4-1. Homologous genes and proposed gene functions in the asperipin-2a BGC

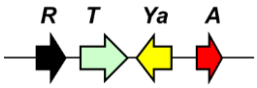

Gene ID in NCBI	Gene name in this thesis	Homologue gene ID in *A. orzyae* (sequence identity)	Proposed function
AFLA_041370	*aprR*	AOR_1_508054 (99%)	Isoflavone reductase related gene
AFLA_041380	*aprT*	AOR_1_510054 (99%)	MFS transporter
AFLA_041390	*aprY*	AOR_1_512054 (99%)	UstY homologue
AFLA_041400	*aprA*	AOR_1_514054 (92%)	Precursor peptide protein

After confirming these genes co-expressed each other in the production of asperipin-2a, they employed gene deletions of *aprA* and *aprY* and found that the resultant mutants abolished the production of asperipin-2a. Then they determined the unique bicyclic structure of this compound and established that it has one of the core peptide sequence FYYTGY (Figure 4-2). These data suggested that AprY may catalyze two oxidative cyclizations of core peptide to afford a macrocyclic peptide. Compared with ustiloxin B biosynthesis that requires four genes for construction of macrocyclic core scaffold, asperipin-2a biosynthesis is rather simple, indicating that oxidative cyclization system with a single enzyme AprY may readily reconstitute *in vitro* using synthetic peptides.

Based on these observations, the author decided to reconstitute the biosynthetic pathway of asperipin-2a.

(A)

AprA
MHLSRYIAVLLSASSFVSALPLQND
VISDDGKPIDAIMATAMEHKVVNP
ENLDATPATPENPEDLD**KR**
*FYYTGY***KR**NAETPEDLD**KR**
*FYYTGY***KR**NAETPEDLD**KR**
*FYYTGY***KR**NAETPEDLD**KR**
*FYYTGY***KR**NAETPEDLD**KR**
*FYYTGY***KR**NAETPDDLD**KR**
*FYYTGY***KR**NAETPEDLD**KR**
*FYYTGY***KR**NAETPEDLD**KR**
*FYYTGY***KR**TAETPEDLD**K**

(B)

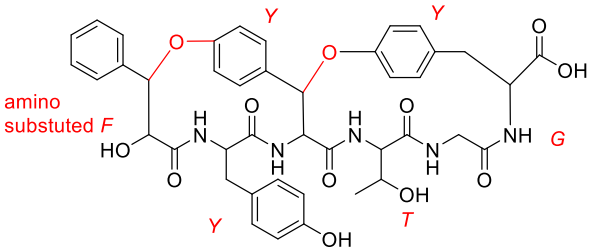

asperipin-2a

Figure 4-2. (A) primary amino acid sequence of AprA. (B) Planar structure of asperipin-2a

4-2. Heterologous expression of asperipin-2a biosynthetic gene cluster.

4-2-1 Construction of plasmids and transformation of *A. oryzae* NSAR1

As mentioned in 4-1, four genes were proposed to constitute the BGC for asperipin-2a production, thus the author started heterologous expression of these genes. AprA, Y, T have their corresponding counterparts in ustiloxin B BGC, so their functions were easily predicted. However, *aprR* is unique in asperipin-2a BGC, and its function remains unknown. We transformed the wild-type NSAR1 strain with plasmids as Table 4-2 shows. While *aprY* and *aprA* gene deletion experiments in *A. flavus* conducted by Nagano *et al* [10] proved they were involved in asperipin-2a production, the AO-*aprAY* transformant was constructed to examine whether these two enzymes-minimal set was enough to afford asperipin-2a or not. AO-*aprAYaT* transformant was constructed here to elucidate AprR's function. Also, the transporter's function could be checked in AO-*aprAYaR* transformant.

Table 4-2. *A. oryzae transformants and* corresponding plasmids

*A. oryza*e transformant	Transformation plasmids
AO-*aprAYRT*	pUARA2-*aprAY* pAdeA2-*aprRT*
AO-*aprAYR*	pUARA2-*aprAY* pAdeA2-*aprR*
AO-*aprAYT*	pUARA2-*aprAY* pAdeA2-*aprT*
AO-*aprAY*	pUARA2-*aprAY*

4-2-2. LC-MS analysis of the metabolites produced by the transformants.

After obtaining the transformants the author cultured them in rice medium and potato/starch medium to screen the production of metabolites. As potato/starch medium gave a cleaner background, their UPLC/MS results were shown in Figure 4-2. AO-*aprAYaRT* produced a new peak corresponding to asperipin-2a, indicating that these four genes are sufficient for heterologous production of asperipin-2a. Asperipin-2a was also isolated from the AO-*aprAYaRT* rice medium. The yield is 1.7 mg/Kg rice, 5 times the amount of that isolated from *A. flavus* cultured in maize[10]. The pure compound was subjected to extensive NMR analysis.

On the other hand, asperipin-2a production was not observed in AO-*aprAY* (data not shown) and dramatically decreased in transformants lacking either AprR or AprT, and no intermediates were observed. As shown in Table 4-1, *A. oryzae* wild type genome has the same gene cluster with almost identical enzyme sequences. The low expression of AprR's counterpart AOR_1_508054 in AO-*aprAYaT* transformant would result in trivial production of asperipin-2a.

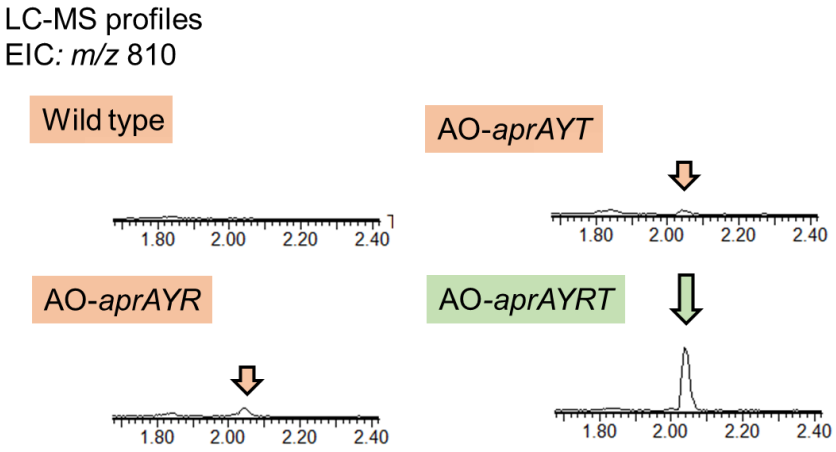

Figure 4-2. The LC/MS profile of *apr* gene transformants

Although the function of AprR could not be determined currently, yet some information could still be obtained from sequence analysis of AprR. It contains NAD(P)H-binding motif and conserves homology to isoflavone reductase (IFR) which converts 2'-hydroxyformononetin stereospecifically to

(*3R*)-vestitone (Scheme 4-1A)[96]. Thus AprR was speculated to have reductive activity to reduce ketone double bond. Accordingly the proposed the biosynthetic pathway of asperipin-2a was shown in scheme 4-1 B.

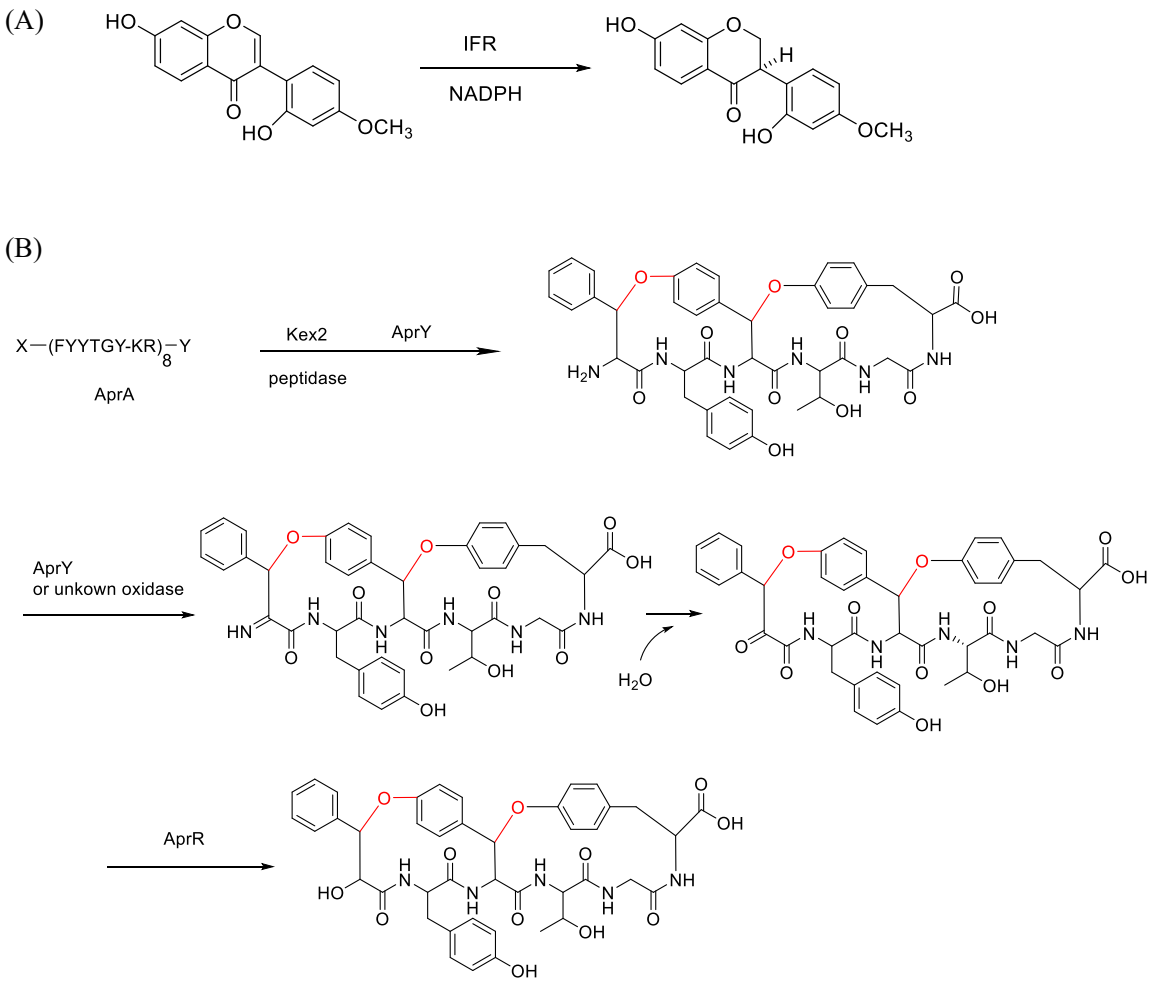

Scheme 4-1. A) Double bond reduction catalyzed by AprR homologue IFR. (B) Proposed biosynthetic pathway of asperipin-2a

Precursor peptide AprA was digested by Kex2 and unknown peptidase to give FYYTGY. UstYa homologue AprY catalyzed two rounds of oxidative cyclizations to afford bicyclic intermediate through ether bonds. Amino group of the phenylalanine residue was oxidized by either AprY or unknown oxidase to imine which would readily be hydrolyzed to ketone. Finally, AprR would reduce the ketone into hydroxy group at the α position.

4-3. Absolute configuration of asperipin-2a.

The absolute configuration of asperipin-2a, which has eight chiral centers, had not been determined yet. Since asperipin-2a is derived from peptide, the advanced Marfey's method[97] was applied to determine its stereochemistry. However, the existence of two ether rings interfered to obtain at least 3-phenyllactic acid, the second and the third tyrosine residues. For this reason, hydrogenolysis of asperipin-2a was initially conducted. Thus, the following Scheme 4-2 was designed to determine the absolute configuration of asperipin-2a.

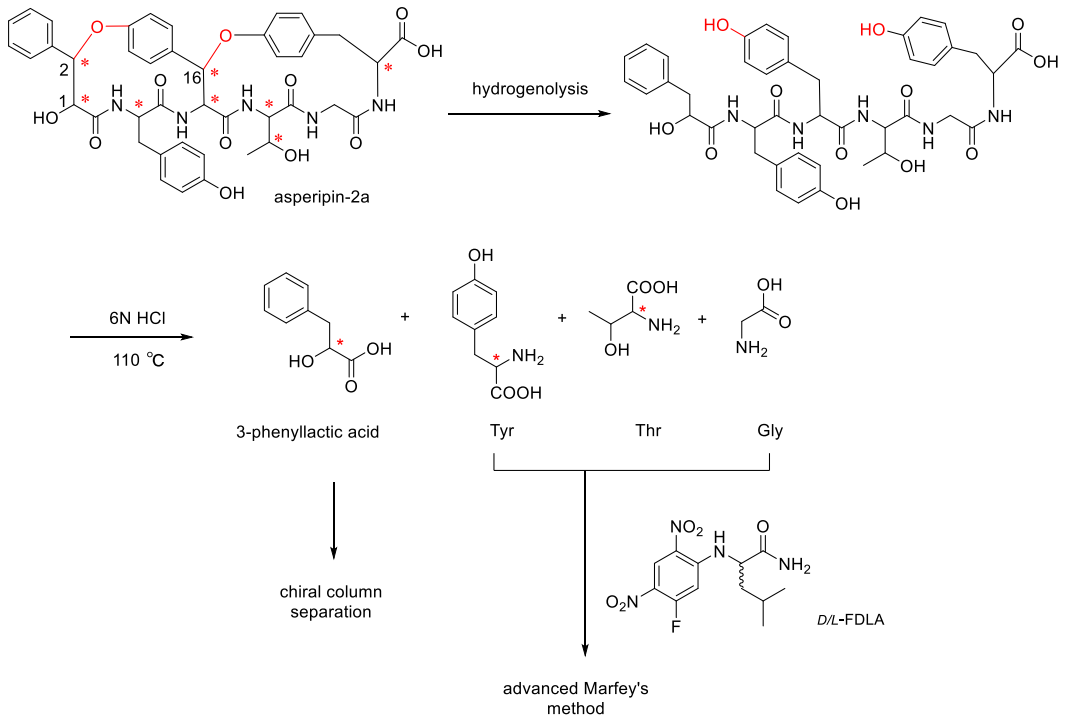

Scheme 4-2. Experiment design for asperipin-2a absolute configuration determination

Since hydrogenolysis using H_2 and Pearlman's catalyst[98] did not proceed, the hydrogen donor was changed from H_2 to $HCOONH_4$ catalyzed by 10% Pd/C[99] as shown in scheme 4-3.

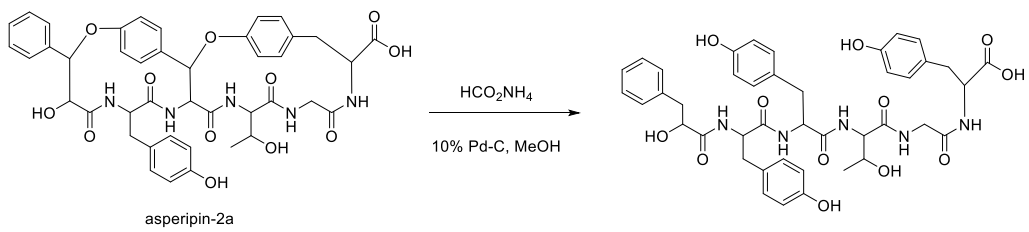

Scheme 4-3. Hydrogenolysis of asperipin-2a

Purified linear product was subjected to hydrolysis in 6 N HCl for 13 hours. After evaporating out of HCl, the product mixture was analyzed by UPLC-MS equipped with chiral column (CHIRALPAK® ZWIX(+)). The LC-MS profile (Figure 4-3) was compared with that of authentic (*R*)- and (*S*)-3-phenyllactic acid, and the 3-phenyllactic acid residue of asperipin-2a was determined to be *R* configuration.

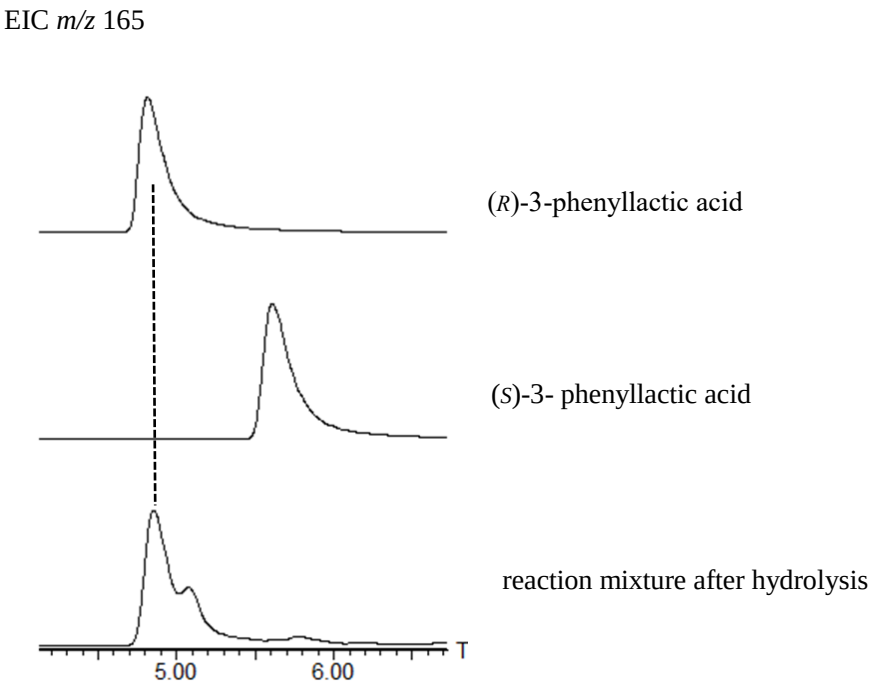

Figure 4-3 LC-MS analysis of hydrolyzed products with chiral column for separation of (*R*)- and (*S*)-enantiomer of 3-phenyllactic acid.

Following the last step of scheme 4-2, the chiral derivatization of hydrolyzed products using L-FDLA was conducted. Derivatized products were analyzed by UPLC UV or MS as shown in Figure 4-4. By comparing with the synthetic standards, the tyrosine and threonine residues are determined to be L configuration. Based on the peak area in the UPLC-UV analysis, the mole ration of derivatized L-tyrosine and glycine was estimated to be 3 in the reaction mixture, further proving that the asperipin-

2a was completely linearized after hydrogenolysis and all the three tyrosine residues are of the same configuration.

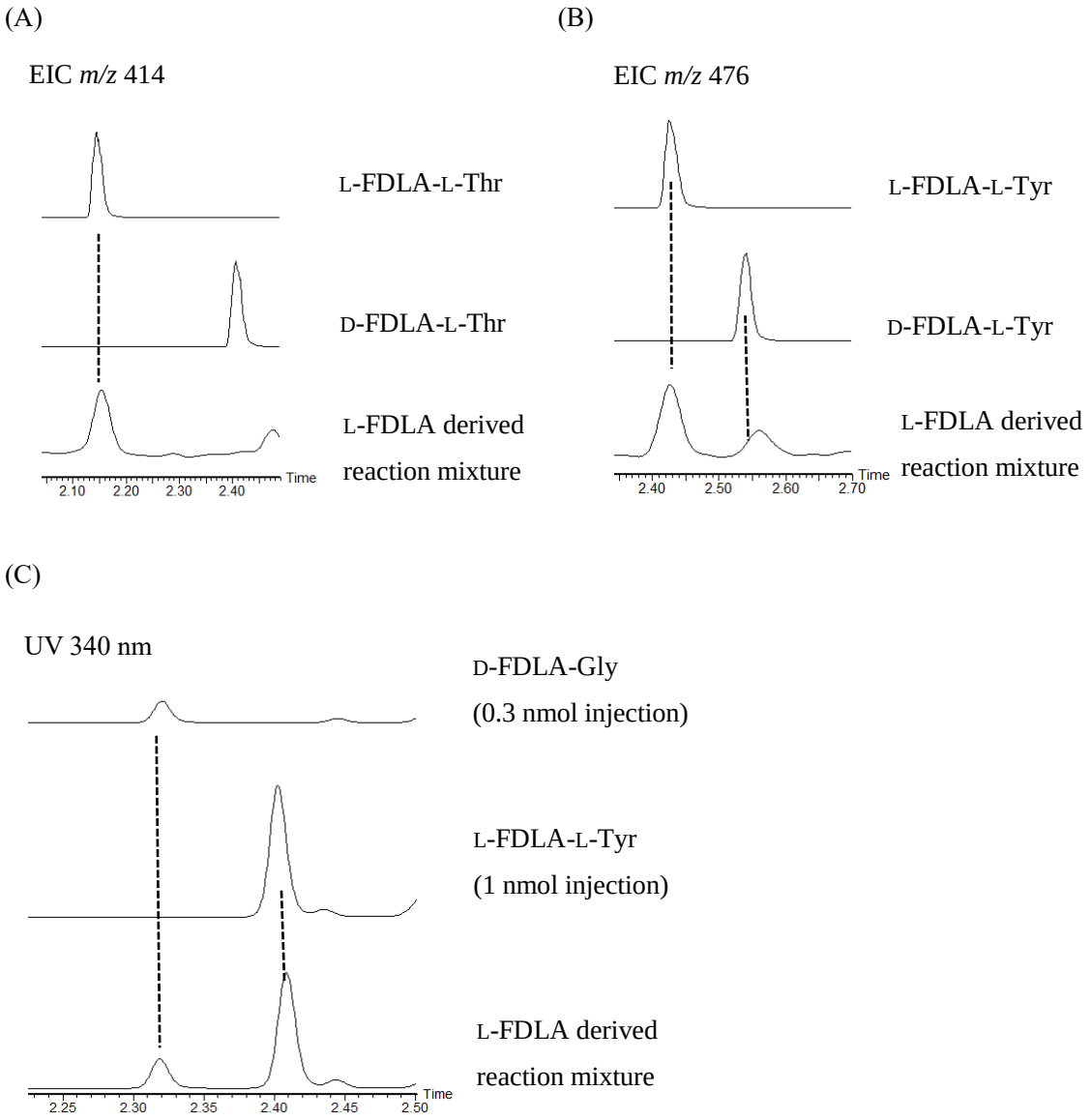

Figure 4-4. LC-MS and HPLC profiles of FDLA-derivatives of hydrolyzed asperipin-2a. A) Extracted ion chromatograms for FDLA-Thr. B) Extracted ion chromatograms for FDLA-Tyr. C) UPLC-UV chromatograms for FDLA-Gly and FDLA-Tyr at 340 nm

After determination of the absolute configurations of 3-phenyllactic acid and amino acid residues, the

author moved to determine the stereochemistry of ether moieties at C2 and C16. NOESY correlations observed in Figure 4-5A allowed to fix the confirmation of 14-membered para-cyclophane system A, thus making the relative stereochemistry at C15 and C16 determined. Although determinative NOE correlation was not observed at H2, the *J* value between H1 and H2 was nearly 0, indicating their dihedral angel was nearly 90° with the H2 facing upward (Figure 4-5).

(A)

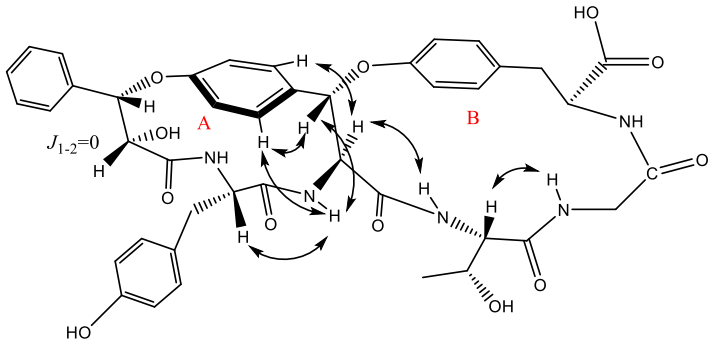

(B)

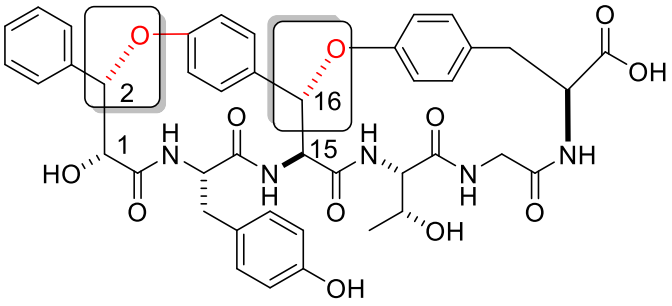

Figure 4-5. (A) NOE correlation and (B) absolute configuration of asperipin-2a.

Taken together, the author determined the absolute configuration of asperipin-2a as shown in Figure 4-5B. Notably, the C-O bond formation in the sequential cyclization occurs from the same orientation, suggesting that cyclase catalyzes stereospecific C-O bonding formation with the same mechanism. In addition, the orientation of C1 hydroxy group which might be controlled by AprR, was the opposite of that of amino group in the natural L-phenylalanine.

As mentioned in section 3-3, UstYaYb were proposed to abstract hydrogen at β position of amino acids and to form the ether ring through radical mechanism. In the case of asperipin-2a, AprY abstracted hydrogen at β position of phenylalanine and the second tyrosine, the resultant radicals were attacked by phenols from the same orientation in the active site of AprY (Scheme 4-4). Notably, a single enzyme AprY catalyzed two rounds of oxidative cyclizations.

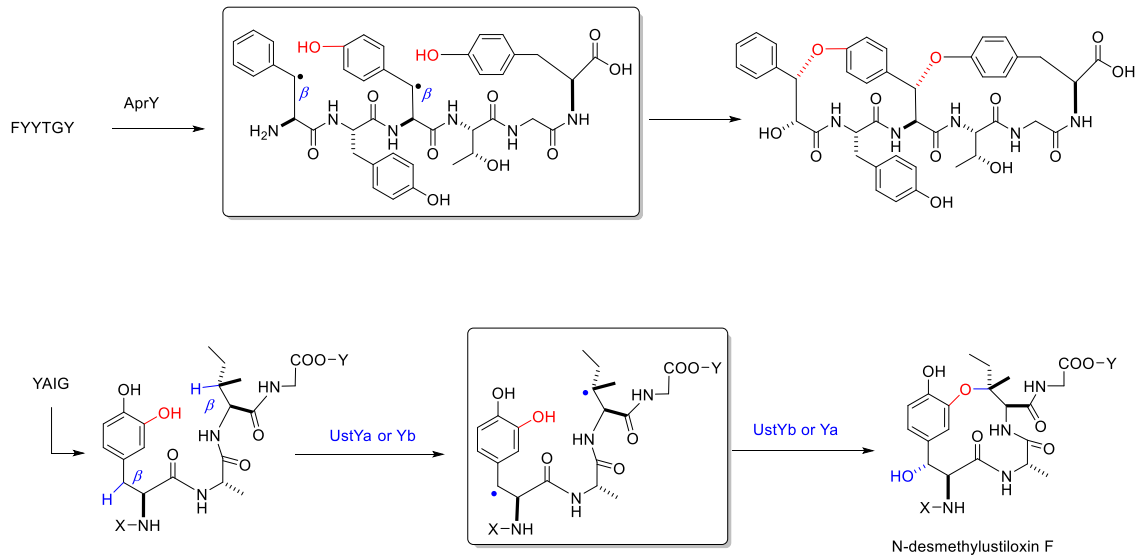

Scheme 4-4. Proposed mechanism of AprY and UstYaYb cyclization mechanism

4-4. Discussion

In this thesis, the author demonstrated the reconstitution of two RiPPs core cyclic peptides essential for the biosynthesis of ustiloxin B and asperipin-2a. While ustiloxin B had complex macrocyclic core assembly system (1 protein and 3 enzymes) and modification reactions (5 enzymes), asperipin-2a had very simple system (1 protein and 1 enzyme) and a simple modification (1 reductase). Recent bioinformatics analysis revealed a significant number of RiPPs gene cluster in the various fungal

genomes. In general, these clusters consisted of mainly precursor peptide and UstY homologue with a few modification enzymes. This indicated that asperipin-2a type RiPPs are major group in this family and elucidation of catalytic mechanism of AprY is very important to understand RiPPs biosynthesis. Observation that a single DUF3328 protein AprY catalyzes two-step oxidative cyclization in the biosynthesis of asperipin-2a suggested that AprY is suitable for in vitro study of macrocyclization using various synthetic peptide.

The sequence alignment of AprY, UstYaYb and phomYb (which was the UstY homologue found in the BGC of phomopsin[80]) was shown in Figure 4-6. The presence of HxxHC motif that is reminiscent of non-heme iron oxidases suggests involvement of metal cofactors in the catalysis[88].

```
AprY        MEPFSKFFKSF---------RRYHRFHPLDSS-SASD-DELAGKYEEHLLMDERLKRET-
UstYb       ----------------------------------MSD-LYAHRESDEYLLKPEHFAEKK-
UstYa       --MFSYFFRSREIKMAERSSNGYKEVPV-----RHSEESTIAEEEKDTLLEDRSYSRRDR
phomYb      -------------------MDGYSSKKPRSASPSRSSLTEVEEEERDTLLKTVSLEEEDK
                                             *.       :  : **       ..

AprY        -------VIFKSRIWILLTITNLIILGITVSMIVTSHCQLYAGKN--ADLRPISWWSPIL
UstYb       ---------NRPKRWDCLRPIIYTSLAFVGFIEILFFGIFFAQVTRKTPERLLGELNGLV
UstYa       K------RSCSKAVWFLIALLLLSNIGLLGGLIH-----YFRKTH--HKEKDVPWLP--P
phomYb      SGENGPRKLRRSRFLYAIGILMLSNIAFIAAFLT-----VFVQKRALEPARLPPWAP--P
                              :       :. :   :        :         :

AprY        DAIEIPTYETTLNGTFFA---KPEVSIAREEPGPENDADWEQYETIRTHIVSREDILRLG
UstYb       GDFP-------ARRVIFRSDPLAASDHKTEESRNATMNNWLSYMPRGNGFIAVNQTERYT
UstYa       KTTP-------TRKLF-VF-----QTLYGEPLNPEAEKAWDELMPIGRGFVNINNDTALP
phomYb      ERYE--------SRVF-KY-----MDVYGGEPGPKSEEAWTNLIPKGKGWIKVHNETAIP
                              :                        * .       :  .:
```

```
AprY        KDPDTVMRFDNDYWGFGDDAYMVQLDVMHQIHCLNMLRKAAFHDYPGYVPTGA--H----
UstYb       LPPPI-K-------QLGQDTY--SIAVFHQLHCLYAIMSVYDDLAAAKSAADLNAHHSRD
UstYa       DQPGLDQ-------SLPQQRA--MISVFHQLHCIYMTREGYYAAREG--------------
phomYb      DMPGLDQ-------SLPEQSA--LVSVFHQLHCLYMTRAGYFAARSG--------------
              *             : ::      : *:**:**:              .
                                      HxxHC motif
AprY        ------TDANNTHASRWTHLGHCVDILLQNIQCNANTEVITLAWVEGRTQPW--PDFSVN
UstYb       DTHSNEHPHEQVHVHSHDHVDHCFQYLRQSLLCCGDTA---LEGQDPRTDNPGTDGTGAV
UstYa       ----------NLDQVNAAHLMHCWDYLRQAIMCHADTT---LEWIPAPPNDKGSTGWGVE
phomYb      ----------NLDEVNVVHVSHCWDYLRQAIMCHSDTT---LEWLHAPPDNFGSTGWGYE
                     : .      *: ** : * * : * .:*    *       :     . .
                              HxxHC motif
AprY        RKCRDFEAIYKWQLENSVDAGKFDRMPIPHDAYVWPAPWENRESELGEKLGKHQKQEGVL
UstYb       HICKDFEGILAWADSRRLVDAKHN-----------------------------------
UstYa       HTCGDFDAIARWAEDNRLKTTYGIH-----------------------------------
phomYb      HQCRDYEAIFAFATEHRAGERQVIHG-----------------------------------
            : * *::.*  :  ..

AprY        GQAGHQHTKRHE
UstYb       ------------
UstYa       ------------
phomYb      ------------
```

Figure 4-6. Amino acids sequence alignments of UstY homologues

Although containing macrocyclic ether rings that are also found in ustiloxin B and phomopsin, asperipin-2a possesses the following unique features: 1) It is derived from $FY_1Y_2TGY_3$ containing 4 aromatic rings. 2) it contains unique bicyclic ether rings cyclized between Phe benzylic C with Tyr2 phenol O; and Tyr2 benzylic C with Tyr3 phenol O. To undergo these transformations, two oxidative cyclizations are required. 3) there is no hydroxylation at benzylic carbon observed in ustiloxin B and phomopsin. Instead, the phenylalanine amino group was replaced by hydroxy group. These points indicate that asperipin-2a belongs to a novel kind of fungal RiPPs.

We compared biosynthetic gene clusters of ustiloxin B, phomopsin and asperipin-2a together with their structures (Figure 4-7).

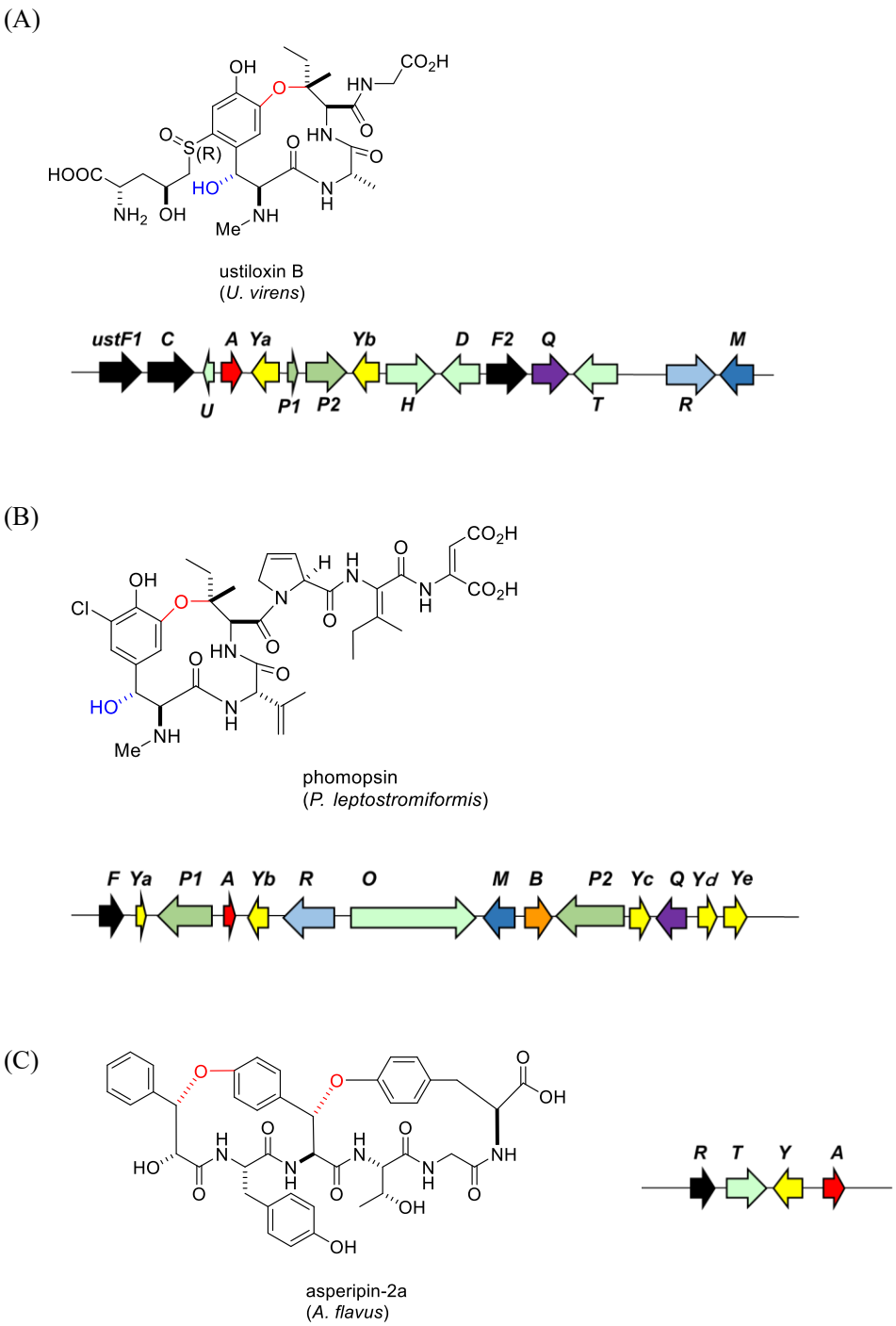

Figure 4-7 Structures of fungal RiPPs and their BGCs. A) ustiloxin B. B) phomopsin. C) asperipin-2a.

The oxidative modifications involved in formation of ustiloxin B (not including tyrosine residue sidechain modifications), phomopsin and asperipin-2a are shown in Table 4-3 as well as the UstY homologues on each BGC. Of particular interest is that the number of oxidative modifications on each

compound reflects the number of UstY homologues on corresponding BGC. Thus we proposed that UstY homologues are multifunctional enzymes catalyzing oxidative cyclization, hydroxylation, double bond formation and chlorination. Different numbers of UstY homologues may bring the oxidative state diversity in fungal RiPP products.

Table 4-3. Oxidative modifications and UstY homologues on their BGCs

compounds	putative oxidative modifications[a]	UstY homologues on BGC
ustiloxin B	➢ ether ring formation ➢ benzylic hydroxylation	UstYa, UstYb
phomopsin	➢ ether ring formation ➢ benzylic hydroxylation ➢ chlorination ➢ double bond formation×3	Phom A~E
asperipin-2a	➢ ether ring formation	AprY

[a] Not including ustilxoin B tyrosine residue sidechain modifications which had been characterized in chapter 3.

Another intriguing issue that needs to be discussed is that, why multiple core peptide motifs appear in the precursor pepetides of fungal RiPPs, while usually only one core peptide motif is retained in bacterial RiPP precursor peptides. It is known that the average cellular transcription rate is about two mRNA molecules per hour and translation rate constant of about 140 proteins per mRNA per hour[100]. A plausible hypothesis can be proposed that multiple repeated sequence can response more rapidly for production of core peptides for production of RiPPs, further suggesting that the RiPPs play some significant roles in fungal life cycles.

Conclusions

In this chapter, biosynthetic study of asperipin-2a was carried out.

1. Asperipin-2a was heterologously produced in AO-*aprAYRT* with 5 times the yield compared with original producing strain *A. flavus*. Thus the complete biosynthetic gene cluster of asperipin-2a was confirmed, and function of UstY homologue as an oxidative cyclase has been again proved.

2. With the help of improved yield of asperipin-2a in *A. oryzae* transformant, its absolute configuration was determined by applying advanced Marfey's method and conformational analysis. Based on these results, cyclization mechanism of AprY was proposed that a single enzyme AprY catalyzed two-step oxidative cyclization in a stereoselective manner.

Asperipin-2a was discovered through bioinformatics studies based on the sequence characteristics of precursor peptide and oxidative cyclases. *A. oryzae* heterologous expression helped determine its BGC and absolute configuration. Therefore, asperipin-2a represents a successful example of genome mining of fungal RiPPs and inspires further discovery of novel RiPPs. However, many questions remain unsolved concerning AprY and AprR functions. *In vitro* characterizations are required to look further into the oxidation mechanism of AprY.

Experimental

General.

All reagents commercially supplied were used as received. Optical rotations were recorded on JASCO P-2200 digital polarimeter. ^{1}H- and ^{13}C-NMR spectra were recorded on Bruker AMX-500 spectrometer or Bruker DRX-500. NMR spectra were recorded in dimethyl Sulfoxide-d_6 (99.9%D with 0.03%TMS, kanto chemical). ^{1}H chemical shifts were reported in δ value relative to DMSO: δ_H 2.50 ppm). Data are reported as follows: chemical shift, multiplicity (s = singlet, d = doublet, t = triplet, q = quartet, m = multiplet, br = broad), coupling constant (Hz), and integration. Column chromatography was carried out on C18 open column (Wakosil, 30~50 μm). Oligonucleotides for polymerase chain reaction (PCR) were purchased from Hokkaido System Science Co., Ltd.

Strain and Culture Conditions.

Escherichia coli HST08 and *E. coli* DH5α were used for cloning, following standard recombinant DNA techniques. *Aspergillus oryzae* NSAR1, a quadruple auxotrophic mutant (*niaD*$^{-}$, *sC*$^{-}$, Δ*argB*, *adeA*$^{-}$), was used for the fungal expression.

Preparation of expression plasmids.

The *aprA*, *aprR*, *aprT* were amplified from genomic DNA, *aprY* from c-DNA of *A. flavus* (obtained from chapter 2) with primer set as shown in Table 4-4. PCR reactions were performed with the KOD-Plus-Neo (TOYOBO). Each PCR product was inserted into appropriate restriction site (site 1 and/or site 2) of pUARA2 or pAdeA2 using In-Fusion Advantage PCR cloning kit (Clontech Laboratories) to construct expression plasmids.

Table 4-4. Oligonucleotides used for construction of *A. oryzae* expression plasmids.

Insert	Restriction site	Sequence 5'-3'	Size vector
aprA	*NheI*	F: ATCGATTTGAGCTAGATGCATCTCTCGCGCTAC R: TAGTGCGGCCGCTAGTTACTTGTCAAGATCCTCGG	663 bp pUARA2
aprY	*KpnI*	F: ATGGCCGTGGAATATTTCCAGGAAAAACTA R: ACGACTACCCGGGTCACTAATACGTATAACATA	1005 bp pUARA2
aprR	*NheI*	F: ATCGATTTGAGCTAGATGACTATCAAAGTGATTGTTG R: TAGTGCGGCCGCTAGTCAACCTTTCAGAATACTAGC	946 bp pAdeA2
aprT	*KpnI*	F: CGGAATTCGAGCTCGATGTCGGATCTCTACGCAC R: ACTACAGATCCCCGGCTAATTATGCTTAGCATCCAC	1559 bp pAdeA2

Transformation of *Aspergillus oryzae*.

Transformation of *A. oryzae* NSAR1 or transformant (1.0 x 10^8 cells) were performed by the protoplast-polyethylene glycol method as in chapter 1 experimental.

Extraction of metabolites.

Rice medium: Mycelia of *A. oryzae* transformants were inoculated into a solid medium containing polished rice (20 g). Each culture was incubated at 30°C for 7 days followed by extraction with 80% acetone/H_2O overnight. After centrifuge, 300 μL aqueous acetone supernatant was evaporated out of acetone and washed with an equal volume of ethyl acetate to give the analytical sample.

Potato/starch medium: Mycelia of *A. oryzae* transformants were inoculated into potato/starch medium (potato infusion 200 g, soluble starch 20 g for 1 L medium) 20 mL. Each culture was incubated at 30°C, 200 rpm for 3 days followed by adding 80 mL acetone and keeping still overnight. After centrifuge, 500 μL aqueous acetone supernatant was evaporated out of acetone to give the analytical sample.

Analysis of the metabolites.

An 5 μL aliquot of each water extract was analyzed by UPLC (Waters ACQUITY^{TM} UPLC H-Class system) equipped with a ACQUITY^{TM} UPLC BEH C18 column (50 mm ×2.1 mm, 1.7 μm particle size) at the following conditions: Flow rate; 0. 7 mL/min, Solvent system: A linear gradient from 5 to 50% of CH_3CN with 0.1% HCOOH in water with 0.1% TFA over 2 min, 50 to 95% of CH_3CN with 0.1% HCOOH in water with 0.1% HCOOH for 1 min. An ACQUITY QDa MS was used for detection.

Isolation of asperipin-2a from *A. oryzae* transformant AO-*aprAYRT*

Mycelia of AO-*aprAYRT* was inoculated into a solid medium containing polished rice in 500 mL Erlenmeyer flasks for 1 week. The fungal mycelia were than extracted with 80% aqueous acetone (200 mL) for overnight at room temperature. After vaporizing the acetone, the water layer was washed with AcOEt and then extracted by butanol. Butanol layer was subjected to C18 column chromatography. The fraction containing asperipin-2a was separated by HPLC (Shimazu Class VP system) equipped with Wakopak Navi C18-5 column (10 x 250 mm, A linear gradient from 25 to 75% of MeOH with 0.1% TFA in water with 0.1% TFA over 25 min, and 75% MeOH with 0.1% TFA for 10 min; flow rate of 3 mL/min) to give asperipin-2a (Yield: 1.7 mg/ kg rice).

Asperipin-2a hydrogenolysis

0.35 mg asperipin-2a (0.43 μmol) was stirred with 1.7 mg 10% Pd/C in 1 mL methanol. A total of 0.5

g ammonium formate was added in 10 portions. The resulting reaction mixture was stirred at 70℃ and the reaction was monitored by UPLC-MS. After completion of reaction, the catalyst was removed by filtration through a celite pad. After C18 open column and HPLC purification, the two-ring opened linear target product and one-ring opened intermediates were obtained at 80:20.

Chiral separation of （*S*） and (*R*)-3-phenyllactic acid

(*S*) and (*R*)-3-phenyllactic acid were separated by UPLC-MS UPLC (Waters ACQUITY™ UPLC H-Class system) equipped with a CHIRALPAK® ZWIX(+) (250 mm ×4 mm, 3 μm particle size) at the following conditions: 0. 8 mL/min, Solvent system: 10 mM HCOOH+10 mM HCO_2NH_4 in MeOH/H_2O 98:2 (v/v). An ACQUITY QDa MS was used for detection.

Derivatization of amino acids by L/D FDLA

The derivatization reactions were listed as Table 4-5. Common derivatization method follows like this: 0.3~0.9 mM amino acids water solution was mixed with 2 mM $NaHCO_3$. L/D-FDLA acetone solution was added to final 3.7 mM. 170 μL reaction solution was kept in 37℃ for 1 h and quenched by 20 μL 1N HCl to prepare for the final sample of UPLC analysis. (Waters ACQUITY™ UPLC H-Class system) equipped with a ACQUITY™ UPLC BEH C18 column (50 mm ×2.1 mm, 1.7 μm particle size) at the following conditions: Flow rate; 0. 7 mL/min, Solvent system: A linear gradient from 5 to 50% of CH_3CN with 0.1% HCOOH in water with 0.1% HCOOH over 2 min, 50% of CH_3CN with 0.1% HCOOH in water with 0.1% HCOOH for 1 min. An ACQUITY QDa MS or PDA e λ detector was used for detection.

Table 4-5. List of chiral derivatizations

Amino acid	chiral reagent	product
L-tyrosoine	L-FDLA	L-FDLA-L-Tyr
	D-FDLA	D-FDLA-L-Tyr
L-threonine	L-FDLA	L-FDLA-L-Thr
	D-FDLA	D-FDLA-L-Thr
glycine	D-FDLA	D-FDLA-Gly
sample	L-FDLA	

AprY Cloning and Expression in *E. coli*

To generate the overexpression construct for AprY, *aprY* was amplified from the cDNA of the *A. flavus* (chapter II experimental) using primer sets as Table 4-6 shows. The PCR products were directly infused into each vector and separately introduced into *E. coli* BL21-Gold(DE3) for overexpression. The transformant was grown at 37°C at an OD_{600} of ~0.6 in a 500 mL flask. After the culture was cooled at 4°C, isopropyl β-d-thiogalactopyranoside (0.1 mM) was added to it. After incubation at 16°C for 18 h, the cells were harvested by centrifugation at 4000 rpm. The harvested cells were resuspended in disruption buffer (50 mM Tris–HCl (pH 7.5), 200 mM NaCl, 10 mM 2-Mercaptoethanol) and disrupted by sonication. After centrifugation, the supernatant was applied to an Ni-NTA-agarose resin (Qiagen) to purify the expressed protein.

For co-expression of N or C-His-$AprY_{78\sim334}$ with tg chaperon, the chaperone competent cell pTf16/BL21 (TAKARA) was used according to manufacture manual.

Table 4-6. Oligonucleotides used for construction of *E. coli* expression plasmids

Insert	Restriction site	Sequence 5'-3'	Size vector
aprY for N-His-AprY	*NdeI*	F: TCGAAGGTAGGCATATGTCGCACTGCCAACTCA R: GTACCGAGCTCCATATTAACTTCCAGGAACAGCTG	1005 bp pColdI

aprY for C-His-AprY	*HindIII*	F: CTCCGTCGACAAGCTTATGGAGCCCTTCTCTAAATT R: GTGCGGCCGCAAGCTTTTCGTGCCTTTTCGTATGTT	1005 bp pET22b-
aprY (short) for N-His-AprY$_{78\sim334}$	*NdeI*	F: TCGAAGGTAGGCATATGCACTGTCAGCTTTACGCGGG R: GGGTACCGAGCTCCATACTATTCGTGCCTTTTCGTAT	774 bp pColdI
aprY (short) for C-His-AprY$_{78\sim334}$	*NdeI* *BamHI*	F: AAGGAGATATACATATGCACTGTCAGCTTTACGCGGG R: GCTCGAATTCGGATCTTCGTGCCTTTTCGTATGTT	774 bp pET22b-

Chapter 5. Summary

In previous chapters, biosynthetic studies of three different fungal metabolites were performed. The chapter 2 described genome mining of bifunctional terpene synthases in fungal strains. The chapter 3 and chapter 4 focused on the biosynthesis of two fungal RiPPs ustiloxin B and asperipin-2a respectively.

In chapter 2, phylogenetics analysis of bifunctional terpene synthases from fungal genomes were performed and four candidates from different clades were chosen. The candidate genes were introduced into *A. oryzae* among which *NfSS* transformant produced a novel sesterterpene named sesterfisherol. The cyclization mechanism of NfSS was elucidated from *in vivo* and *in vitro* labeling experiments and exhibited its uniqueness through a series of hydride shifts. On the basis of this mechanism, a unified biogenesis for group A sesterterpenes from bicyclic (5-15), tricyclic (5-12-5) and tetracyclic (5-6-8-5) cation intermediates was proposed. Especially, the first cyclization mode of each synthase may be reflected by phylogenetic clades it belongs to. Although not yet proved, this promising hypothesis suggested that phylogenetic analysis will be the roadmap to guide future genome mining of novel di/sesterterpenes.

In the chapter 3, I focused on the biosynthetic pathway of ustiloxin B, whose BGC was the firstly identified RiPPs BGC from filamentous fungi. At first, based on the structural elucidation of the metabolites accumulated in a series of gene deletion mutants of *A. flavus*. I proposed the biosynthetic pathway of ustiloxin B. Heterologous expression of *ustAQYaYb* revealed that these four genes were involved in the biosynthesis of the first cyclic intermediates, *N*-desmethylustiloxin F. Especially, UstYa and UstYb, both of which contained Duf3328, were proposed as novel oxidative enzymes responsible for the formation of ether linked macrocycle. I also characterized the enzymes involved in the late stage using recombinant enzymes. The FAD-dependent UstF2 catalyzed two rounds of

hydroxylation on amino group followed by decarboxylative dehydration. The PLP-dependent UstD catalyzed unprecedented C-C bond formation through a decarboxylative condensation. Based on the above results, the biosynthetic pathway of ustiloxin B was characterized in detail.

In the chapter 4, asperipin-2a, which was recently discovered by bioinformatics study, was chosen as the subject for biosynthetic study on fungal RiPPs. Based on the prediction of its BGC proposed by gene expression analysis, four genes *aprAYRT* were cloned and introduced into *A. oryzae*. Resultant AO-*aprAYRT* produced asperipin-2a. confirming that these four genes were actually involved in the biosynthesis. Notably, AprY likely catalyzed two oxidative cyclizations to form the two ether bonds of asperipin-2a. This result also indicated that ustY homologues, which contained Duf3328 and were often found in fungal RiPPs gene clusters, would be universal enzymes that were responsible for oxidative cyclization. In addition I also determined the absolute configuration of asperipin-2a, taking advantage of the high production achieved by the *A. oryzae* heterologous expression. Also the expression of transmembrane region truncated AprY in *E. coli* was achieved, which may give purified enzyme for detailed analysis of its catalytic mechanism.

In this chapter, I also want to arrange these three stories into two topics to develop some discussions and prospects.

1. *Aspergillus oryzae* vs *E. coli.*

In a long history of efforts to heterologously express genes from various organisms, many classical systems have been established. *E. coli* is widely used for the expression of proteins from bacteria, fungi, plants or even animals. However, higher organism hosts such as *Saccharomyces cerevisiae* are also indispensable tools in biosynthesis researches because eukaryotic protein expression sometimes requires proper cellular localization and/or co-factors specific to higher organisms for proper protein

folding.

In my studies, *Aspergillus oryzae* was established as a versatile host for the reconstitution of the pathway of two different biosynthetic origins, terpenes and RiPPs. It has been developed to be an excellent system to express multiple fungal genes in a reasonable time interval and even becomes a successful platform for screening di/sesterterpene synthases in my studies. The most outstanding merits are the following two: 1) there is no need to delete the introns from insert genes derived from filamentous fungi. 2) the overexpressed proteins are more likely to be functional than in other hosts. For the first merit, it is very important for genome mining: to get the intron-less gene sequences which are required for *E. coli* or yeast expression are usually complex, time-consuming, or impossible for some genes not expressed in standard culturing conditions. Because *A. oryzae* shares the same mRNA splicing mechanism with most filamentous fungi and constitutive/inducible promoters for the expression of exogenous genes are available, introduction of genomic sequence of target genes would readily result in the production of functional proteins. This host strain can also be used for the preparation of matured mRNAs for heterologous expression in other hosts, such as *E. coli* or *S. cerevisiae*. For the second merit, it is also essential to characterize fungal enzymes that retain unknown motifs, cofactors or proteins that *E. coli* is reluctant to express. The most convincing example is the characterization of UstY homologues in chapter 3 and 4. After the introduction of *ustYa*, *Yb* and *AprY* into *A. oryzae,* they were expressed as functional proteins and helped to characterize this novel family of oxidative cyclases. However, their overexpression in *E. coli* were proved to be difficult due to their hydrophobic transmembrane region.

On the other hand, *E. coli* also plays an essential role in my studies. 1) NfSS was expressed and purified as a functional enzyme in *E. coli*. *In vitro* labelling experiments presented a clear evidence for a 1, 5- and 1, 2-shift of two hydrides both from C12 on the sesterfisherol cation intermediate. Such detailed mechanistic elucidation was often limited to *in vitro* enzymatic characterizations. 2) In the late stage

of ustiloxin B biosynthesis, UstF2 and UstD were expressed and purified from *E. coli*. *In vitro* enzymatic assay not only showed their unique reaction mechanisms but also identified the exact structures and products in each reaction. Particularly, ustiloxin C, which was proposed as an intermediate by initial gene deletion experiment, was proved to be a shunt product by *in vitro* experiments.

A. oryzae or *E. coli*, *in vivo* or *in vitro*, they are not contradicting to each other. Instead, they are collaborating and supplementing to each other. We should make clever strategies to let all the hosts or techniques working together to solve the ever-challenging problems of biosynthetic studies.

2. Terpenes vs RiPPs

In my studies, the two subjects are terpenes and RiPPs. Interestingly, they are quite different to each other, and offered me a good chance to compare the study methods of these two.

Terpenes are the most well-known family of natural products, and we have accumulated a great amount of knowledge for their biosynthesis. Their biosynthetic machinery is relatively simple: the terpene skeleton was formed by the prenyltransferases and cyclized by terpene synthases and modified by other tailoring enzymes through oxidation, acylation or hybrid with other indole or PKS products[30, 101]. However, the interests around the terpene synthases have never diminished in this long time. On the contrary, how the terpene synthases contribute to the structural diversity of terpenes and how they precisely controlled the cyclization pattern always amaze us. In NfSS case, its C terminal functioned as prenyltransferase domain and its N terminal cyclase domain catalyzed the formation of tetracyclic (5-6-8-5) skeleton through a complex program of hydride shifts. The secret of this precise control lies behind the amino acids sequence of NfSS, as suggested by the phylogenetic analysis. To solve this mystery, our group and collaborators are looking deep into this enzyme and uses various techniques such as amino acid mutation, protein crystallography, chemical calculations. We hope that one day the

cyclization pattern of terpene synthases could be predicted or even be engineered.

On the other hand, the fungal RiPPs are at the beginning of been characterized, with limited examples and limited information. As in the case of ustiloxin B, the discovery of its BGC was the result of a universal BGC prediction program called MIDDAS-M[78]. After we got the first example of fungal RiPPs BGC, the most important task was to elucidate the biosynthetic machinery and establish the roadmap for further mining of novel RiPPs. After the effort of us and our collaborators, we found out the precursor peptide protein UstA and oxidative cyclases UstY homologues can serve as such "probes". Extensive bioinformatics studies by our collaborators and experimental confirmation conducted by me enabled the discovery of asperipin-2a, a novel kind of fungal RiPPs. This is a promising success and will inspire many other efforts to discover fungal RiPPs based on solid bioinformatic clues.

Although my two subjects, terpenes and fungal RiPPs, are quite different species of natural products, they actually tell the same story: the new discoveries in biosynthetic studies are hidden in the vast raw data of DNA and protein sequences. Our work is to look deep into the mechanism of existing reactions or pathways and establish the roadmap which can guide us to the hidden treasure of natural products and enzymes that nature bequeaths us.

Reference

1. Fleming, A., On the antibacterial action of cultures of a penicillium, with special reference to their use in the isolation of *B. influenzae*. *British Journal of Experimental Pathology* **1929,** *10* (3), 226-236.

2. Endo, A.; Kuroda, M.; Tsujita, Y., ML-236A, ML-236B, and ML-236C, new inhibitors of cholesterogenesis produced by *penicillium citrinum*. *Journal of Antibiotics* **1976,** *29* (12), 1346-1348.

3. Bucknall, R. A.; Moores, H.; Simms, R.; Hesp, B., Antiviral effects of aphidicolin, a new antibiotic produced by *Cephalosporium aphidicola*. *Antimicrobial Agents and Chemotherapy* **1973,** *4* (3), 294-298.

4. Long, K. S.; Hansen, L. H.; Jakobsen, L.; Vester, B., Interaction of pleuromutilin derivatives with the ribosomal peptidyl transferase center. *Antimicrobial Agents and Chemotherapy* **2006,** *50* (4), 1458-1462.

5. Bennett, J. W.; Klich, M., Mycotoxins. *Clinical Microbiology Reviews* **2003,** *16* (3), 497-+.

6. Williams, J. H.; Phillips, T. D.; Jolly, P. E.; Stiles, J. K.; Jolly, C. M.; Aggarwal, D., Human aflatoxicosis in developing countries: a review of toxicology, exposure, potential health consequences, and interventions. *American Journal of Clinical Nutrition* **2004,** *80* (5), 1106-1122.

7. Medema, M. H.; Kottmann, R.; Yilmaz, P.; Cummings, M.; Biggins, J. B.; Blin, K.; de Bruijn, I.; Chooi, Y. H.; Claesen, J.; Coates, R. C.; Cruz-Morales, P.; Duddela, S.; Dusterhus, S.; Edwards, D. J.; Fewer, D. P.; Garg, N.; Geiger, C.; Gomez-Escribano, J. P.; Greule, A.; Hadjithomas, M.; Haines, A. S.; Helfrich, E. J. N.; Hillwig, M. L.; Ishida, K.; Jones, A. C.; Jones, C. S.; Jungmann, K.; Kegler, C.; Kim, H. U.; Kotter, P.; Krug, D.; Masschelein, J.; Melnik, A. V.; Mantovani, S. M.; Monroe, E. A.; Moore, M.; Moss, N.; Nutzmann, H. W.; Pan, G. H.; Pati, A.; Petras, D.; Reen, F. J.; Rosconi, F.; Rui, Z.; Tian, Z. H.; Tobias, N. J.; Tsunematsu, Y.; Wiemann, P.; Wyckoff, E.; Yan, X. H.; Yim, G.; Yu, F. G.; Xie, Y. C.; Aigle, B.; Apel, A. K.; Balibar, C. J.; Balskus, E. P.; Barona-Gomez, F.; Bechthold, A.; Bode, H. B.; Borriss, R.; Brady, S. F.; Brakhage, A. A.; Caffrey, P.; Cheng, Y. Q.; Clardy, J.; Cox, R. J.; De Mot, R.; Donadio, S.; Donia, M. S.; van der Donk, W. A.; Dorrestein, P. C.; Doyle, S.; Driessen, A. J. M.; Ehling-Schulz, M.; Entian, K. D.; Fischbach, M. A.; Gerwick, L.; Gerwick, W. H.; Gross, H.; Gust, B.; Hertweck, C.; Hofte, M.; Jensen, S. E.; Ju, J. H.; Katz, L.; Kaysser, L.; Klassen, J. L.; Keller, N. P.; Kormanec, J.; Kuipers, O. P.; Kuzuyama, T.; Kyrpides, N. C.; Kwon, H. J.; Lautru, S.; Lavigne, R.; Lee, C. Y.; Linquan, B.; Liu, X. Y.; Liu, W.; Luzhetskyy, A.; Mahmud, T.; Mast, Y.; Mendez, C.; Metsa-Ketela, M.; Micklefield, J.; Mitchell, D. A.; Moore, B. S.; Moreira, L. M.; Muller, R.; Neilan, B. A.; Nett, M.; Nielsen, J.; O'Gara, F.; Oikawa, H.; Osbourn, A.; Osburne, M. S.; Ostash, B.; Payne, S. M.; Pernodet, J. L.; Petricek, M.; Piel, J.; Ploux, O.; Raaijmakers, J. M.; Salas, J. A.; Schmitt, E. K.; Scott, B.; Seipke, R. F.; Shen, B.; Sherman, D. H.; Sivonen, K.; Smanski, M. J.; Sosio, M.; Stegmann, E.; Sussmuth, R. D.; Tahlan, K.; Thomas, C. M.; Tang, Y.; Truman, A. W.; Viaud, M.; Walton, J. D.; Walsh, C. T.; Weber, T.; van Wezel, G. P.; Wilkinson, B.; Willey, J. M.; Wohlleben, W.; Wright, G. D.; Ziemert, N.; Zhang, C. S.; Zotchev, S. B.; Breitling, R.; Takano, E.; Glockner, F. O., Minimum information about a biosynthetic gene cluster. *Nature Chemical Biology* **2015,** *11* (9), 625-

631.

8. Wallwey, C.; Li, S. M., Ergot alkaloids: structure diversity, biosynthetic gene clusters and functional proof of biosynthetic genes. *Natural Product Reports* **2011,** *28* (3), 496-510.

9. Bentley, S. D.; Chater, K. F.; Cerdeno-Tarraga, A. M.; Challis, G. L.; Thomson, N. R.; James, K. D.; Harris, D. E.; Quail, M. A.; Kieser, H.; Harper, D.; Bateman, A.; Brown, S.; Chandra, G.; Chen, C. W.; Collins, M.; Cronin, A.; Fraser, A.; Goble, A.; Hidalgo, J.; Hornsby, T.; Howarth, S.; Huang, C. H.; Kieser, T.; Larke, L.; Murphy, L.; Oliver, K.; O'Neil, S.; Rabbinowitsch, E.; Rajandream, M. A.; Rutherford, K.; Rutter, S.; Seeger, K.; Saunders, D.; Sharp, S.; Squares, R.; Squares, S.; Taylor, K.; Warren, T.; Wietzorrek, A.; Woodward, J.; Barrell, B. G.; Parkhill, J.; Hopwood, D. A., Complete genome sequence of the model actinomycete *Streptomyces coelicolor* A3(2). *Nature* **2002,** *417* (6885), 141-147.

10. Nagano, N.; Umemura, M.; Izumikawa, M.; Kawano, J.; Ishii, T.; Kikuchi, M.; Tomii, K.; Kumagai, T.; Yoshimi, A.; Machida, M.; Abe, K.; Shin-ya, K.; Asai, K., Class of cyclic ribosomal peptide synthetic genes in filamentous fungi. *Fungal Genetics and Biology* **2016,** *86*, 58-70.

11. Stajich, J. 1KFG updates – another 100 genomes. (accessed http://1000.fungalgenomes.org/home/).

12. Finn, R. D.; Bateman, A.; Clements, J.; Coggill, P.; Eberhardt, R. Y.; Eddy, S. R.; Heger, A.; Hetherington, K.; Holm, L.; Mistry, J.; Sonnhammer, E. L. L.; Tate, J.; Punta, M., Pfam: the protein families database. *Nucleic Acids Research* **2014,** *42* (D1), D222-D230.

13. 2ndFind. (accessed http://biosyn.nih.go.jp/2ndfind/).

14. Medema, M. H.; Blin, K.; Cimermancic, P.; de Jager, V.; Zakrzewski, P.; Fischbach, M. A.; Weber, T.; Takano, E.; Breitling, R., antiSMASH: rapid identification, annotation and analysis of secondary metabolite biosynthesis gene clusters in bacterial and fungal genome sequences. *Nucleic Acids Research* **2011,** *39*, W339-W346.

15. Rutledge, P. J.; Challis, G. L., Discovery of microbial natural products by activation of silent biosynthetic gene clusters. *Nature Reviews Microbiology* **2015,** *13* (8), 509-523.

16. Weld, R. J.; Plummer, K. M.; Carpenter, M. A.; Ridgway, H. J., Approaches to functional genomics in filamentous fungi. *Cell Research* **2006,** *16* (1), 31-44.

17. Salame, T. M.; Ziv, C.; Hadar, Y.; Yarden, O., RNAi as a potential tool for biotechnological applications in fungi. *Applied Microbiology and Biotechnology* **2011,** *89* (3), 501-512.

18. Katayama, T.; Tanaka, Y.; Okabe, T.; Nakamura, H.; Fujii, W.; Kitamoto, K.; Maruyama, J., Development of a genome editing technique using the CRISPR/Cas9 system in the industrial filamentous fungus *Aspergillus oryzae*. *Biotechnology Letters* **2016,** *38* (4), 637-642.

19. Keller, N. P.; Turner, G.; Bennett, J. W., Fungal secondary metabolism - From biochemistry to genomics. *Nature Reviews Microbiology* **2005,** *3* (12), 937-947.

20. Bergmann, S.; Schumann, J.; Scherlach, K.; Lange, C.; Brakhage, A. A.; Hertweck, C., Genomics-driven discovery of PKS-NRPS hybrid metabolites from *Aspergillus nidulans*. *Nature Chemical*

Biology **2007,** *3* (4), 213-217.

21. Slater, S. C.; Voige, W. H.; Dennis, D. E., Cloning and expression in *Escherichia coli* of the *Alcaligenes eutrophus* H16 poly-β-hydroxybutyrate biosynthetic pathway. *Journal of Bacteriology* **1988,** *170* (10), 4431-4436.

22. Trantas, E.; Panopoulos, N.; Ververidis, F., Metabolic engineering of the complete pathway leading to heterologous biosynthesis of various flavonoids and stilbenoids in *Saccharomyces cerevisiae*. *Metabolic Engineering* **2009,** *11* (6), 355-366.

23. Fujii, I.; Ono, Y.; Tada, H.; Gomi, K.; Ebizuka, Y.; Sankawa, U., Cloning of the polyketide synthase gene *atX* from *Aspergillus terreus* and its identification as the 6-methylsalicylic acid synthase gene by heterologous expression. *Molecular & General Genetics* **1996,** *253* (1-2), 1-10.

24. Kennedy, J.; Auclair, K.; Kendrew, S. G.; Park, C.; Vederas, J. C.; Hutchinson, C. R., Modulation of polyketide synthase activity by accessory proteins during lovastatin biosynthesis. *Science* **1999,** *284* (5418), 1368-1372.

25. Chiang, Y. M.; Oakley, C. E.; Ahuja, M.; Entwistle, R.; Schultz, A.; Chang, S. L.; Sung, C. T.; Wang, C. C. C.; Oakley, B. R., An efficient system for heterologous expression of secondary metabolite genes in *Aspergillus nidulans*. *Journal of the American Chemical Society* **2013,** *135* (20), 7720-7731.

26. Tagami, K.; Liu, C. W.; Minami, A.; Noike, M.; Isaka, T.; Fueki, S.; Shichijo, Y.; Toshima, H.; Gomi, K.; Dairi, T.; Oikawa, H., Reconstitution of biosynthetic machinery for indole-diterpene paxilline in *Aspergillus oryzae*. *Journal of the American Chemical Society* **2013,** *135* (4), 1260-1263.

27. **Fujita, C.** *Koji*, an Aspergillus. (accessed http://www.tokyofoundation.org/en/topics/japanese-traditional-foods/vol.-10-koji-an-aspergillus).

28. Tada, S.; Gomi, K.; Kitamoto, K.; Takahashi, K.; Tamura, G.; Hara, S., Construction of a fusion gene comprising the taka-amylase A promoter and the *Escherichia coli* beta-glucuronidase gene and analysis of its expression in *Aspergillus oryzae*. *Molecular & General Genetics* **1991,** *229* (2), 301-306.

29. Watanabe, A.; Ono, Y.; Fujii, I.; Sankawa, U.; Mayorga, M. E.; Timberlake, W. E.; Ebizuka, Y., Product identification of polyketide synthase coded by *Aspergillus nidulans wA* gene. *Tetrahedron Letters* **1998,** *39* (42), 7733-7736.

30. Itoh, T.; Tokunaga, K.; Matsuda, Y.; Fujii, I.; Abe, I.; Ebizuka, Y.; Kushiro, T., Reconstitution of a fungal meroterpenoid biosynthesis reveals the involvement of a novel family of terpene cyclases. *Nature Chemistry* **2010,** *2* (10), 858-864.

31. Heneghan, M. N.; Yakasai, A. A.; Halo, L. M.; Song, Z. S.; Bailey, A. M.; Simpson, T. J.; Cox, R. J.; Lazarus, C. M., First Heterologous reconstruction of a complete functional fungal biosynthetic multigene cluster. *Chembiochem* **2010,** *11* (11), 1508-1512.

32. Jin, F. H.; Maruyama, J.; Juvvadi, P. R.; Arioka, M.; Kitamoto, K., Development of a novel quadruple auxotrophic host transformation system by *argB* gene disruption using *adeA* gene and exploiting adenine auxotrophy in *Aspergillus oryzae*. *Fems Microbiology Letters* **2004,** *239* (1), 79-85.

33. Tagami, K.; Minami, A.; Fujii, R.; Liu, C.; Tanaka, M.; Gomi, K.; Dairi, T.; Oikawa, H., Rapid reconstitution of biosynthetic machinery for fungal metabolites in *Aspergillus oryzae*: total biosynthesis of aflatrem. *Chembiochem* **2014,** *15* (14), 2076-2080.

34. Liu, C. W.; Tagami, K.; Minami, A.; Matsumoto, T.; Frisvad, J. C.; Suzuki, H.; Ishikawa, J.; Gomi, K.; Oikawa, H., Reconstitution of biosynthetic machinery for the synthesis of the highly elaborated indole diterpene penitrem. *Angewandte Chemie-International Edition* **2015,** *54* (19), 5748-5752.

35. 藤居 瑠彌. *Aspergillus oryzae* 異種発現系を用いた糸状菌由来二次代謝産物の全生合成研究. 博士論文, 北海道大学, 2015.

36. Arnison, P. G.; Bibb, M. J.; Bierbaum, G.; Bowers, A. A.; Bugni, T. S.; Bulaj, G.; Camarero, J. A.; Campopiano, D. J.; Challis, G. L.; Clardy, J.; Cotter, P. D.; Craik, D. J.; Dawson, M.; Dittmann, E.; Donadio, S.; Dorrestein, P. C.; Entian, K. D.; Fischbach, M. A.; Garavelli, J. S.; Goransson, U.; Gruber, C. W.; Haft, D. H.; Hemscheidt, T. K.; Hertweck, C.; Hill, C.; Horswill, A. R.; Jaspars, M.; Kelly, W. L.; Klinman, J. P.; Kuipers, O. P.; Link, A. J.; Liu, W.; Marahiel, M. A.; Mitchell, D. A.; Moll, G. N.; Moore, B. S.; Muller, R.; Nair, S. K.; Nes, I. F.; Norris, G. E.; Olivera, B. M.; Onaka, H.; Patchett, M. L.; Piel, J.; Reaney, M. J. T.; Rebuffat, S.; Ross, R. P.; Sahl, H. G.; Schmidt, E. W.; Selsted, M. E.; Severinov, K.; Shen, B.; Sivonen, K.; Smith, L.; Stein, T.; Sussmuth, R. D.; Tagg, J. R.; Tang, G. L.; Truman, A. W.; Vederas, J. C.; Walsh, C. T.; Walton, J. D.; Wenzel, S. C.; Willey, J. M.; van der Donk, W. A., Ribosomally synthesized and post-translationally modified peptide natural products: overview and recommendations for a universal nomenclature. *Natural Product Reports* **2013,** *30* (1), 108-160.

37. Ro, D. K.; Paradise, E. M.; Ouellet, M.; Fisher, K. J.; Newman, K. L.; Ndungu, J. M.; Ho, K. A.; Eachus, R. A.; Ham, T. S.; Kirby, J.; Chang, M. C. Y.; Withers, S. T.; Shiba, Y.; Sarpong, R.; Keasling, J. D., Production of the antimalarial drug precursor artemisinic acid in engineered yeast. *Nature* **2006,** *440* (7086), 940-943.

38. Ajikumar, P. K.; Xiao, W. H.; Tyo, K. E. J.; Wang, Y.; Simeon, F.; Leonard, E.; Mucha, O.; Phon, T. H.; Pfeifer, B.; Stephanopoulos, G., Isoprenoid pathway optimization for taxol precursor overproduction in *Escherichia coli. Science* **2010,** *330* (6000), 70-74.

39. Mander, L. N.; Liu, H. W., *Comprehensive natural products II : chemistry and biology*. Elsevier: Amsterdam ; Boston, 2010; p (10 volumes).

40. Dewick, P. M., *Medicinal natural products : a biosynthetic approach*. 2nd ed.; Wiley: Chichester, West Sussex, England ; New York, NY, USA, 2002; p xii, 507 p.

41. Wang, K.; Ohnuma, S., Chain-length determination mechanism of isoprenyl diphosphate synthases and implications for molecular evolution. *Trends in Biochemical Sciences* **1999,** *24* (11), 445-451.

42. Barton, D. H. R.; Nakanishi, K. O.; Meth-Cohn, O., *Comprehensive natural products chemistry*. 1st ed.; Elsevier: Amsterdam ; New York, 1999.

43. Toyomasu, T.; Tsukahara, M.; Kaneko, A.; Niida, R.; Mitsuhashi, W.; Dairi, T.; Kato, N.; Sassa,

T., Fusicoccins are biosynthesized by an unusual chimera diterpene synthase in fungi. *Proceedings of the National Academy of Sciences of the United States of America* **2007,** *104* (9), 3084-3088.

44. Chiba, R.; Minami, A.; Gomi, K.; Oikawa, H., Identification of ophiobolin F synthase by a genome mining approach: a sesterterpene synthase from *Aspergillus clavatus*. *Organic Letters* **2013,** *15* (3), 594-597.

45. Minami, A.; Tajima, N.; Higuchi, Y.; Toyomasu, T.; Sassa, T.; Kato, N.; Dairi, T., Identification and functional analysis of brassicicene C biosynthetic gene cluster in *Alternaria brassicicola*. *Bioorganic & Medicinal Chemistry Letters* **2009,** *19* (3), 870-874.

46. Toyomasu, T.; Kaneko, A.; Tokiwano, T.; Kanno, Y.; Niida, R.; Miura, S.; Nishioka, T.; Ikeda, C.; Mitsuhashi, W.; Dairi, T.; Kawano, T.; Oikawa, H.; Kato, N.; Sassa, T., Biosynthetic gene-based secondary metabolite screening: a new diterpene, methyl phomopsenonate, from the fungus *Phomopsis amygdali*. *Journal of Organic Chemistry* **2009,** *74* (4), 1541-1548.

47. Matsuda, Y.; Wakimoto, T.; Mori, T.; Awakawa, T.; Abe, I., Complete biosynthetic pathway of anditomin: nature's sophisticated synthetic route to a complex fungal meroterpenoid. *Journal of the American Chemical Society* **2014,** *136* (43), 15326-15336.

48. Murata, M.; Legrand, A. M.; Ishibashi, Y.; Fukui, M.; Yasumoto, T., Structures and configurations of ciguatoxin from the Moray Eel *Gymnothorax javanicus* and its likely precursor from the Dinoflagellate *Gambierdiscus toxicus*. *Journal of the American Chemical Society* **1990,** *112* (11), 4380-4386.

49. Polavarapu, P. L., Renaissance in chiroptical spectroscopic methods for molecular structure determination. *Chemical Record* **2007,** *7* (2), 125-136.

50. Kawahara, N.; Nozawa, M.; Flores, D.; Bonilla, P.; Sekita, S.; Satake, M.; Kawai, K., Nitidasin, a novel sesterterpenoid, from the Peruvian folk medicine "Hercampuri" (*Gentianella nitida*). *Chemical & Pharmaceutical Bulletin* **1997,** *45* (10), 1717-1719.

51. Krogh, A.; Larsson, B.; von Heijne, G.; Sonnhammer, E. L. L., Predicting transmembrane protein topology with a hidden Markov model: Application to complete genomes. *Journal of Molecular Biology* **2001,** *305* (3), 567-580.

52. Chang, C. C. Y.; Huh, H. Y.; Cadigan, K. M.; Chang, T. Y., Molecular cloning and functional expression of human Acyl-coenzyme A cholesterol acyltransferase cdna in mutant Chinese Hamster Ovary cells. *Journal of Biological Chemistry* **1993,** *268* (28), 20747-20755.

53. Roncal, T.; Cordobes, S.; Sterner, O.; Ugalde, U., Conidiation in *Penicillium cyclopium* is induced by conidiogenone, an endogenous diterpene. *Eukaryotic Cell* **2002,** *1* (5), 823-829.

54. Seo, S.; Uomori, A.; Yoshimura, Y.; Takeda, K.; Seto, H.; Ebizuka, Y.; Noguchi, H.; Sankawa, U., Biosynthesis of sitosterol, cycloartenol, and 24-methylenecycloartanol in tissue cultures of higher plants and of ergosterol in yeast from [1,2-$^{13}C_2$]- and [2-$^{13}C^2H_3$]-acetate and [5-$^{13}C^2H_2$]MVA. *Journal of the Chemical Society-Perkin Transactions 1* **1988,** (8), 2407-2414.

55. Renner, M. K.; Jensen, P. R.; Fenical, W., Mangicols: Structures and biosynthesis of a new class of sesterterpene polyols from a marine fungus of the genus Fusarium. *Journal of Organic Chemistry* **2000,** *65* (16), 4843-4852.

56. Santini, A.; Ritieni, A.; Fogliano, V.; Randazzo, G.; Mannina, L.; Logrieco, A.; Benedetti, E., Structure and absolute stereochemistry of fusaproliferin, a toxic metabolite from *Fusarium proliferatum*. *Journal of Natural Products* **1996,** *59* (2), 109-112.

57. Singh, S. B.; Reamer, R. A.; Zink, D.; Schmatz, D.; Dombrowski, A.; Goetz, M. A., Variculanol - structure and absolute stereochemistry of a novel 5/12/5 tricyclic sesterterpenoid from *Aspergillus variecolor*. *Journal of Organic Chemistry* **1991,** *56* (19), 5618-5622.

58. Sadler, I. H.; Simpson, T. J., Determination by NMR methods of the structure and stereochemistry of astellatol, a new and unusual sesterterpene. *Magnetic Resonance in Chemistry* **1992,** *30*, S18-S23.

59. Kaneda, M.; Iitaka, Y.; Shibata, S.; Takahashi, R., Retigeranic acid, a novel sesterterpene isolated from lichens of *Lobaria retigera* group. *Tetrahedron Letters* **1972,** (45), 4609-4611.

60. Kawahara, N.; Nozawa, M.; Flores, D.; Bonilla, P.; Sekita, S.; Satake, M., Sesterterpenoid from *Gentianella alborosea*. *Phytochemistry* **2000,** *53* (8), 881-884.

61. Kawahara, N.; Nozawa, M.; Kurata, A.; Hakamatsuka, T.; Sekita, S.; Satake, M., A novel sesterterpenoid, nitiol, as a potent enhancer of IL-2 gene expression in a human T cell line, from the Peruvian folk medicine “Hercumpuri” (*Gentianella nitida*). *Chemical and Pharmaceutical Bulletin* **1999,** *47* (9), 1344-1345.

62. Wang, Y.; Oberer, L.; Dreyfuss, M.; Sutterlin, C.; Riezman, H., Conformation and relative configuration of a very potent glycosylphosphatidylinositol-anchoring inhibitor with an unusual tricarbocyclic sesterterpenoid delta-lactone skeleton from the fungus *Paecilomyces inflatus*. *Helvetica Chimica Acta* **1998,** *81* (11), 2031-2042.

63. Wang, Y.; Dreyfuss, M.; Ponelle, M.; Oberer, L.; Riezman, H., A glycosylphosphatidylinositol-anchoring inhibitor with an unusual tetracarbocyclic sesterterpene skeleton from the fungus *Codinaea simplex*. *Tetrahedron* **1998,** *54* (23), 6415-6426.

64. Schmidt, E. W.; Nelson, J. T.; Rasko, D. A.; Sudek, S.; Eisen, J. A.; Haygood, M. G.; Ravel, J., Patellamide A and C biosynthesis by a microcin-like pathway in *Prochloron didemni*, the cyanobacterial symbiont of *Lissoclinum patella*. *Proceedings of the National Academy of Sciences of the United States of America* **2005,** *102* (20), 7315-7320.

65. Lee, S. W.; Mitchell, D. A.; Markley, A. L.; Hensler, M. E.; Gonzalez, D.; Wohlrab, A.; Dorrestein, P. C.; Nizet, V.; Dixon, J. E., Discovery of a widely distributed toxin biosynthetic gene cluster. *Proceedings of the National Academy of Sciences of the United States of America* **2008,** *105* (15), 5879-5884.

66. Hallen, H. E.; Luo, H.; Scott-Craig, J. S.; Walton, J. D., Gene family encoding the major toxins

of lethal Amanita mushrooms. *Proceedings of the National Academy of Sciences of the United States of America* **2007,** *104* (48), 19097-19101.

67. Meindl, K.; Schmiederer, T.; Schneider, K.; Reicke, A.; Butz, D.; Keller, S.; Guhring, H.; Vertesy, L.; Wink, J.; Hoffmann, H.; Bronstrup, M.; Sheldrick, G. M.; Sussmuth, R. D., Labyrinthopeptins: A new class of carbacyclic lantibiotics. *Angewandte Chemie-International Edition* **2010,** *49* (6), 1151-1154.

68. Engelhardt, K.; Degnes, K. F.; Kemmler, M.; Bredholt, H.; Fjaervik, E.; Klinkenberg, G.; Sletta, H.; Ellingsen, T. E.; Zotchev, S. B., Production of a new thiopeptide antibiotic, TP-1161, by a marine Nocardiopsis species. *Applied and Environmental Microbiology* **2010,** *76* (15), 4969-4976.

69. Ireland, C. M.; Durso, A. R.; Newman, R. A.; Hacker, M. P., Anti-neoplastic cyclic peptides from the marine tunicate *Lissoclinum patella*. *Journal of Organic Chemistry* **1982,** *47* (10), 1807-1811.

70. Meinecke, B.; Meinecketillmann, S., Effects of alpha-amanitin on nuclear maturation of porcine oocytes *in vitro*. *Journal of Reproduction and Fertility* **1993,** *98* (1), 195-201.

71. Truman, A. W., Cyclisation mechanisms in the biosynthesis of ribosomally synthesised and post-translationally modified peptides. *Beilstein Journal of Organic Chemistry* **2016,** *12*, 1250-1268.

72. Burkhart, B. J.; Hudson, G. A.; Dunbar, K. L.; Mitchell, D. A., A prevalent peptide-binding domain guides ribosomal natural product biosynthesis. *Nature Chemical Biology* **2015,** *11* (8), 564-U56.

73. Link, A. J., Biosynthesis leading the way to RiPPs. *Nature Chemical Biology* **2015,** *11* (8), 551-552.

74. Hou, Y. P.; Tianero, M. D. B.; Kwan, J. C.; Wyche, T. P.; Michel, C. R.; Ellis, G. A.; Vazquez-Rivera, E.; Braun, D. R.; Rose, W. E.; Schmidt, E. W.; Bugni, T. S., Structure and biosynthesis of the antibiotic bottromycin D. *Organic Letters* **2012,** *14* (19), 5050-5053.

75. Ortega, M. A.; Hao, Y.; Zhang, Q.; Walker, M. C.; van der Donk, W. A.; Nair, S. K., Structure and mechanism of the tRNA-dependent lantibiotic dehydratase NisB. *Nature* **2015,** *517* (7535), 509-+.

76. Dunbar, K. L.; Melby, J. O.; Mitchell, D. A., YcaO domains use ATP to activate amide backbones during peptide cyclodehydrations. *Nature Chemical Biology* **2012,** *8* (6), 569-575.

77. Ding, W.; Li, Y. Z.; Zhao, J. F.; Ji, X. J.; Mo, T. L.; Qianzhu, H. C.; Tu, T.; Deng, Z. X.; Yu, Y.; Chen, F. E.; Zhang, Q., The catalytic mechanism of the class C radical *S*-adenosylmethionine methyltransferase NosN. *Angewandte Chemie-International Edition* **2017,** *56* (14), 3857-3861.

78. Umemura, M.; Nagano, N.; Koike, H.; Kawano, J.; Ishii, T.; Miyamura, Y.; Kikuchi, M.; Tamano, K.; Yu, J. J.; Shin-ya, K.; Machida, M., Characterization of the biosynthetic gene cluster for the ribosomally synthesized cyclic peptide ustiloxin B in *Aspergillus flavus*. *Fungal Genetics and Biology* **2014,** *68*, 23-30.

79. Koiso, Y.; Natori, M.; Iwasaki, S.; Sato, S.; Sonoda, R.; Fujita, Y.; Yaegashi, H.; Sato, Z., Ustiloxin - a phytotoxin and a mycotoxin from false smut balls on rice panicles. *Tetrahedron Letters* **1992,** *33* (29), 4157-4160.

80. Ding, W.; Liu, W. Q.; Jia, Y. L.; Li, Y. Z.; van der Donk, W. A.; Zhang, Q., Biosynthetic investigation of phomopsins reveals a widespread pathway for ribosomal natural products in Ascomycetes.

Proceedings of the National Academy of Sciences of the United States of America **2016,** *113* (13), 3521-3526.

81. Koiso, Y.; Morisaki, N.; Yamashita, Y.; Mitsui, Y.; Shirai, R.; Hashimoto, Y.; Iwasaki, S., Isolation and structure of an antimitotic cyclic peptide, Ustiloxin F: Chemical interrelation with a homologous peptide, ustiloxin B. *Journal of Antibiotics* **1998,** *51* (4), 418-422.

82. Matoba, Y.; Kumagai, T.; Yamamoto, A.; Yoshitsu, H.; Sugiyama, M., Crystallographic evidence that the dinuclear copper center of tyrosinase is flexible during catalysis. *Journal of Biological Chemistry* **2006,** *281* (13), 8981-8990.

83. Gibson, D. G.; Young, L.; Chuang, R. Y.; Venter, J. C.; Hutchison, C. A.; Smith, H. O., Enzymatic assembly of DNA molecules up to several hundred kilobases. *Nature Methods* **2009,** *6* (5), 343-U41.

84. Yazaki, K., Transporters of secondary metabolites. *Current Opinion in Plant Biology* **2005,** *8* (3), 301-307.

85. Costa, C.; Dias, P. J.; Sa-Correia, I.; Teixeira, M. C., MFS multidrug transporters in pathogenic fungi: do they have real clinical impact? *Frontiers in Physiology* **2014,** *5*.

86. Groves, J. T.; McClusky, G. A., Aliphatic hydroxylation via oxygen rebound. Oxygen transfer catalyzed by iron. *Journal of the American Chemical Society* **1976,** *98* (3), 859-861.

87. Broderick, J. B.; Duffus, B. R.; Duschene, K. S.; Shepard, E. M., Radical *S*-adenosylmethionine enzymes. *Chemical Reviews* **2014,** *114* (8), 4229-4317.

88. Bruijnincx, P. C. A.; van Koten, G.; Gebbink, R., Mononuclear non-heme iron enzymes with the 2-His-1-carboxylate facial triad: recent developments in enzymology and modeling studies. *Chemical Society Reviews* **2008,** *37* (12), 2716-2744.

89. van Berkel, W. J. H.; Kamerbeek, N. M.; Fraaije, M. W., Flavoprotein monooxygenases, a diverse class of oxidative biocatalysts. *Journal of Biotechnology* **2006,** *124* (4), 670-689.

90. Eliot, A. C.; Kirsch, J. F., Pyridoxal phosphate enzymes: Mechanistic, structural, and evolutionary considerations. *Annual Review of Biochemistry* **2004,** *73*, 383-415.

91. 五十嵐　祐也. 糸状菌リボソームによる新規ペプチド骨格生合成経路に関する研究.卒業論文, 北海道大学, 2015.

92. Zhu, Y. G.; Zhang, Q. B.; Li, S. M.; Lin, Q. H.; Fu, P.; Zhang, G. T.; Zhang, H. B.; Shi, R.; Zhu, W. M.; Zhang, C. S., Insights into Caerulomycin A biosynthesis: A two-component monooxygenase CrmH-catalyzed oxime formation. *Journal of the American Chemical Society* **2013,** *135* (50), 18750-18753.

93. Fesko, K.; Gruber-Khadjawi, M., Biocatalytic methods for C-C bond formation. *Chemcatchem* **2013,** *5* (6), 1248-1272.

94. Chen, H. J.; Ko, T. P.; Lee, C. Y.; Wang, N. C.; Wang, A. H. J., Structure, assembly, and mechanism of a PLP-dependent dodecameric L-aspartate *beta*-decarboxylase. *Structure* **2009,** *17* (4), 517-529.

95. Koiso, Y.; Li, Y.; Iwasaki, S.; Hanaoka, K.; Kobayashi, T.; Sonoda, R.; Fujita, Y.; Yaegashi, H.;

Sato, Z., Ustiloxins, antimitotic cyclic-peptides from false smut balls on rice panicles caused by *Ustilaginoidea virens*. *Journal of Antibiotics* **1994,** *47* (7), 765-773.

96. Wang, X. Q.; He, X. Z.; Lin, J. Q.; Shao, H.; Chang, Z. Z.; Dixon, R. A., Crystal structure of isoflavone reductase from alfalfa (*Medicago sativa* L.). *Journal of Molecular Biology* **2006,** *358* (5), 1341-1352.

97. Fujii, K.; Ikai, Y.; Mayumi, T.; Oka, H.; Suzuki, M.; Harada, K., A nonempirical method using LC/MS for determination of the absolute configuration of constituent amino acids in a peptide: Elucidation of limitations of Marfey's method and of its separation mechanism. *Analytical Chemistry* **1997,** *69* (16), 3346-3352.

98. Li, Y.; Manickam, G.; Ghoshal, A.; Subramaniam, P., More efficient palladium catalyst for hydrogenolysis of benzyl groups. *Synthetic Communications* **2006,** *36* (7), 925-928.

99. Ram, S.; Spicer, L. D., Rapid debenzylation of *N*-benzylamino derivatives to amino derivatives using ammonium formate as catalytic hydrogen transfer agent. *Tetrahedron Letters* **1987,** *28* (5), 515-516.

100. Schwanhausser, B.; Busse, D.; Li, N.; Dittmar, G.; Schuchhardt, J.; Wolf, J.; Chen, W.; Selbach, M., Global quantification of mammalian gene expression control. *Nature* **2011,** *473* (7347), 337-342.

101. Xu, Z. L.; Baunach, M.; Ding, L.; Hertweck, C., Bacterial synthesis of diverse indole terpene alkaloids by an unparalleled cyclization sequence. *Angewandte Chemie-International Edition* **2012,** *51* (41), 10293-10297.

Acknowledgement

Firstly, I would like to thank my Ph. D. supervisor, professor Hideaki Oikawa. Under Prof. Oikawa's guidance, I have obtained great chances to carry on interesting research projects and to publish in academic journals and meetings. More importantly, he led me to this laboratory where I feel ambitious and enjoyable to do researches, to join discussions and to collaborate. His great knowledge and talent prompt me never to stop improving myself, and his devotion to research and education will always guide me in the future academic road.

I would like to thank associate professor Atsushi Minami. Out of his great experiences and sharp mind, he always gave me important suggestions and advices, and inspired me to think deep and work efficiently.

I would like to thank assistant Professor Taro Ozaki. In the final year of my Ph. D, he supported me a lot when I was facing the great difficulty of Duf3328 characterization. His enthusiasm in research and teaching also impressed me.

I would like to thank Professor Tohru Dairi, Keiji Tanino, Takanori Suzuki and Masaya Sawamura who are the sub-advisers of my course. Their advices and suggestion are important for me to accomplish this thesis.

I would like to thank collaborators Dr. Myco Umemura in ustiloxin project, Dr. Attila Mandi in sesterfishrol project and Dr. Eri Fukushi for NMR measurements. Thanks to Prof. Hiroshi Tomoda for measuring the bioactivity of sesterfisheric acid. Daicel Corporation for providing chiral column

I would like to thank all lab members. The everyday discussions and mutual supports make here a wonderful team. Thanks to Yuya Igarashi for working together in ustiloxin project. Special thanks to Momoka Yamane and secretory Ms. Saze. These two lovely ladies gave me sweet memories of friendship.

Lastly, I would like to thank Professor Chengwei Liu. He taught me everything of experiment details, and helped me overcome the foreignness and loneliness when I first came here. 谢谢师兄！

June 2017